STUDIES OF SELECTED HEAVY METALS REMOVAL FROM NAKURU INDUSTRIAL WASTEWATER USING SUGARCANE BAGASSE AND VALORISED BAGASSE

EZEKIEL KIPKORIR LANG'AT

A Thesis Submitted to the Graduate School in Partial Fulfilment of the Requirements for the Master of Science Degree in Chemistry of Egerton University

EGERTON UNIVERSITY

AUGUST, 2025

DECLARATION AND RECOMMENDATION

Declaration

This thesis is my original work and has not, wholly or in part, been presented for the award of a degree in this University or any other University.

Signature  Date:……17 / 08 / 2025…….

Ezekiel Kipkorir Lang'at

SM11/11771/16

Recommendation

This thesis has been submitted for examination with our approval as University supervisors.

Signature:……  …….. Date……18/08/2025……

Prof. Josiah O. Omolo, PhD

Department of Chemistry

Egerton University

Signature:……  …… Date…18/08/2025……

Dr. Peter O. Ongoma, PhD

Department of Chemistry

Egerton University

COPYRIGHT

DEDICATION

This work is dedicated to my wife Juliet and our children Joy, Jesse, Sarah. To my mother Rebecca Ng'eny and sisters Faith and Charity

ACKNOWLEDGEMENTS

I thank God for His abundant grace and care. I would like to acknowledge and thank Egerton University for allowing me to pursue my Master of Science degree in Chemistry. Gratitude goes to Chemistry Department for providing the equipment and laboratory space for my studies. Special thanks go to my supervisors, Prof. Josiah Omolo and Dr. Peter Ongoma for their advice, academic guidance and support. Their useful suggestions and comments enabled me complete my work successfully. Also, my gratitude goes to technical staff at Chemistry department, especially Mr. Paul Kamau; Mr. Kevin Odhiambo (USIU-Africa, Nairobi) and Mr. Leonard Bii (TRI-KALRO, Kericho) for their technical support. Last but not least, I am indebted to my family and mother for their encouragement, patience and prayers during my studies.

May God richly bless you all, in your endeavours.

ABSTRACT

Adsorption of heavy metals is a novel technology for treatment of wastewaters containing different types of heavy metals. This study aimed at using sugarcane bagasse (NSCB) and valorised bagasse (VSCB) adsorbents made out of sugarcane bagasse, a viable and low cost agricultural waste material from Nzoia sugar factory in Western Kenya, to investigate kinetic and thermodynamic properties for the removal of selected heavy metals (cadmium(II), copper(II), chromium(III), nickel(II) and lead(II)) from industrial wastewater at controlled pH, using Atomic Absorption Spectrophotometer (AAS). Sugarcane bagasse (NSCB) was divided into smaller particle sizes and air-dried at room temperature, dried in a drying oven at 70 °C for 24 h; while Valorised sugarcane bagasse (VSCB) was prepared by slowly heating bagasse at 300 °C for 3 hours. NSCB and VSCB were sieved through standardized sieves of 150-595µm. Batch experiments were done to get the optimum conditions of pH, adsorbent dosage, particle size, contact time, concentration and temperature. Eleven (11) industrial wastewater samples were collected randomly from three major locations (**A**, **B**, and **C**), lying between 0° 10' 0'' S and 36°10' 00'' E within Nakuru City in Nakuru County, Kenya. The levels of heavy metals in the untreated wastewater ranged respectively from: 0.02 – 2.02 ppm for lead, 0.02-0.81ppm for copper, 0.02-0.10 ppm for cadmium, 0.024-0.670 ppm for nickel and 0.004-9.94 ppm for chromium. The levels of lead, copper, cadmium and chromium in some of the wastewater samples were above the limits set by the Kenya Bureau of Standardisation (KEBs). The study showed that the adsorption efficiency of NSCB and VSCB powder was higher in aqueous solution than in wastewater. The removal kinetics of the metal ions fitted well with the pseudo-second-order model. For NSCB, the adsorption isotherm models of Pb^{2+} and Ni^{2+} showed better fitting for Freundlich isotherm while Cd^{2+}, Cu^{2+} and Cr^{3+} showed better fit on the Langmuir isotherm model. While Pb^{2+}, Ni^{2+}, Cd^{2+}, and Cu^{2+} had a better fit for the Freundlich isotherm as Cr^{3+} has a better fit with the Langmuir isotherm model on VSCB. The negative free energy change (ΔG) values revealed spontaneous adsorption process of the metal ions onto NSCB and VSCB, respectively. The enthalpy change (ΔH) and entropy change (ΔS) ranged from 28.34 - 74.84 $kJmol^{-1}$ and 111.70-344.23 $Jmol^{-1}K^{-1}$ for NSCB and VSCB further reflecting higher affinity of the metal ions onto NSCB and VSCB. This study addresses sustainable developmental goal 6 (SDG 6) which seeks to improve water quality by reducing pollution and proportions of heavy metals in untreated wastewater using NSCB and VSCB adsorbents.

TABLE OF CONTENTS

LIST OF TABLES

LIST OF FIGURES

LIST OF ABBREVIATIONS AND ACRONYMS

AAS	Atomic Absorption Spectrometry
AC	Activated carbon
AR	Analytical reagent
NSCB	Normal sugarcane bagasse
TDS	Total dissolved solids
UNWD	United Nations World Water Development
VSCB	Valorised sugarcane bagasse
WHO	World Health Organization

CHAPTER ONE
INTRODUCTION

1.1 Background information

Water is a source of life and is regarded as the most essential of natural resources (Connor *et al.*, 2017). The quality of the world's water is increasingly being threatened because freshwater resources are becoming polluted which impacts negatively on humans. As much as 90% of wastewater in developing nations is released in rivers lakes or oceans with little or no treatment (Canton, 2021).

Water contamination is a world-wide challenge (Anastopoulos *et al*., 2017) and is caused by heavy metal pollution, pathogens, turbidity, oil and its derivatives from industries and agricultural effluents (Cutillas *et al*., 2012). When ingested beyond the permitted concentration, heavy metals can cause serious health disorder. Water contamination by heavy metals is emerging as a major environmental issue that requires immediate global attention because these metals are non-biodegradable (persist in the environment indefinitely), have long biological half-lives and are often transformed from one oxidation state to the other, which increases to their mobility and toxicity in the environment (Ezeonuegbu *et al*., 2021; Kibet *et al*., 2023). And thus, cause a danger to public health. Lead and cadmium are the most common heavy metal pollutants (Barakat, 2011; Mudhoo *et al*., 2012). Lead poisoning causes low intelligent quotient, concentration disorders and behavioural changes in children. In women it causes infertility, menstrual disorders, increased the chance of miscarriage and stillbirths (Dahl *et al*., 2014). Prolonged exposure to cadmium ions causes damage to kidneys, lungs, liver and it is also carcinogenic (Fu & Wang, 2011). These metals end up in human bodies either by direct intake or via food chains. What is worse is that heavy metals cannot be degraded or destroyed (Coral *et al*., 2005).

To solve this problem, numerous conventional physicochemical methods such as electrochemical treatment, ion-exchange, precipitation, reverse osmosis, evaporation and oxidation/reduction have been explored. However, all these conventional methods have also had their limitations. They are expensive, not eco-friendly, and inefficient for removing trace levels of heavy metals (Vera *et al*., 2019). In addition, adsorption has been used for centuries by Egyptians for removing odours and purification of drinking water (Hijab, 2017).

Annual sugarcane production in Kenya is 7.2 million metric tonnes per year, which generates about 2.4 million metric tonnes of sugarcane waste or bagasse (Sugar Industry Stakeholder's Taskforce Report 2019). Sugarcane bagasse is an inexhaustible material that

has greater selectivity for bio-sorption studies on heavy metal ions, particularly when valorised which increases its efficiency and high adsorption capacity (Adegoke & Bello, 2015), high surface area and surface reactivity (Arshadi *et al.*, 2014). Bagasse is rich in lignocellulose and has abundant pores giving it a large internal surface area (Mahamadi, 2011). Due to this property, sugarcane bagasse has also been applied to remove some heavy metal ions from contaminated water. The degree of success in removing these ions from water differs from one metal to another and depends on prevailing experimental conditions such as temperature, concentration contact time, pH, and particle size (Bhatnagar & Mika, 2010; Gupta & Sharma, 2003; Ibrahim *et al*., 2006).

Sugarcane bagasse has not been fully explored as an economic and effective material for removing heavy metal pollutants from wastewater (Abdulrazak *et al*., 2017; Chan *et al*., 2022; Raj *et al*., 2022). It is friendly to the environment and cost effective bio-sorbent. Sugarcane bagasse contains around 50% cellulose, 27% polyoses, and 23% lignin (Aksu & Isoglu, 2005). These substances contain abundant carboxyl and amine functional groups that can strongly bind metal ions in an aqueous solution; thus, enabling sugarcane bagasse to have great potential as an excellent bio-sorbent (Aksu & Isoglu, 2005; Kawwsarn, 2002).

There is, therefore, a need to investigate the kinetic and thermodynamic behaviour of sugarcane bio-sorbent to remove cadmium (Cd^{2+}), chromium (Cr^{3+}), copper ($Cu^{2+)}$, Nickel (Ni^{2+}) and lead (Pb^{2+}) ions from industrial wastewater under varying experimental conditions of pH, contact time, particle size, initial concentration, adsorbent dosage and temperature to obtain a detailed understanding of the adsorption mechanism. This is of vital importance because sugarcane bagasse is a low-cost farm waste sorbent that can be regenerated for reuse and exhibits high efficiency in detoxifying extremely dilute effluents. To describe the interactions between liquid and solid phases (Saleh, 2022), numerous equations have been used to correlate experimental adsorption isotherm data to determine the best-fit isotherms model (Chen, 2015). The Freundlich isotherm is reported to be suitable for non-ideal adsorption caused by different functional groups on the surface. The Langmuir isotherm, on the other hand, is derived from the assumption of monolayer adsorption (Al-Ghouti *et al*., 2020). The Langmuir, Freundlich, and Dubinin-Radushkevich adsorption isotherm models (Hu *et al*., 2019; Russakova *et al*., 2021) are used to select the best suitable isotherm for explaining the adsorption process (Babatunde *et al*., 2022).

In this study the adsorption mechanism and maximum adsorption capacity were studied through the application of these adsorption models from which thermodynamic parameters

(ΔG, ΔS and ΔH) were determined. Kinetics of adsorption were studied using pseudo first and pseudo second order rate equations.

1.2 Statement of the problem

A review of the literature has demonstrated that there is increased discharge of heavy metals into the water body system as a result of industrialization, and the use of fertilizers, pesticides, and herbicides in agriculture. Others include surface runoffs and Jua Kali garages posing a major concern to marine life as well as human health. This points to unplanned human activities, especially in developing countries. An example is the battery recycling plant (in Owino Uhuru area) at the coastal city of Mombasa which was accused in 2016 of releasing toxic substances, including lead, into the environment that severely impacted the health of the local community. The number of deaths yearly as a result of dirty water and related diseases is estimated at 2.3 million people every year. To protect the current generation and generations to come, there is a need to treat heavy metal-contaminated wastewater before they are released into the environment. Conventional treatments are expensive, require specialized expertise, and pose disposal problems, and thus have not been widely applied at large scale in the Kenyan local context. Due to those drawbacks, adsorption has emerged as a low-cost alternative. Agricultural wastes such as sugarcane bagasse and valorised bagasse are explored in this regard because of their abundance, cheapness, and properties to trap metal ions from aqueous metal ion solutions. They have the advantage of low cost, help in solving the problem of waste, their properties can be enhanced through modification, are fast, and can be reused.

Heavy metal contamination has become a global issue. The quality of world's water is increasingly threatened because surface water has been increasingly polluted due to unplanned human activities especially in developing countries. The number of deaths yearly as a result of dirty water and related diseases is estimated at 2.3 million people every year. Waste from households is approximately 1.3 tonnes per annum and 0.3 tonnes of hazardous waste is thrown out per year. Discharge of such waste water can lead to serious pollution of surface water and underground water. Some of the chemicals polluting water bodies are heavy metals Lead, Chromium, Cadmium Nickel, and Copper among others. A review of literature has demonstrated that there is increased discharge of heavy metals into the water body system. These metals end up in human bodies either by direct intake or via food chains. Heavy metals pose significant risks (Oladimeji *et al*., 2024; Das *et al*., 2023) to both human health and marine ecosystems (Canton, 2021; Ahamad *et al*., 2024). The effects on human

health and marine life can be catastrophic depending on the kind of chemicals and concentrations of the pollutants when they are polluted an example is the Owino uhuru battery recycling plant at the coastal city of Mombasa which was accused in 2016 of releasing toxic substances, including lead, into the environment, which severely impacted the health of the local community. Jua kali sector also is not left behind in contribution to pollution. Cadmium (Cd), lead (Pb), copper (Cu), Nickel (Ni) and Chromium (Cr), even in very low concentration or exposure, cause various diseases like kidney problem, anaemia, liver problem, lowered immune function, allergies and lung disorders, respectively. On top of these diseases the metals also cause various types of cancer. Therefore, it is important to study the chemical and physical properties of these heavy metals in the polluted waters in order to develop new technologies for their removal. Therefore, this study was carried out to investigate optimum conditions of adsorption, Kinetic and thermodynamic behaviour of selected heavy metals on sugarcane bagasse and valorised sugarcane bagasse adsorbents, and to apply the optimum conditions on their removal from wastewater samples.

1.3 Objectives

1.3.1 General objective

To study selected heavy metals removal from Nakuru city industrial wastewaters using sugarcane bagasse and valorised bagasse.

1.3.2 Specific objectives

i. To analyse the concentration of heavy metals (Cd, Pb, Cr, Cu & Ni) in selected Industrial wastewaters in Nakuru city.

ii. To determine the optimal conditions of pH of medium, contact time, particle size, amount of adsorbent used and temperature, and to characterize sugarcane bagasse and valorised bagasse for the presence of functional groups accountable for adsorption using Fourier transform infrared (FTIR) spectroscopy and surface coverage using adsorption isotherms.

iii. To determine the thermodynamic and kinetic properties of adsorption of the heavy metals on normal sugar cane bagasse and valorised bagasse.

iv. To evaluate the efficiency, under optimal conditions, for removal of the heavy metals from industrial waters collected within Nakuru City.

1.4 Research questions

i. What is the concentration of heavy metals (Cd, Pb, Cr, Cu & Ni) in Industrial wastewater in Nakuru city?

ii. What are the optimal conditions of pH medium, contact time, particle size, amount of adsorbent used, temperature and characterize sugarcane bagasse and valorised bagasse for the presence of functional groups accountable for adsorption using Fourier transform infrared (FTIR) and surface coverage using adsorption isotherms?

iii. What are the thermodynamic and kinetic properties of adsorption of the heavy metals on normal sugar cane bagasse and valorised bagasse?

iv. What is the efficacy of the optimal conditions for removal of the heavy metals from industrial waters collected within Nakuru City?

1.5 Justification

In Kenya, the sugarcane crop has the advantage of large-scale production all year round. In 2022/2023 sugarcane production in Kenya was 650,000 metric tonnes per year (Kenya annual USDA sugar report: report number: KE2023-0003). This translates to 198,000 metric tonnes of bagasse as waste, which this study explores to develop a low-cost adsorbent for the removal of heavy metal pollutants (Cu, Cr, Cd, Ni, and Pb) from wastewater by adopting its adsorptive properties. Toxicity due to copper leads to kidney damage, haemolytic anaemia, and liver problems. Lead toxicity leads to delayed puberty, anaemia, cardiovascular, central nervous system, kidney damage, high blood pressure and fertility problems. Cadmium toxicity results in low birth weight in infants, kidney and liver problems. Excess effects of chromium include accelerated development of several cancers affecting lungs, larynx, bladder, kidneys, bone, and thyroid while excess nickel results in allergic reaction, dermatitis, respiratory and reproductive problems. The above-mentioned metals target the major organs (kidney, lungs, liver, brain, bones) and they also accelerate developments of cancer. There is therefore a need to remove these heavy metal pollutants from wastewater, using safe low-cost adsorbent with high adsorption capacity and is highly efficient like sugarcane bagasse and valorised bagasse. The use of sugarcane bagasse to remove heavy metals contributes to United nation environment programme sustainable development goal number 6 (SDG 6), which aims to improve water quality by reducing pollution, eliminating dumping and minimizing the release of hazardous chemicals and materials, halving the proportion of untreated wastewater and substantially increasing recycling and safe reuse

globally (Arora & Mishra, 2022). Therefore, this study was carried out to come up with optimum conditions of adsorption, isotherm studies, Kinetic and thermodynamic behaviour of sugarcane bagasse and valorised sugarcane bagasse. The findings from this study will provide reference material for future researchers using agricultural waste as an adsorbent.

1.6 Limitations

Despite the comprehensive nature of this study, several limitations were encountered. While both raw and valorized sugarcane bagasse were investigated, the valorized form showed superior removal efficiencies. One limitation was difficulty in accessing equipment (ICP-OES and FTIR). The samples were however sent for analysis in places that had the required equipment, *i.e.* USIU-A (Nairobi) and Tea research institute, Kericho.

Secondly, although kinetic, isotherm, thermodynamic models were applied and FTIR analysis done, deeper mechanistic studies— such as metal speciation or advanced surface characterization of the adsorbent-adsorbate interface such as SEM (scanning electron microscopy), XRD (x-ray diffraction) and others—were beyond the scope of this work, and could be explored in future research. Last but not least, experiments were done under controlled laboratory conditions, so industrial scale applicability that may reflect field-scale complexities was beyond the scope of this work and could be explored in future research.

CHAPTER TWO
LITERATURE REVIEW

2.1 Heavy metal pollution of industrial wastewaters and surface waters

Industrial uses of heavy metals include metal processing in refineries and petroleum combustion among others. Pollution could also result from mine waste spills. Other sources are leaded gasoline, paints, and land application of fertilizers among others.

2.1.1 Definition of heavy metals and their sources

There is no clear definition of a heavy metal and in most cases density is the determining factor in defining a heavy metal (Järup *et al*., 2003). Heavy metals are defined a naturally occurring inorganic substances with atomic numbers above 20 and characteristic densities of more than 5g cm^{-3} (Garcia *et al*., 2025; Ranaweera *et al*., 2023) and they are characterized by their potential toxicity to living organisms at concentrations beyond permissible levels (Ungureanu *et al.,* 2022). Sources of heavy metals are either Natural or Anthropogenic (Human made). Naturally they may be found in soils as a result of volcanic emissions and weathering (Oves *et al.,* 2016). Anthropogenic activities include mining, smelting , domestic and technological agricultural activities (Tchounwou *et al.*, 2012) such as application of certain phosphate based fertilizers add Cd (Wuana & Okieimen, 2011) also as a result of industrial wastewater discharge (Ranaweera *et al*., 2023).

Table 1: Sources of heavy metals**:**

Heavy metal	Source
Cu	Plumbing and tap fittings, motor vehicle parts, Cu-based agrochemicals, (Rehman *et al.*, 2019)
Pb	Automobile battery processing, mobile phone battery, lead smelting, Leaded fuel, (Raj & Das, 2023)
Cd	Weathering of rocks, welding or smelting, metallurgy, electroplating, Cd-based batteries, Phosphatic fertilizers (Emiliani *et al.*, 2021)
Cr	Dental implants, leather tanning, dye-manufacturing, chrome plating (Coetzee *et al.*, 2020)
Ni	Clothing industry, electrical appliances , alloy in steel industry, electroplating, Ni/Cd batteries, paints (Genchi *et al*., 2020).

Road dust can have heavy metals including Fe, Zn, Pb, and Cr in it (Oves *et al.*, 2016). It is estimated that approximately 20 million hectares of arable land worldwide (Trotta *et al*., 2024) are irrigated using wastewater (Hettiarachchi & Ardakanian, 2018), particularly in various cities across Asia and Africa, where agriculture reliant on wastewater irrigation (Angon *et al*., 2024) contributes to around 50% of the vegetables supplied to urban populations (Makoni *et al*., 2010). This can be attributed to water scarcity challenges in many regions, leading to the reuse of wastewater for agricultural purposes. Farmers generally may not bother about environmental benefits or hazards (Wuana & Okieimen, 2011; Khalid *et al*., 2021). Heavy metals and their compounds are characterized by relatively high stability and solubility in atmospheric precipitation (Dzyadevych & Jaffrezic-Renault, 2014). In the stomach the acid medium converts them to their stable oxidation states (Zn^{2+}, Pb^{2+}, Cd^{2+}, As^{5+}, As^{3+}, Hg^{2+} and Ag^{+}) which combine with the body's proteins and enzymes. Their levels in water depend on the physicochemical parameters of water such as pH, turbidity and conductivity among others (Radulescu *et al.*, 2014).

Industrial sources include metal processing refineries and petroleum combustion among others. It could also result from mine waste spills. Collapse of a dam in lead mine in Hunan, southern china led to the spread of mining waste spills on the farmlands along rivers. Seventeen years later certain soils were still heavily polluted with As, Cd, Zn, Pb and Cu (Liu *et al.*, 2005). There is increased use of heavy metals in process industries such as the electroplating, tanning and textile industries (Yu *et al*., 2001). Other sources of heavy metals are leaded gasoline and paints, land application of fertilizers, animal manures, sewage sludge , pesticides, wastewater irrigation, coal combustion residues, spillages of petrochemicals and atmospheric deposition (Wuana & Okieimen, 2011). Thus, heavy metal contaminated waters are growing at an alarming rate and is a growing concern (Sharma *et al*., 2021).

2.1.2 Methods of determination of heavy metals in water samples

Several methods previously used include evaporation, solvent extraction and ion chromatography whereby heavy metals are separated by elution and determined with a conductometric detector. Chelates have also been analysed using thin layer chromatography (Zolotov *et al.*, 1987). Atomic absorption (AAS) is a common and reliable way to analyse metals and metalloids in water samples (Kassim *et al.*, 2023). Mineralization of samples is performed by using a digester (Radulescu *et al.*, 2014). It uses a flame to atomize the sample and then measures intensity of incident radiation adsorbed by metal atoms. AAS technique is

accurate in analysis of trace amounts of metals since it is sensitive, selective and precise (Salih, 2024; Bakırcıoğlu *et al.*, 2003).

Inductively Coupled Plasma Mass Spectrometry (ICP-MS) is a very sensitive (Van *et al*., 2023)

and accurate technique to find and measure trace amounts of elements in a wide range of samples (Chen *et al*., 2022). It involves ionizing the sample in an inductively coupled plasma and then analysing the mass-to-charge ratio of the ions produced (Acker *et al*., 2023). Inductively Coupled Plasma Optical Emission Spectrometry (ICP-OES) is Similar to ICP-MS. ICP-OES measures the concentration of elements in a sample by analysing the light emitted by excited atoms in an inductively coupled plasma (Khan *et al*., 2022). The method used will rely on factors such as the range of heavy metal concentration, how sensitive the method is, and what equipment is available (Poljak *et al*., 2024).

2.1.3 Permissible levels of heavy metals in waters

As heavy metals have been proven to show toxicological effects even at very low concentrations, organizations such as the World Health Organization (WHO) have set permissible exposure limits of these contaminants in drinking water (Ranaweera *et al*., 2023). Maximum permissible level for Cadmium is 0.03 mg/L, 0.01 mg/L for lead, 0.05 mg/L for Chromium, 0.02 mg/L for Nickel and 0.07 mg/L for Cu. WHO guidelines for drinking water (WHO, 2011). More information on Table 2.

Table 2: Maximum permissible levels

Metal	WHO	EU	USEPA	EAC	KEBs
Pb	0.01mg/L	0.01mg/L	0.015mg/L	0.01mg/L	0.05mg/L
Cu	2mg/L	2mg/L	1.3mg/L	2.00mg/L	0.1mg/L
Cd	0.03mg/L	0.01mg/L	0.005mg/L	0.03mg/L	0.005mg/L
Ni	0.07mg/L	0.02mg/L	0.1mg/L	0.02mg/L	-
Cr	0.05mg/L	0.05mg/L	0.1mg/L	0.05mg/L	0.05mg/L

2.1.4 Problems associated with heavy metals

Trace elements are important when present in the required amount. The steady growth in human population has magnified the release of heavy metals into water bodies. Heavy metals may bio accumulate in various organs of aquatic organisms, particularly fish, which in turn may enter the human body through food chain causing serious health implications. Heavy metals have a tendency to accumulate in selective tissues of living organisms (Rajeshkumar & Li, 2018). Copper at lower concentration acts as co-factor for various enzymes which are involved in fundamental physiological processes (Oves *et al.*, 2016). Copper is essential in maintaining the metabolism of the human body. Small amounts of Nickel are needed by the human body to produce red blood cells. Cadmium and lead, have no known physiological activity (Wuana & Okieimen, 2011).

Once inside the human body, they are likely to cause multiple adverse medical conditions. Metal toxicity depends on the amount absorbed, route of exposure, and duration of exposure. This can lead to various disorders and can also result in excessive damage due to oxidative stress induced by free radical formation. Other conditions associated include nausea, anorexia, gastrointestinal abnormalities, and dermatitis. Additionally, they have the potential of damaging the central nervous system and can alter blood composition. These metal toxins may also harm vital organs such as the lungs, and kidney (Jaishankar *et al*., 2014; Oves *et al.*, 2016). Other medical conditions are given in Table 3.

Table 3: Medical conditions associated with excess heavy metals

Heavy metal	Medical condition
Cu	- kidney damage, haemolytic anaemia, liver problems (Taylor *et al.*, 2020).
Pb	- delayed puberty, anaemia, cardiovascular, central nervous system, kidney damage, high blood pressure and fertility problems (Gull *et al.*, 2018; A. Kumar *et al.*, 2020)
Cd	- low birth weight in infants, kidney and liver problems (Emiliani *et al.*, 2021 & Gull *et al.*, 2018)
Cr	- accelerate the development of several cancers affecting lungs, larynx, bladder, kidneys, bone, and thyroid (Deng *et al*., 2019; Balali-Mood *et al.*, 2021)
Ni	- allergic reaction, dermatitis, respiratory and reproductive problems (Buxton *et al.*, 2019)

2.2 Presence of heavy metals in Nakuru wastewaters and surface waters

Rift Valley lakes such as Lake Nakuru and Lake Naivasha are important habitats for fish, birds and other wildlife (Aloo *et al*., 2013; Ochieng *et al.*, 2007). Lake Nakuru is fed by freshwater springs and five rivers namely: Njoro, Nderit, Larmudiak, Makalia and Naishi in addition to direct rainfall and ground water (Nantongo, 2021), in addition to direct rainfall and groundwater, these rivers-mainly seasonal- drain into the lake. Challenges emerging from unplanned urban development are evident as majority of urban areas are faced with challenges of solid and wastewater disposal, and some like Nakuru, Naivasha and Kisumu have directly discharged sewage into the lakes thus affecting water quality (Githaiga *et al*., 2021).

Lake Nakuru water quality has been declining over time due to pollutants emanating from discharge of waste from industrial activities and human settlements (Ochieng *et al.*, 2007). In 2003 it was found that fish from lake Nakuru had accumulated traces of Cd, Cr, Hg, Ni and Pb (Mavura & Wangila, 2003). In addition, flamingo deaths were attributed to poisoning by heavy metals (Ndetei & Muhandiki, 2005).

In 2007 water samples and sediments taken from sites in Lake Nakuru were analysed for of heavy metals and findings indicated that some of the sites had relatively high concentration levels of metals (Nantongo *et al*., 2024) Cd, Co, Cu, Pb, Ni, and Zn (Esilaba *et al*., 2020;

Ochieng *et al.*, 2007). Water samples analysed from Lake Nakuru were found to have traces of Ni, Cu, Zn, As, Cd and Hg (Yang *et al.*, 2017). Recent studies on fish from Lake Nakuru were found to have high levels of lead (Nantongo *et al*., 2024).

2.3 Adsorption and desorption studies

Liquid–solid adsorption is based on the ability of certain solids to accumulate molecules (Alkhaldi *et al*., 2024) and ions from liquid phase onto the surface of solid material (Abdullah *et al*., 2019). This is generally attributed to weak interactions i.e in chemical adsorption involves electrostatic interactions (Zhu *et al.*, 2020) between the charged sites on adsorbents and adsorbates (Moreno *et al.*, 2010). Different researchers have studied these interactions and found that plant based adsorbents consists groups such as C=S, S=O, S-S, C=O (Krishnan & Anirudhan, 2003), numerous hydroxyl and carboxyl groups operate as exchangeable cation sites, which play a critical role in cation exchange processes by supplying negatively charged sites that that adsorb positively charged ions (cations) via reversible chemical reactions (Yadav *et al*., 2023; Gao *et al.*, 2020).

Most adsorption studies done have found that the adsorbents that have a negatively charged surface and negatively charged functional group are most favourable for adsorption of positively charged metal ions (Lui *et al*., 2013) due to electrostatic attraction (Yang *et al*., 2019). Thus the main mechanisms for adsorption by these groups includes H-bonding, π–π interactions, n–π electron-donor–acceptor ion exchange and complexation (Mariska *et al*., 2024)/chelation (Huang *et al.*, 2019; Vera *et al*., 2019). The adsorption can be due to either chemisorption or physiosorption. In physiosorption weak van der waals attraction is observed between an adsorbate (metal ion) and an adsorbent surface while chemisorption when there is formation of chemical bonds between the adsorbent surfaces and metal ion (Sahmoune, 2019).

pH is a critical parameter in these interactions because it affects the charges of the active sites of the adsorbents (Rodriguez *et al*., 2015) and the metal behaviour in the solution (Ahmed *et al*., 2023). The pH of a solution is important in both adsorption and desorption processes (Gkika *et al*., 2025; Ghosh *et al*., 2023; Chien *et al*., 2018) because it affects surface charge properties, ionization states, and electrostatic interactions between adsorbents and adsorbates (Chien *et al*., 2023; Umeh *et al*., 2023). Some researchers have achieved desorption by changing pH of the solution to about pH 2 (Kallel *et al.*, 2016) or by placing adsorbent in dilute acidic solution (Dawodu *et al.*, 2020 ; Vijayalakshmi *et al.*, 2017) .

Alkaline solutions such as dilute NaOH (0.1M) have also been investigated as desorbing agents (Ranaweera *et al*., 2023).

2.3.1 Thermodynamic and kinetic properties of adsorption and desorption

Adsorption and desorption processes involve both thermodynamic and kinetic properties, which are crucial for understanding and predicting the behaviour of adsorbates (Suter *et al*., 2024) and adsorbents (Saleh, 2022). Adsorption by activated carbons are analysed using Langmuir, Freundlich, Dubinin–Radushkevich among others (Song *et al*., 2014). Kinetics of adsorption is one of the important characteristics defining the efficiency of adsorption and is studied using pseudo first order or second order model data fitting while thermodynamic parameters of adsorption are calculated using Van't hoff's plot (Zhou *et al*., 2024; Anastopoulos *et al*., 2017).

2.3.2 Review of thermodynamic and kinetic studies of heavy metals adsorption

Mabuza *et al*. (2022) observed that thermodynamic parameters including the standard enthalpy change (ΔH^o), Gibbs free energy change (ΔG^o), and the entropy change (ΔS^o) are evaluated for adsorption systems to establish thermodynamic parameters governing the adsorption process (Mabuza *et al.*, 2022) i.e. whether the adsorption process is spontaneous, and whether endothermic or exothermic (Argun *et al.*, 2007). Thermodynamic parameters can be evaluated by applying Van't Hoff equation and Gibbs free energy equation (Beyan *et al.*, 2022; Kalavathy *et al.*, 2005). The Van't Hoff's plot is a graphical representation that shows the natural logarithm of equilibrium constant (ln K_{eq}) plotted against reciprocal of absolute temperature ($\frac{1}{T}$) (Bullerjahn *et al*., 2024) and is given as

$$\frac{\mathrm{d}\ \ln K_{eq}}{d\,T} = \frac{\Delta \mathrm{H}}{R}\left(\frac{1}{T^2}\right) \quad \text{or} \quad \ln K_{eq} = \left(-\frac{\Delta \mathrm{H}}{RT} + \frac{\Delta \mathrm{S}}{R}\right) \tag{2.1}$$

The Arrhenius and Eyring equations can also be used to obtain the activation parameters such as activation energy (E_a), and enthalpy (ΔH), entropy (ΔS) and free energy (ΔG) of activation for the adsorption system (Chowdhury *et al.*, 2011). Arrhenius equation describes the temperature dependence of reaction rates, including adsorption processes. The modern form of Arrhenius equation accounts for temperature dependence of pre-exponential factor. The equation is given by

$K = A\,.T^{n}.e\left(\frac{-E_a}{RT}\right)$ also written as $ln\,K = lnA + n\,\ln T + \left(\frac{-E_a}{RT}\right)$

2.2

Where, K is the rate constant, A is the pre-exponential factor, E_a is the activation energy, R is the gas constant, T is the temperature and *n* is an empirical exponent accounting for temperature dependence of pre-exponential factor.

Eyring equation is given by $K=\frac{K_B.T}{h}.e\,(\frac{-\Delta H}{RT})\,.\,e\,(\frac{\Delta S}{RT})$ whereby k_B is the Boltzman constant. Thermodynamic parameters can also be obtained by using the adsorption isotherms namely Langmuir Model, Freundlich and Dubinin-Radushchevik Model as described below;

Langmuir Model , $q = q_{max}\frac{K_L C}{1+K_L C}$

2.3

Freundlich Model , $q = K_f C^{\frac{1}{n}}$

2.4

and Dubinin-Radushchevik Model , $q_e = q_s\, e^{(-K_{ad}\varepsilon^2)}$

The equilibrium constant (K_c) is given as

$K_c = \frac{q_e}{C_e}$

2.5

where K_c is the equilibrium constant, C_e is the equilibrium concentration in solution (mg/L) and q_e is the amount adsorbed at equilibrium (P. S. Kumar *et al.*, 2010).

$\Delta G = -RT ln\,K_c$

2.6

$ln\,K_c = \frac{\Delta S}{R} - \frac{\Delta H}{RT}$

2.7

The values of ΔS and ΔH are determined from the slope and the intercept of the plots of plots of $ln\,K_c$ versus $\frac{1}{T}$. The enthalpy change (ΔH^o) and the entropy change (ΔS^o) are calculated from a plot of $\ln b$ versus $\frac{1}{T}$.

$\Delta G = -RT \ln b$

2.8

$\ln b = \frac{\Delta S}{R} - \frac{\Delta H}{RT}$

2.9

Kinetic parameters for the adsorption process are done analyse the rate at which adsorption occurs over time and is usually studied for a range of contact times (Chang *et al*., 2012). The pseudo-first-order, pseudo-second-order, and intrapartile diffusion models are widely used to study adsorption kinetics and processes (Al-Harby *et al*., 2021; Simonin, 2016). The obtained data is regressed against two equations the Lagergren pseudo first-order kinetic equation (Ezzati *et al*., 2024) and also against a pseudo-second-order kinetic equation (Ezzati *et al*., 2024; Karaman *et al*.,2022; Yuh-Shan, 2004).

$$\log(q_e - q_t) = \log q_e - \frac{K_1 t}{2.303}$$

2.10

$$\frac{t}{q_t} = \frac{1}{k_2 q_e^2} + \frac{1}{q_e} t$$

2.11

Where q_t = the metal uptake per unit weight of adsorbent (mg g^{-1}) at time t.

q_e = the metal uptake per unit weight of adsorbent (mg g−1) at equilibrium.

k_1 = the rate constant of the first-order kinetics equation (min^{-1}).

k_2 = the rate constant of pseudo-second-order kinetics equations (g $mg^{-1}min^{-1}$).

The slopes and intercepts of plots generated from adsorption data are used to calculate the rate constants k_1 and k_2 and equilibrium adsorption capacity q_e (Qi *et al*., 2021; Khan *et al*., 2017; Argun *et al.*, 2007). The one that give the best fit is the one with a higher R^2 value.

2.3.3 Influence of thermodynamic and kinetic properties on removal of heavy metals from polluted waters

Thermodynamic properties play a significant role in the removal of heavy metals from polluted waters. They thermodynamic factors and their impact include Gibb's free energy, enthalpy and entropy (Al-Harby *et al*., 2021). The Gibbs free energy change (ΔG) is a critical parameter (Chowdhury *et al*., 2012) that determines the spontaneity of the adsorption process. A more negative ΔG means value indicates higher adsorption capacities and thus a stronger driving force for the adsorption (Tong *et al*., 2019).

Enthalpy change (ΔH) determines whether the process is endothermic (+ΔH) or exothermic (- ΔH) in studying the heat exchange during the adsorption. Endothermic adsorption means that adsorption will increase at higher temperatures. Exothermic process means that adsorption is favourable at lower temperatures (Sahmoune, 2019). Entropy change (ΔS) provides insights into the randomness of the system i.e whether adsorption is accompanied by an increase (ΔS > 0) or decrease (ΔS < 0) in randomness. Positive entropy

means the adsorption is entropy driven. Positive ΔS values indicate an increase in disorder, which is often favourable for adsorption (Ramadhani *et al*., 2020).

Adsorbent adsorption typically consists of four stages: (i) the movement of solute molecules from the bulk solution to the thin boundary layer surrounding the adsorbent, (ii) diffusion of the solute from this boundary layer to the adsorbent's surface, (iii) transfer of solute molecules from the surface into the adsorption sites, and (iv) the actual interaction or binding between the solute molecules and these active sites on the adsorbent. These consecutive processes jointly regulate the efficiency and kinetics of the adsorption process. After adsorption onto the surface, adsorbate molecules may also undergo surface diffusion (Argun *et al.*, 2007; Sahu *et al*., 2020). Intraparticle diffusion is typically defined as a relationship between the amount of adsorbate adsorbed at any given time (q_t) and the square root of time ($t^{1/2}$) (Al-Harby *et al*., 2021; Wang *et al*., 2022; Argun *et al.*, 2007).

Thus, the kinetics of sorption on the activated carbon as adsorbent can be analysed using linearized form of pseudo-first-order and pseudo-second-order kinetic models. The plots of experimental data are made at different initial concentration of metal ion for pseudo-first order and second order models, respectively. Calculated kinetic parameters indicate which kinetic model better represents the experimental data (Rai *et al.*, 2016).

2.4 Effects of activation of adsorbent on removal of heavy metals from polluted waters

Activation of adsorbent is achieved by modifying the adsorbent's surface. Adsorbents surface can be modified by either chemical activation or by physical activation which often involves heat (Abegunde *et al*., 2020). Some common effects of activation include; increased surface area, improved porosity and enhanced surface reactivity.

High surface area: Activation often leads to an increase in the surface area of the adsorbent material (Heidarinejad *et al*., 2020). Barman & Saikia (2025) noted that a higher surface area provides more active sites for heavy metal ions to bind to, thereby enhancing adsorption capability of an adsorbent.

Additionally activation process of an adsorbent can dramatically enhance its porosity by producing new pores, which improves its overall surface area and adsorption effectiveness (Li *et al*., 2024). Increased porosity improves the accessibility of heavy metal ions to active sites within the adsorbent structure (Ankrah *et al*., 2022), facilitating their removal from the solution (Qasem *et al*., 2021; Hong *et al*., 2019).

Enhanced Surface Reactivity**:** Activation processes can introduce functional groups or defects on the surface of the adsorbent (Li *et al*., 2020). These functional groups have the

ability to interact chemically or physically with heavy metal ions, improving the adsorbent's selectivity and affinity for particular heavy metals (Yang *et al*., 2019).

2.4.1 Heat activated adsorbent surfaces

Using heat as a means of activation for agricultural waste for adsorption purposes is a common technique in environmental and waste management applications (Yunus *et al*., 2022). Heat treatment activates adsorbents, which improves their adsorption capabilities (Kharrazi *et al*., 2020).

Activation Process**:** Heat treatment, also known as pyrolysis, involves subjecting the agricultural waste to high temperatures in the absence of oxygen (Karić *et al*., 2022). This process breaks down the complex organic structure of the waste material, creating a highly porous structure (Ren *et al*., 2021). The heat decomposes organic molecules in agricultural waste, resulting in an adsorbent material with enhanced surface area that can participate in adsorption process (Lawtae & Tangsathitkulchai, 2021; Karić *et al*., 2022).

The first step usually involves selection of a suitable agricultural waste material for valorisation. Common agricultural waste materials used include groundnut shells, rice husks, coconut shells, wood chips, sawdust, and various types of straws. The material undergoes cleaning, drying, and crushing or grinding into tiny particles in order to maximize its surface area and enable consistent heating during activation.

Heat Treatment is done by subjecting the material to high temperatures under oxygen free conditions ie in a furnace (Agboola *et al*., 2024; Saleem *et al*., 2019). Temperatures typically range between 400°C and 900°C, depending on the precursor material and desired qualities of the activated adsorbent. Karić *et al*. (2022) synthesized activated carbon using potato peels and valorisation was performed exclusively at a high temperature of 500 °C for 30 min while Elleta *et al*. (2020) synthesized activated carbon using Cocoa pod husk (CPH) which was valorised at 700 ^{o}C for 2 hours.

The duration of heating, also known as residence time, is an essential parameter in the activation process. Different researchers have used different resident times varying from several minutes to several hours, depending on the adsorbent material and required properties of the activated adsorbent of the activated adsorbent (De Rose *et al*., 2023). Olawale *et al*. (2015) used activation time of 20 to 60 min and temperatures of 200 and 400°C to make adsorbent from nutshell. Odubiyi *et al*. (2012) used 120 minutes and temperature of 700 ^{o}C to prepare adsorbent from cocoa pod husk.

After the heating process is complete, cooling and stabilization is done. Activated sample is allowed to cool down gradually to room temperature. This helps in stabilizing the material (Abate *et al*., 2020).

2.4.2 Removal of heavy metals from polluted waters using activated adsorbent surfaces

Activated carbon's efficiency in adsorptive removal of inorganic pollutants is largely determined by the type of functional groups and ions present on its surface (Yang *et al*., 2019). Rice husk and coconut shell activated carbons are low cost adsorbents that remove dyes from aqueous solutions (Oribayo *et al*., 2020; Kheddo *et al*., 2020) i.e malachite green dye from aqueous solution (Abate *et al*., 2020) and Pb^{2+} from aqueous solutions respectively (Chowdhury *et al.*, 2011; Song *et al.*, 2013). Sugar beet bagasse activated carbon was used for the adsorption of nitrates (Demiral & Gündüzoğlu, 2010).

Cotton stalk and dried mango kernel activated carbon have been used as an adsorbent for the removal of methylene blue and adsorption of Cr (VI) from aqueous solutions (Deng *et al.*, 2009; Rai *et al.,* 2016). Molasses activated carbon has been used for adsorption of methylene blue dye (Legrouri *et al.,* 2005). In India activated carbon prepared from bagasse pith was used for the adsorption of Cd(II) (Krishnan & Anirudhan, 2003).

CHAPTER THREE
MATERIALS AND METHODS

3.1 Sampling sites and sample collection

Eleven (11) composite industrial waste samples were collected randomly from three major locations (**A**, **B**, and **C**), lying between 0° 10’ 0’’ S and 36°10’ 00’’ E within Nakuru City in Nakuru County, Kenya (Figure 1). The samples comprised industrial wastewater from the following sampling regions: **A**: *Jua Kali industrial sites*- {S9 (0°16'28.6"S 36°02'49.6"E), S10 (0°16'56.3"S 36°03'44.6"E), and S11(0°17'40.2"S 36°03'28.8"E)} ; **B**: {*Tannery* {S1 (0°17'48.5"S 36°03'22.7" E) and S8 (0°17'48.5"S 36°03'22.7"E)}, *Textile* {S4 (0°17'24.4"S 36°03'39.2"E) and S5 0°17'24.4"S 36°03'39.2"E)}, and *Soap processing* S2 (0°17'13.6"S 36°02'42.1"E)}; and **C**: {*Milk processing* S3 (0°17'25.4"S 36°06'43.6"E), and *Potable water treatment plants* {(S6 (0°24'47.9"S 36°08'49.2"E) and S7 (0°16'56.3"S 36°03'44.6"E)}.

The samples were collected in pre-cleaned one-litre plastic bottles that had been thoroughly washed with detergent and tap water, then consecutively rinsed with nitric acid: distilled water (1:1), hydrochloric acid: distilled water (1:1), and finally with deionized distilled water. This was to ensure the sample containers did not introduce contaminants through leaching or surface desorption, causing positive and negative errors or by reducing the solution concentrations through adsorption. The samples were then acidified with 1.0 mL concentrated HNO_3 bringing the pH to 2-3 and stored in a refrigerator, at approximately 4 °C, to ensure that the metal ions remained in solution in their stable oxidized state before analysis.

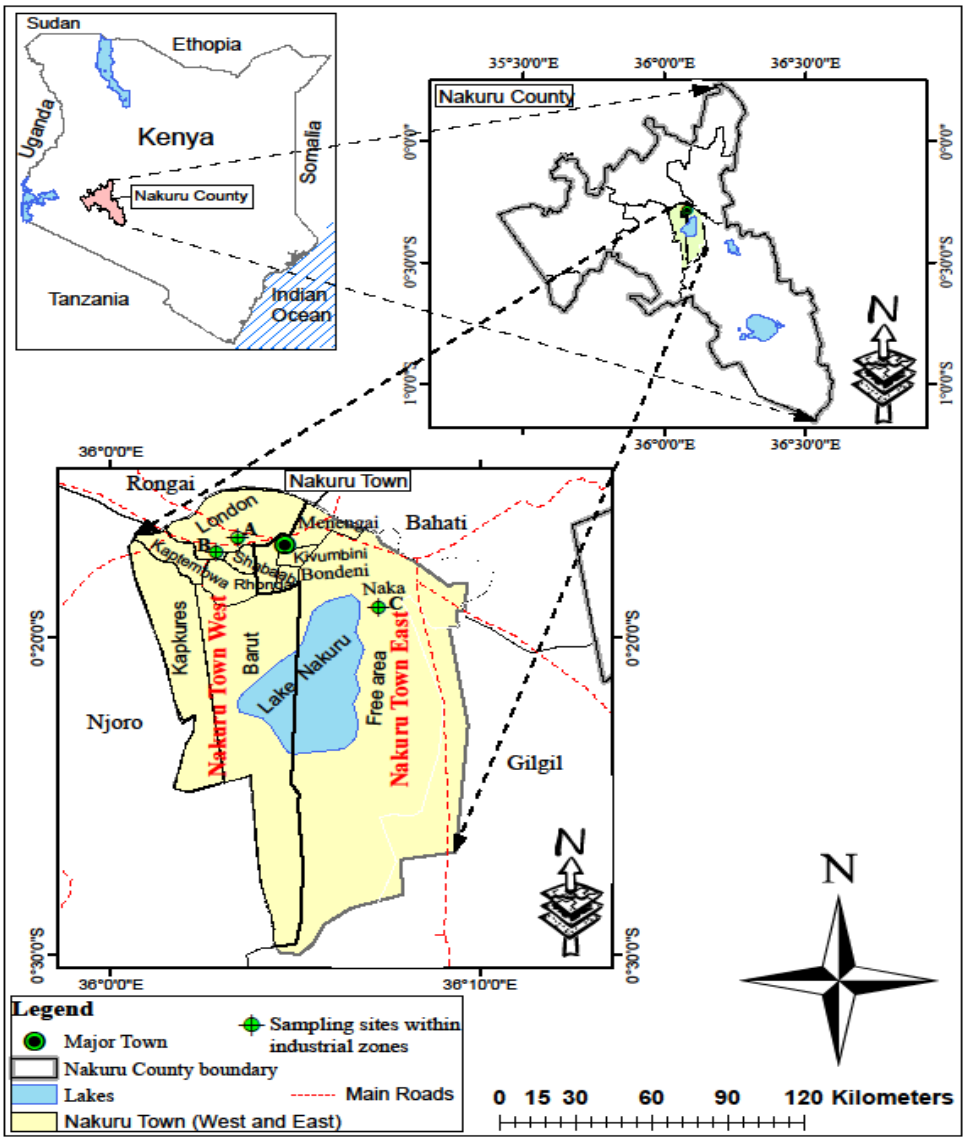

Figure 1: Map of Kenya showing Nakuru City and the sampling sites

3.2.1 Chemicals, reagents and solvents

All the chemicals used throughout this study were analytical-grade reagents. Double-distilled water was used to prepare all solutions and reagents. Stock solutions of the heavy metal standards were prepared by dissolving appropriate amounts of analytical grade salts ($Cu(NO_3)_2$, $Pb(NO_3)_2$, $Cr(NO_3)_3$, $NiCl_2$, and $CdCl_2$ purchased from Sigma Aldrich (Kobian, Nairobi) in distilled water to which 3.0 cm^3 concentrated HNO_3 acid had been added, and then diluted to 1.0 Litre. The working standard solutions of each metal were obtained by dilution of appropriate amounts of heavy metal solution using distilled water. A few drops of Caesium-lanthanum ($CsCl/LaCl_3$; 5:20 g/L) solution was added to each of the working

standards as an interference suppressant. 0.1 M HCl or 0.1 M NaOH was used to adjust the appropriate initial pH of solutions during analyses.

3.2.2 Preliminary laboratory preparations and storage of the samples

The samples were preserved immediately after sampling by acidification with 10 mL of concentrated nitric acid per litre of sample bringing the pH to 2-3. After acidification the sample was stored in a refrigerator, at approximately 4 °C, to ensure that the metal ions remained in solution in their stable oxidized state.

3.2.3 Collection and preparation of sugarcane bagasse and valorised bagasse

Sugarcane bagasse was collected from the Nzoia sugar factory in Western Kenya. The bagasse sample was washed with excess distilled water to remove extraneous materials such as dirt, sand, and other impurities. The Sugarcane bagasse was divided into smaller particle sizes and air-dried at room temperature, dried in a drying oven at 70 °C for 24 h and then ground into a fine powder using a blender (Heavy duty blender model 24CB10C). It was labelled as normal sugarcane bagasse (**NSCB**) and stored in labelled air-tight plastic jars before use.

The Valorised sugarcane bagasse (**VSCB**) was prepared by placing some of the oven-dried bagasse in a glass beaker) and slowly heated at 300 °C for 3 hours in an oxygen-free environment in a muffle furnace (Gallenkamp muffle furnace, size 2, tactical 308). The sample was left to cool to room temperature and then kept in a desiccator. The resulting biochar is referred to as **VSCB**.

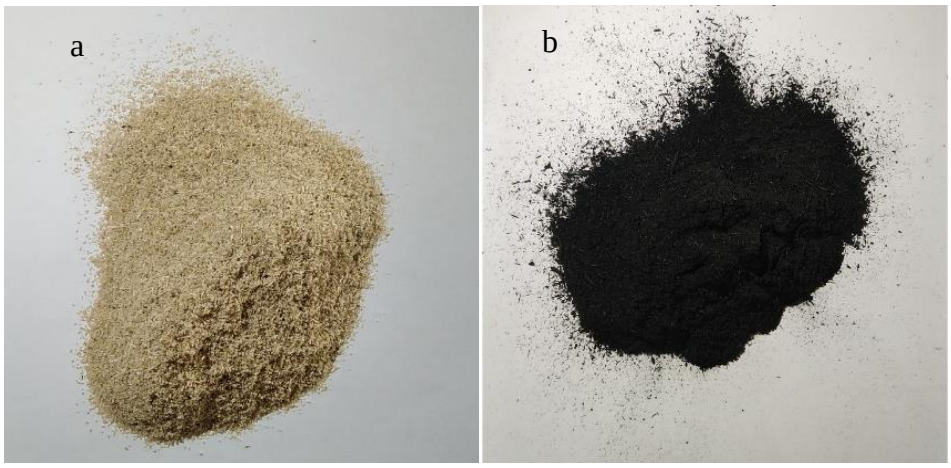

Plate1: (a) Normal sugarcane bagasse (**NSCB**) and (b) valorised sugarcane bagasse (**VSCB**)

3.2.4 Functional group analysis

Fourier transform infrared (FTIR) spectroscopy analysis was carried out to determine the surface functional groups of the biochar samples using a FTIR – 6100 JASCO spectrometer in the range 4000–400 cm^{-1}.

3.2.5 Digestion of samples

From the refrigerated samples, 10 mL of each was measured in separate 100 mL conical flasks. To each, 20 mL a 1:4 aqueous hydrochloric acid solution (i.e. hydrochloric acid: distilled water) followed by addition of 10mL a 1:1 aqueous nitric acid solution. The sample mixture was digested using a hotplate for 25 minutes at 350 ^{o}C. The digested sample was left to cool for 5 minutes then filtered into a 50 mL volumetric flask through Whatman no 1 filter paper. The volume was be topped to 50 mL.

To check whether bagasse could be having residual heavy metals, 5 g of powdered sugarcane bagasse was placed in a 100 mL conical flask. To this 20 mL of a 1:4 aqueous hydrochloric acid solution followed by addition of 10 mL a 1:1 aqueous nitric acid solution. The mixture was then digested on a hotplate for 25 minutes at 350 °C. The resulting digested sample was left to cool for 5 minutes, then filtered into a 50 mL volumetric flask through Whatman no1 filter paper and the volume topped up to 50 mL.

3.2.6 Preparation of stock and standard solutions

A stock solution 500mg/L for each metal analysed in this study were obtained by dissolving an amount of their respective salts in distilled water namely; Cr from 3.848g $Cr(NO_3)_3$, Ni from 2.025g $NiCl_2$, Cd from 0.815g $CdCl_2$, Pb from 0.799g $Pb(NO_3)_2$ and Cu from 1.478g $Cu(NO_3)_2$. 1.5 mL of concentrated nitric acid was added to the solution and the volume made up to 500 mL. From the respective stock solutions different standard concentrations ranges in mg/L for each metal was prepared. The standard concentration ranges were prepared using serial dilution from a higher concentration of each. The serial dilution was done by pipetting 10 mL of the stock solution and diluting to 100 mL to make 50ppm solutions for each of the metals. The 50ppm was serially diluted to get the required concentration range using the dilution formula.

$C_1V_1=C_2V_2$

The working range concentration for the metals was as follows;

(i) Chromium standard concentration range between 1.0µg/ mL up to 5.0 µg/ mL.

(ii) Nickel standard concentration between 1.5 µg/ mL up to 5 µg/ mL.

(iii) Cadmium standard concentration between 0.25 µg/ mL up to 2.0 µg/ mL.

(iv) Lead standard concentration between 2 µg/ mL up to 15 µg/ mL.

(v) Copper standard concentration between 0.7 µg/ mL up to 4.0 µg/ mL.

During the analysis of the prepared samples and standards solutions, caesium-lanthanum interference suppressant solution was used. The suppressant solution was prepared by adding 400 mL of concentrated hydrochloric acid (AR grade) slowly and carefully (in a fume cupboard) to 47.0 g of lanthanum oxide (AR grade) in a beaker. The mixture was stirred until the lanthanum oxide completely dissolved. To the obtained lanthanum solution, 12.7 g of caesium chloride (AR grade) was added, and stirred until everything dissolved. Finally, the volume was adjusted to 2 L with distilled water, making a concentration of 5 g/L caesium and 20 g/L lanthanum.

3.2.7 Atomic absorption spectroscopic (AAS) analysis of heavy metal in the samples

The metal ions in the prepared standard and sample solutions were analysed using atomic absorption spectrophotometer, AAS (Model S11 from Thermo Jarell Ash Cooperation of Waltham, MA, USA.). For each metal ion analysed a hollow cathode lamp was used so as to provide the specific wavelength emitted by that particular element. For all the analyses the air-acetylene burner was installed, and the burner head position adjusted and aligned to the path of radiation from the lamp. The oxidant (air) was turned on and flow rate adjusted to that specified by manufacturer to give maximum sensitivity for the metal being measured. Acetylene was turned ON at specified flow rate value, and then the flame was ignited. A blank solution made of double distilled deionized water plus the interference suppressant was aspirated into the AAS so as to set the background signal capture before the standards are analysed. To obtain maximum response (sensitivity) a standard solution from middle of the linear working range, derived from the prepared standard concentration range for each metal, was used by aspirating as the burner is adjusted vertically and horizontally until optimal absorbance value.

The prepared standard solutions for each of the metal (refer section 3.1.6) was aspirated into the AAS and in each case the aspiration rate of the nebulizer (if variable) was adjusted to obtain maximum sensitivity. For each of the standards analysed the corresponding absorbance was recorded and used for plotting of calibration curve. The sample solutions were aspirated under the same conditions as the standards for each of the metals to be analysed and absorbance values recorded.

From the calibration curve, the absorbance values of the corresponding metals in the analysed sample solution were read off to give the concentration value. The value obtained was multiplied by dilution factors to give the actual concentration in collected sample. The plotting and calculation were done by programming the respective formulae and functions in Microsoft Excel (2016 Edition) according to Miller and Miller (2010). Table 4 shows operating conditions for heavy metal analysis.

Table 4: Atomic absorption spectrophotometer settings

Heavy metal	**Cr**	**Ni**	**Cd**	**Pb**	**Cu**
Wavelength (nm)	357.9	232.0	228.8	217.0	324.7
Burner height (mm)	5	5	5	5	5
Band pass (nm)	0.5	0.3	1	1	1
Lamp current (A)	6	10	3	5	5
Linear range (ppm)	5	5	2	15	4

3.3 Adsorption experiments

Adsorption experiments were done by weighing 0.1 g of normal bagasse in a glass beaker, followed by the addition of 100 ml of different concentrations of the respective heavy metal solutions. The optimal adsorption conditions were monitored and evaluated by varying pH, particle size, contact time, concentration and temperature as described in the following subsections.

3.3.1 Particle size

The normal SCB was sieved to get different particle sizes i.e. 50, 150, 250, 425, 500, 595µm, and 1mm. For each of the particle size grades, 0.1 g of the SCB was placed in a glass beaker. Then 100 mL of the respective heavy metal solutions were added. The middle of the working range concentrations for the respective heavy metals was added (i.e. Cr = 2.5 ppm, Ni = 3 ppm, Cd = 1.5 ppm, Pb = 5 ppm and Cu = 2 ppm). The mixtures were shaken using a water bath shaker (65 rpm) for 30minutes and then filtered. The filtrate was analysed by AAS for the respective heavy metals that were not adsorbed as per the procedure described in sections 3.1.6 and 3.1.7 above.

This was repeated by changing the amounts of SCB to 0.3, 0.5, 0.7, 0.9, 1.5 and 2.0g. The data was analysed using the procedure described in section 3.1.8 to find the best amount (g) SCB for the heavy metal absorption.

3.3.2 Contact time

The best amount (g) of SCB obtained from section 3.2.2.1 and particle size was weighed into a glass beaker and to which 100 mL of the respective heavy metal solutions were added. The middle of the working range concentrations for the respective heavy metals was added to the mixture (i.e. Cr = 2.5ppm, Ni = 3ppm, Cd = 1.5ppm, Pb = 5ppm and Cu = 2ppm). The mixtures were shaken using a water bath shaker (65rpm) 1 minute and then filtered. The filtrate was analysed by AAS for the respective heavy metals were not absorbed as per the procedure described in sections 3.1.6 and 3.1.7 above. The experiments were repeated by changing the contact time to 2, 3, 4, 5, 30 and 60mins and the last one shaken for 24hrs for the same concentrations and volumes of solutions for each of the heavy metals. And the data analysed using the procedure described in section 3.1.8 to find the best optimal contact time (hrs) for the heavy metal absorption.

3.3.3 pH optimisation

The initial pH was adjusted with 0.1 M HCl or 0.1 M NaOH. Fresh 0.1 M hydrochloric acid was prepared by dissolving 9.2 mL of concentrated hydrochloric acid in distilled water to make a 1000 mL solution. Equally fresh 0.1 M sodium hydroxide solution was made by dissolving 4g of sodium hydroxide pellets in distilled water then be made to 1000 mL in a volumetric flask. The solutions were used to adjust the pH of mixture of SCB and heavy metal solutions to be prepared in the following paragraph.

The best amounts (g) of SCB obtained from section 3.2.1.1 was weighed in a glass beaker, to which 100 mL of the respective heavy metal solutions was added (i.e. Cr = 2.5ppm, Ni = 3ppm, Cd = 1.5ppm, Pb = 5ppm and Cu = 2ppm). Using few drops of 0.1M HCl the pH of mixture was adjusted to pH 2. The mixtures were shaken in a water bath shaker (65 rpm) for the optimum contact time obtained from section 3.2.1.1. The filtrate was analysed by AAS for the respective heavy metals that were not adsorbed as described in sections 3.1.6 and 3.1.7 above.

The experiments were repeated by changing the pH to, 4, 6, 7, 8, and 10 for the same concentrations and volumes of solutions for each of the heavy metals. The data was analysed

using the procedure described in section 3.1.8 to find the best optimal contact time (hrs) for the heavy metal absorption.

3.3.4 Heavy metals concentration

Different concentration of the respective heavy metal solutions were built within each metal's sensitivity range namely:

(i) Chromium solutions were 1.0, 2.0, 3.0, 4.0 and 5.0 ppm.

(ii) Nickel solutions were 1.5, 2.0, 2.5, 3.0, 3.5, 4.0, 4.5 and 5.0 ppm.

(iii) Cadmium solutions were 0.25, 0.5, 0.75, 1, 1.5, 1.75 and 2.0 ppm.

(iv) Lead solutions were 2.0, 4.0, 6.0, 8.0, 10.0, 12.0 and 15.0 ppm.

(v) Copper solutions were 0.7, 1.0, 1.5, 2.0, 2.5, 3.0, 3.5, and 4.0 ppm

At each of the concentrations, the optimum amount of adsorbent needed and particle size was weighed into a glass beaker, 100 mL of heavy metal solution was placed into each beaker. The pH of solution was adjusted to the optimum value. The mixtures were shaken using a water bath shaker (50 rpm) for the optimum contact time obtained from section 3.2.1.1. The filtrate was analysed by AAS for the respective heavy metals not absorbed as per the procedure described in sections 3.1.6 and 3.1.7 above. The data was analysed using the procedure described in section 3.1.8 to find the best optimal contact time (hrs) for the heavy metal adsorption.

3.3.5 Temperature

In this section the optimised values for particle size, amount (g) of SCB, contact time, pH and the concentration were factored where optimising the temperature. The SCB was weighed into a glass beaker then100 mL of heavy metal solution was added. The optimum pH and concentration was maintained as the mixtures were shaken using a water bath shaker (65 rpm) for the optimum contact time. The filtrate was analysed by AAS for the respective heavy metals not adsorbed as per the procedure described in sections 3.1.6 and 3.1.7 above. The experiments were repeated by changing the temperatures 20, 25, 30, 35, and 40 °C for the same concentrations and volumes of solutions for each of the heavy metals. The data was analysed using the procedure described in section 3.1.8 to find the best optimal temperature (°C) for the heavy metal absorption.

3.3.6 Thermodynamic data modelling

In order to model the thermodynamic data for the adsorption, the equilibrium time (t_e), amount adsorbed at equilibrium (q_e) and equilibrium concentration (c_e) were determined. In adsorption studies, q basically represents adsorption capacity which is the amount of heavy metal ions adsorbed. It is expressed by the formula

$$q = \frac{amount\ of\ adsorbate\ (mg)}{amount\ of\ adsorbent\ used\ (g)} \quad 3.1$$

Solutions of known concentrations were prepared and their initial heavy metal concentration (C_o) determined. For chromium, nickel, cadmium, lead and copper, the initial concentrations are 2.5 ppm, 3 ppm, 1.5ppm, Pb = 5ppm and 2 ppm, respectively. Optimized amount of adsorbent was weighed into a glass beaker then 100 mL of heavy metal solution was added. For each metal solution, 13 beakers were setup in triplicate to allow analysis after different contact times. A contact time study was done by determining the concentration of heavy metals remaining in the solutions at 1,2,3,4,5,30 and 60 mins then the last one for 24hours (1440 minutes) from the start of the experiment. The concentration obtained at any given time t was denoted C_t. The adsorption capacity q_t was calculated at any given time t, using the formula

$$q_t = \frac{C_o - C_t}{m} xV \quad 3.2$$

A plot was made of q_t versus time and from the plot a point was determined where q_t became constant which was the equilibrium time. Equally the corresponding q_t value was be the q_e value and the concentration value of heavy metals adsorbed was C_e.

$$q_e = \frac{C_o - C_e}{m} xV \quad 3.3$$

whereby C_e is the equilibrium concentration (mg/L) and q_e is the amount of heavy metal adsorbed (q_e, mg g^{-1}). The values found for C_o, C_e and q_e were used for thermodynamic data modelling vide Langmuir Model, Freundlich Model and Dubinin-Radushchevik Model as described below:

(i) Langmuir Model simulation

$$q = q_{max} \frac{K_L C}{1 + K_L C} \quad 3.4$$

The Langmiur equation was tranformed to its linear form;

$$\frac{1}{q_e} = \frac{1}{q_{max}} + \frac{1}{q_{max} K_L C} \quad 3.5$$

Values of K_L and q_{max} was computed from the slope and intercept, respectively from the plot of $\frac{1}{q_e}$ against $\frac{1}{C_e}$

Langmuir equilibrium parmeter (R_L) given by

$$R_L = \frac{1}{1 + (1 + K_L C_o)} \quad 3.6$$

R_L was calculated to check whether the equilibrium sorption is be favourable. R^2 value was calculated to see whether the sorption data fitted well to Langmiur model.In order to determine thermodynamic parameters experiment was carried out in three different temperatures

$$\Delta G = -RT ln b \quad 3.7$$

$$\ln \frac{K}{T} = -\frac{\Delta H}{R}.\frac{1}{T} + \ln \frac{K_B}{h} + \frac{\Delta S}{R} \quad 3.8$$

The Gibb's energy change is related to enthalpy change (ΔH) and entropy change (ΔS) by Eyring equation which can be abbreviated by ln $b = \frac{\Delta S}{R} - \frac{\Delta H}{RT}$ (equation 2). A plot of ln b versus $\frac{1}{T}$ was made. The entropy change was calculated from the intercept (intercept = $\frac{\Delta S}{R}$) and the enthalpy change calculated from the slope (slope = - $\frac{\Delta H}{R}$).

(ii) Freundlich Model Simulation

$$q = K_f C^{\frac{1}{n}} \quad 3.9$$

The linearized equation be

$$log\, q_e = log\, K_f + \frac{1}{n} log\, C_e \quad 3.10$$

Amount adsorbed q_e was plotted against equilibrium concentration of the heavy metal solution C_e K_f and n was characteristic of sorbent-sorbate system. If n lie between 1 and 10 it indicates a favourable sorption process. R^2 value was calculated to see whether the sorption data fitted well to Freundlich model

$$K_c = \frac{q_e}{C_e} \quad 3.11$$

A plot of ln K_c vs $\frac{1}{T}$ was plotted to estimate the thermodynamic parameters ΔG, ΔS, and ΔH

$$\Delta G = -RT ln\, K_c \quad 3.12$$

$$ln\, K_c = \frac{\Delta S}{R} - \frac{\Delta H}{RT} \quad 3.13$$

(iii) Dubinin-Radushchevik *(DR) Model*

Linearized form of Dubinin-radushchevik equation is given as;

$$\ln q_e = lnq_s - K_{ad}\,\varepsilon^2 \quad 3.14$$

The parameter ε (is the Polanyi potential) can be calculated as

$$\varepsilon = RT\ ln\ (1 + \frac{1}{C_e}) \quad 3.15$$

Adsorption data at different temperatures was plotted as a function of logarithm of amount adsorbed ln q_e vs ε^2. The values of q_s (maximum sorption capacity) and K_{ad} (Dubinin- radushkevich coefficient) is determined from the linear plot of DR model.

$$K_c = \frac{q_e}{C_e} \quad 3.16$$

$\ln K_c$ vs $\frac{1}{T}$ was plotted to estimate the thermodynamic parameters ΔG, ΔS, and ΔH

$$\Delta G = -RT ln\ K_c \quad 3.17$$

$$lnK = \frac{\Delta S}{R} - \frac{\Delta H}{RT} \quad 3.18$$

3.3.7 Kinetic data modelling

For kinetic studies, the optimum amount of sugarcane bagasse was brought into contact with 100 mL of heavy metal solution in the following concentration ranges.

(i) Chromium solutions were 1.0, 2.0, 3.0, 4.0 and 5.0 ppm.

(ii) Nickel solutions were 1.5, 2.0, 2.5, 3.0, 3.5, 4.0, 4.5 and 5.0 ppm.

(iii) Cadmium solutions were 0.25, 0.5, 0.75, 1.00, 1.50, 1.75 and 2.00 ppm.

(iv) Lead solutions were 2.0, 4.0, 6.0, 8.0, 10.0, 12.0 and 15.0 ppm.

(v) Copper solutions were 0.75, 1.00, 1.50, 2.00, 2.50, 3.00, 3.50, and 4.00 ppm.

The solutions were placed in a shaker at room temperature. At time intervals of 1 hr, 2 hr, 4 hr, 8 hr and 24 hrs, the amount of uptake of heavy metals were evaluated using Atomic Absorption Spectrophotometer and the kinetic data recorded.

Amount of heavy metal adsorbed (q_e, mg g^{-1}).

$$q_e\ (\text{mg}\ g^{-1}) = \frac{(C_o - C_e)}{m} xV \quad 3.19$$

(i) Pseudo first order simulation

$$\log(q_e - q_t) = \log\ q_e - \frac{K_1 t}{2.303} \quad 3.20$$

The value of q_e calculated were fitted in Lagregen pseudo-first-order equation. The value of rate constant for adsorption (K_1) from the slope of linear plot of log $(q_e - q_t)$ versus time

From the plot the regression coefficient R^2 value were calculated for each of the ions being studied.

(ii) Pseudo second order simulation

$$\frac{t}{q_t} = \frac{1}{k_2 q_e^2} + \frac{1}{q_e} t \qquad 3.21$$

The value of q_e calculated were fitted in the pseudo second order equation. The value of rate constant for adsorption (K_2) were obtained from the slope of linear plot of log $(\frac{t}{q_t})$ versus time (t). From the plot the regression coefficient R^2 value were calculated for each of the ions being studied.

3.3.8 Desorption experiments

50 mL of 2M hydrochloric acid were added to 100g of adsorbent and agitated for 24 hours to remove the adsorbed heavy metals ions then filtered. It was washed with 50 mL distilled water to remove any residual acid then dried in an oven and it was ready for use in the next cycle of adsorption and desorption.

3.4 Thermodynamic data modelling and kinetic data modelling for adsorption of heavy metals on heat valorised sugar cane bagasse

The sugarcane bagasse (SCB) was thoroughly washed with water to remove dirt and grime then rinsed a few times with distilled water, then dried at a room temperature. The dried materials were ground into fine powder using a blender (Heavy duty blender model 24CB10C).The powdered bagasse was placed in 500 mL beaker and placed in a muffle furnace (Gallenkamp muffle furnace, tactical model 308). The temperature was set at 300 ^oC (temperatures beyond 350^oC might lead to ashing) and the sample was left to heat in the furnace for 3 hours. After cooling the prepared carbon was pre-served until use. The thermodynamic and kinetic properties of adsorption/desorption of heavy metals were done following procedures and protocols describes under section 3.2 above.

3.5 Evaluation of the efficacy of the optimal conditions for removal of the heavy metals from surface and industrial waters collected within Nakuru City

The optimised values for amount of SCB, particle size, contact time, pH, concentration and temperature obtained in section 3.3 were used.

3.5.1 Digestion of samples

From the stored sample, 10 mL was measured into a 100 mL conical flask, to which 20 mL of 1:4 (Hydrochloric acid: distilled water) was added. Then finally 10 mL of 1:1 (Nitric acid: distilled water) was added. The mixture was heated in a hotplate at 350^{o}C for 25 minutes. The solution was left to cool, filtered into a 50 mL volumetric flask and the volume made up to 50 mL mark.

3.5.2 Soaking of the samples with NSCB and VSCB optimized conditions

Optimum amount of SCB was weighed into a glass beaker, 50 mL of digested sample was placed into each beaker. The determined optimized conditions (from section 3.1 for normal SCB and 3.2 for valorised SCB) were used to evaluate the removal of heavy metals in the collected samples from Nakuru Municipality. Finally, AAS analysis of the respective heavy metals in the filtrate according to procedure described under sections 3.1.6, 3.1.7 and 3.1.8 above for both normal and valorised SCB.

3.5.3 Calculation of removal efficiency and amount adsorbed

Removal efficiency (%) and amount adsorbed in mg/g are calculated as per the equations given below:

$$Removal\ efficiency\ (\%) = \frac{C_o - C_t}{C_o} x100 \qquad 3.22$$

$$Amount\ adsorbed\ \ q_t = \frac{C_o - C_t}{m} xV \qquad 3.23$$

0.1 g of NSCB and VSCB were placed in separate 100 mL aqueous solution of lead solution of concentration 10mg/L, residual lead was found to be 0.392 mg/L.

C_o =100mg/L, C_t = 0.392, m = 0.1 g and V = 0.1 L

$$i) \quad Removal\ efficiency\ (\%) = \frac{10 - 0.392}{10} x100$$

=96.080%

$$ii) \quad Amount\ adsorbed\ \ q_t = \frac{10 - 0.392}{0.1} x0.1$$

= 9.608mg/g

3.5.4 Calculation of number of molecules ions per gram

Conversion of q_{max} (maximum adsorption capacity) into moles per gram. The moles per gram were then multiplied by avogadros number to convert them into number of molecules per gram according to the equations below:

$$Number\ of\ molecules\ or\ ions\ per\ gram = moles/g\ x\ N_A \quad (3.24)$$

$$Number\ of\ molecules\ or\ ions\ per\ gram = \frac{q_{max}}{M\ X\ 1000}\ x\ N_A \quad (3.25)$$

Whereby q_{max} is the maximum Langmuir adsorption capacity (mg/g), M is the molar mass of adsorbed metal and N_A is the avogadro's number 6.022 x 10^{23}

i.e. Adsorption of lead on NSCB had a q_{max} = 44.053, M_{Pb} = 207.2, N_A = 6.022 x 10^{23}

$$Number\ of\ Pb\ molecules\ or\ ions\ per\ gram = \frac{44.053}{207.2\ X\ 1000} x 6.022 \text{ x } 10^{23}$$

$$= 2.12 \text{ moles/g x } 6.022 \text{ x } 10^{23}$$

$$= 1.28 \text{ x } 10^{20} \text{ molecules/ions}$$

CHAPTER FOUR

RESULTS AND DISCUSSIONS

4.1 Concentration of heavy metals in wastewaters

The sampled sites were already given in section 3.1. The concentrations of heavy metals (Cd, Pb, Cr, Cu & Ni) in Nakuru Industrial wastewaters and surface waters are provided in Table 5.

Table 5: Heavy metal concentration (Mean ± SD)

Sampling Site	Lead	Copper	Cadmium	Nickel	Chromium
S1	0.02 ± 0.004	0.020 ± 0	0.020 ± 0.001	0.200 ± 0.017	9.940 ± 1.930
S2	0.010 ± 0.001	0.010 ± 0.001	0.020 ± 0.003	ND	0.007 ± 0.002
S3	0	0	0.096 ± 0.020	0.024 ± 0.006	0.045 ± 0.009
S4	0.100 ± 0.020	0.010 ± 0.002	0.020 ± 0.000	ND	0.011 ± 0.004
S5	0.033 ± 0.002	0.006 ± 0.002	0.007 ± 0.000	ND	0.045 ± 0.000
S6	0	0.004 ± 0.003	0	ND	ND
S7	0.100 ± 0.01	0.001 ± 0	0.020 ± 0.004	0.320 ± 0.004	0.004 ± 0.001
S8	0.033 ± 0.003	0.004 ± 0.002	0.022 ± 0.007	0.119 ± 0.000	ND
S9	1.044 ± 0.022	0.002 ± 0.001	0.057 ± 0.006	ND	0.348 ± 0.135
S10	1.150 ± 0.001	0.810 ± 0.010	0.100 ± 0.009	0.670 ± 0.006	0.664 ± 0.049
S11	2.202 ± 0.002	0.002 ± 0	0.086 ± 0.007	0.341 ± 0.014	0.424 ± 0.132

WHO *MPL Pb = 0.01, Cu = 2, Cd = 0.03, Ni = 0.07 and Cr = 0.05 mg/L

*MPL= maximum permissible limits in wastewater

From the results the lead levels were high except for three samples (sample 2, 3 and 6). Lead was found in textile waste and this can be attributed to metal complexed dyes which are widely used in textile industry (Kishor *et al*., 2021).

Copper levels were within the permitted limits. Cadmium levels were high in samples 3,9,10 and 11. Cadmium is used in automobile coatings (Giacomin *et al*., 2019). Nickel was high in samples 1, 7, 8, 10, 11 but was within permissible levels in sample 3 and was not

detected in the rest of the samples. Nickel was found in waste from tannery and this can be attributed to Nickel salts, such as nickel sulfate which are occasionally used in the tanning process and also in other stabilizing agents that help stabilize tanning chemicals (Khalid *et al*., 2021). Nickel contamination in jua kali garages can be attributed motor vehicle parts and paints that contain nickel when these parts are replaced or disassembled (Giacomin *et al*., 2019).

Chromium was high in four samples (1, 9, 10 and 11) while the rest were within permissible levels. Chromium was found in tannery waste and it can be attributed to chromium sulfate as a tanning agent to make leather durable (Gezahegn *et al*., 2021; Laxmi *et al*., 2020). Chromium was found in garage waste and this can be attributed to motor vehicle parts like brake pads and also chrome based paints (Nduka *et al*., 2019).

4.1.2 Characterization (FTIR)

Examination of FTIR spectra shows a number of functional groups indicating the complex nature of adsorbent surface. The spectra showed wavenumbers in the regions 3334 (-OH), 1700 (-C=O) and 1600cm^{-1} (C=C). On adsorption there was a high frequency shift in these wavenumbers indicating that on adsorption the metal ion is attached to SCB and VSCB through O-H or carboxylate, carbonyl and C=C aromatic groups. Wavenumbers before and after adsorption on SCB are shown in Table 6.

Table 6: Characterization of NSCB

Before adsorption		**After adsorption of Copper**	
Frequency (cm^{-1})	Functional group	Frequency (cm^{-1})	Functional group
3334	-OH stretch (alcoholic, phenols)	3336	-OH stretch (alcoholic, phenols)
1700	-C=O stretch (ketones)	1727	-C=O stretch (ketones)
1600-1500	C=C, alkene (aromatic ring)	1530	C=C, alkene (aromatic ring)

Observation was that there was a high frequency shift (from initial value of -OH 3334, -C=O 1700 and C=C 1500), showing that the metal was attached to the raw SCB through O-H

or carboxylate, carbonyl and C=C aromatic groups. Wavenumbers before and after adsorption on VSCB are shown in Table 7.

Table 7: Characterization of VSCB

Before adsorption		**After adsorption of Copper**	
Frequency (cm^{-1})	Functional group	Frequency (cm^{-1})	Functional group
3796	-OH stretch (alcoholic, phenols)	3860	-OH stretch (alcoholic, phenols)
1702	-C=O stretch (ketones)	1705	-C=O stretch (ketones)
1591, 1509	C=C, alkene (aromatic ring)	1597	C=C, alkene (aromatic ring)

Observation was that there was high frequency shift (from 3796 to values above 3800) indicating adsorption took place mainly from Si–O-H or carboxylic acid.

The presence of functional groups on the surface of adsorbents was confirmed using FTIR analysis. FTIR analysis also provides more information on possible mechanism(s) involved in metal ion adsorption. Both the Sugarcane bagasse and valorised bagasse displayed similar functional groups on their surfaces. The absorption band at 3405–3334 cm^{-1} corresponds to the stretching vibration of –OH and the extension vibration of –NH (Putra *et al*., 2014). The band at 2925–2856 cm^{-1} was assigned to CH stretching, meanwhile the band at 1703 cm^{-1} represents carbonyl (C=O) groups, and at 1600-1536 cm^{-1} represents C=C for alkene groups (Ahmad *et al*., 2018; Putra *et al*., 2014). The absorption bands at 1029 and 1034 cm^{-1} was attributed to C–O stretching vibration of cellulose, lignin and hemicelluloses (Putra *et al*., 2014). Additional bands appeared at 3796 and 3734 cm^{-1} after combustion in valorised bagasse. After interaction with metal ions, the absorption band of –OH groups in the sugarcane bagasse and valorised bagasse shifted 3334 cm^{-1} to 3346 cm^{-1}; and from 3796 to 3800 cm^{-1} in valorised bagasse only. Meanwhile, the absorption band representing the carbonyl group shifted from 1704 cm^{-1} to 1727 cm^{-1}. The absorption intensity of this band increased significantly. The wavenumber of C–O stretch shifted from 1029 cm^{-1} to 1024 cm^{-1} following interaction of sugarcane bagasse and valorised bagasse with the metal ions. From FTIR study, the formation of new absorption bands, the change in absorption intensity, and the shift in wavenumber of functional groups could be due to

interaction of metal ions with active sites of adsorbents. The metal ions bound to the active sites of the adsorbents through either electrostatic attraction or complexation mechanism. The electrostatic attraction was between metal ion and carboxylate group, while the complexation mechanism involved electron pair sharing between electron donor atoms (O) and the metal ions. The results from this study as shown in tables 6 and 7 suggest that carbonyl, hydroxyl and aromatic alkene functional groups are the main adsorption sites in sugarcane bagasse as well as in the valorised bagasse.

4.2 Removal efficiency (%) and amount adsorbed (q)

Removal efficiency and amount of heavy metal adsorbed on NSCB and VSCB were calculated using equation provided in section 3.5.3 and results provided in Table 8.

				Removal efficiency (%)		Amount adsorbed (q) in mg/g	
	$C_{initial}$ (mg/L)	C_{NSCB} (mg/L)	C_{VSCB} (mg/L)	NSCB	VSCB	NSCB	VSCB
Pb	10	0.392	0.000	96.080	100.000	9.608	10.000
	20	4.041	2.570	79.795	87.150	15.959	17.430
	40	10.392	7.284	74.020	81.790	29.608	32.716

Table 8: Removal efficiency and amount adsorbed for lead and cadmium ions on NSCB and VSCB

	60	21.878	17.778	63.537	70.370	38.122	42.222
Cd	10	0.321	0.185	96.790	98.150	9.679	9.815
	20	3.0505	1.665	84.748	91.675	16.950	18.335
	40	9.8394	5.675	75.402	85.813	30.161	34.325
	60	26.536	14.301	55.773	76.165	33.464	45.699

Here it is observed that at low concentrations the removal efficiency is high because there are many available adsorption sites on the adsorbent surface to which the metal ions get attached to. As the concentration increases number of adsorption sites continue diminishing due to the high competition for the few remaining sites which are eventually depleted as shown by a decrease in removal efficiency at high concentration for both NSCB and VSCB. The study showed that VSCB had higher removal efficiencies than NSCB. (Results for Ni, Cu and Cr in Appendix H).

4.2.1 Effects of optimization conditions for adsorption of heavy metals

Experimental conditions such as pH, particle size, contact time, adsorbent dose and temperature on adsorption of heavy metals on normal sugarcane bagasse (**NSCB**) from aqueous solution were investigated and the findings are presented as follows.

4.2.2 Effect of particle size of adsorbent(s)

The initial heavy metal concentration (C_o) used for lead, chromium, copper, cadmium and nickel were 5, 2.5, 2, 1.5 and 2.5ppm respectively. The quantity of heavy metal ions (Cu^{2+} and Ni^{2+}) adsorbed from the aqueous solutions generally increased with decreasing particle size of the adsorbent in the order 150>250 ≈ 425 >500>595μm (Figure 2 and Appendix D for Pb^{2+}, Cd^{2+} and Cr^{3+}). Smaller particles adsorbed the heavy metals better than the bigger particles. The smaller particles have a higher surface area-to-volume ratio compared to the larger particles. Which means smaller particles provide more surface area for a given mass of adsorbent, offering more active sites for adsorption, while the larger particles have a lower surface area-to-volume ratio, resulting in fewer available adsorption sites (Sharma *et al*., 2018). In addition, at large particle size, there is a slower adsorption kinetics (Kumar *et al*., 2019). Subsequently, the adsorbent particle size 150 μm was chosen and used in all experiments for both normal sugarcane bagasse and valorised sugarcane bagasse.

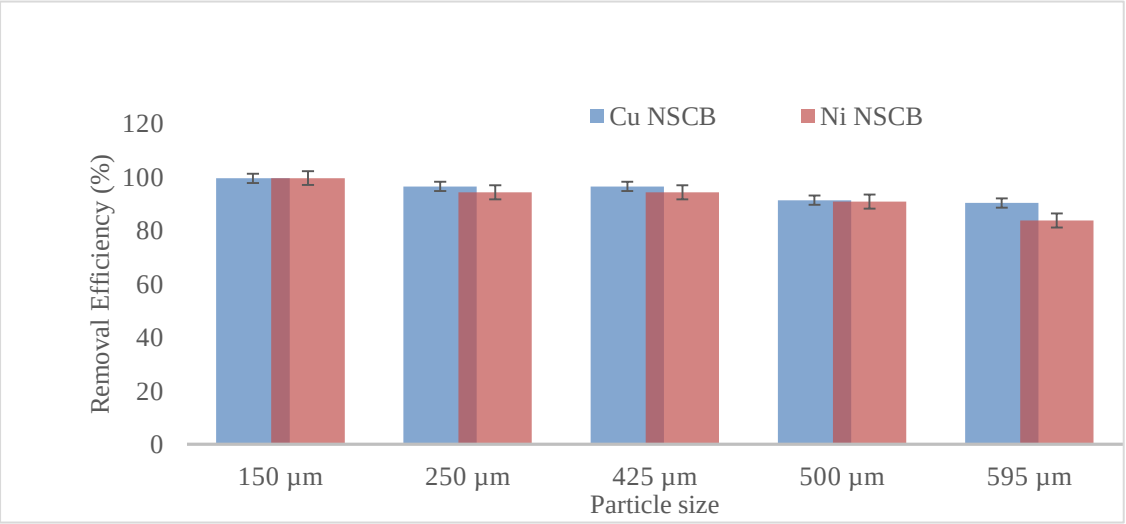

Figure 2: Effect of particle size (pH 5.0, 0.1 g Adsorbent dose, at 20 °C)

4.2.3 Effect of adsorbent dose

To study the best adsorbent dosage, different amounts of adsorbent (0.05 g to 2.0 g) were added to individual heavy metal solutions (Lead, C_o = 5 ppm, Chromium, C_o = 2.5 ppm, Copper, C_o = 2 ppm, Cadmium, C_o = 1.5 ppm, and Nickel, C_o = 3.0 ppm). The results are presented in Figures (3a & 3b) below. The removal efficiencies of NSCB and VSCB (Fig. 2a & 2b) increased with the increase in the adsorbent dosage from 0.05 to 0.70 g for NSCB and from 0.05 to 0.30 g for VSCB. Further increments in adsorbent dosages had no significant effect on metal removal efficiency. This may be attributed to the fact that higher adsorbent dosage provides an increased number of adsorption sites which enhance the overall capacity of the adsorbent (Ezeonuegbu *et al*., 2021), and/or may remain unused during the sequestration reaction (Al-Ghouti *et al*., 2020 & Liu 2015). Overall, it was observed that for both normal sugarcane bagasse and valorised sugarcane bagasse, the optimum adsorbent mass was taken as 0.1 g and was used in subsequent experiments.

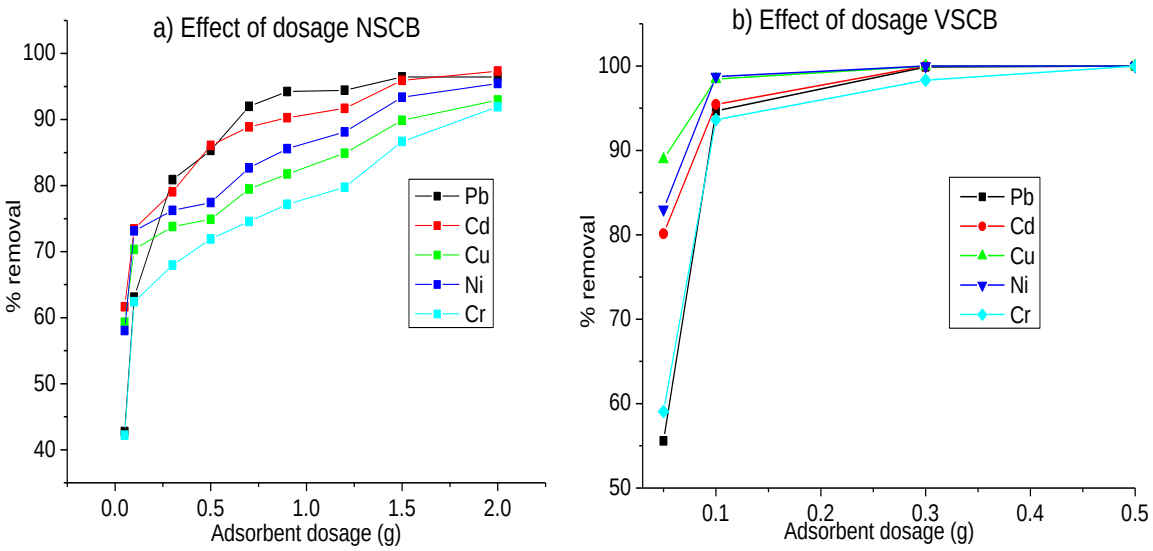

Figure 3:Effect of adsorbent dose on removal of $Pb^{2+,}$ Cd^{2+}, $Cu^{2+,}$ $Ni^{2+,}$ and Cr^{3+} ions (particle size 150 µm, pH 5.0, Adsorption time 60 minutes, at 20 °C)

Earlier studies have shown that adsorbent dosage is a significant parameter that affects the ability of adsorption and the effectiveness of removal. It was observed that the higher the adsorbent dose the higher the removal efficiency and this can be attributed to increased adsorption sites which provides more surface area for contaminants to adhere to, enhancing the overall capacity of the adsorbent (Ezeonuegbu *et al*., 2021).

The removal efficiency of NSCB increased with increase in adsorbent dosage from 0.05 to 0.5 g. This could be due to an increase in the number of active sites available for metal adsorption (Amran *et al*., 2021 and Zhou *et al*., 2018). Further increase in adsorbent dosage had no significant increase in metal removal efficiency. This is ascribed to the fact that higher adsorbent dosage provides more active sites which may remain unused during the sequestration reaction (Al-Ghouti ; Da'ana 2020; Liu 2015). It may also be due to overlapping of adsorption sites as a result of overloading of the adsorption site (Amran *et al*., 2021; Omran *et al*., 2016).

4.2.4 Effect of contact time

The effect of contact time was determined by monitoring the uptake of the Pb(II), Cu(II, Cd(II) , Cr(III) and Ni(II) ions over a period of 60 min at room temperature. A concentration of 10 mg/L of each heavy metal ion solution, at pH 5.0, was used to study how the percentage of its removal was changing for different time intervals.

The results on the effect of contact time on the removal of the heavy metals are shown in Figures 4 (a, & b). The results indicate that with increase in time the removal of the metal ions increased up to a certain point of equilibrium. The removal of the metal ions increased rapidly in the first five minutes and thereafter increased steadily until it reached a point of equilibrium after one hour, where no more metal ions were removed from the solution. This trend was observed for all the metals under investigation. The rapid uptake of Cd(II), Cr(III), Pb(II), Cu(II) and Ni(II) from solution suggests that the binding sites are on surface functional groups, which enhance the interaction between the adsorbent and the metal ions in the solution. During the first thirty minutes of the reaction in the ions-adsorbent adsorption systems, 96.02% of the total amount of Cu (II) and 92.03% Pb(II), 94.57% Ni(II), 96.48% Cd(II), and 99.55% of Cr(III) was immobilised on NSCB, respectively. The state of ion equilibrium was attained after 60 minute in the NSCB structure, and at that time, 96.23% of Cu (II), 96.40% Pb(II), 95.65% Ni(II), 96.79% Cd(II), and 99.55% of Cr(III) were removed by NSCB, respectively. The sequence was the same for the VSCB.

The increased removal efficiencies in both cases, Figures 4 (a, & b), occurred in three stages. In the first stage (0–5 minutes), there was a high concentration gradient between the heavy metal ions in the solution and the adsorbent surface b lting in rapid adsorption. This rapid adsorption was attributed to the availability of many vacant sites, which provided a large surface area for more ions to get adsorbed onto the adsorbent active sites (Musumba *et al*., 2020). In the second stage (5–30 minutes), the adsorption efficiency increased gradually due to the lowering of the available active sites in the surface layers. As a result, the heavy metal ions have to penetrate the underlying layers to reach the empty sites, which in turn increases the mass transfer resistance and lowers the adsorption efficiency (Maddodi *et al*., 2020), and at last stage there was equilibrium and saturation of all adsorption sites after 60 minutes, thus leading to no further adsorption. These results of percentage removal efficiency and time of attainment of equilibrium are, therefore, higher and faster, respectively, than the values reported by other authors (Ezeonuegbu *et al*., 2021).

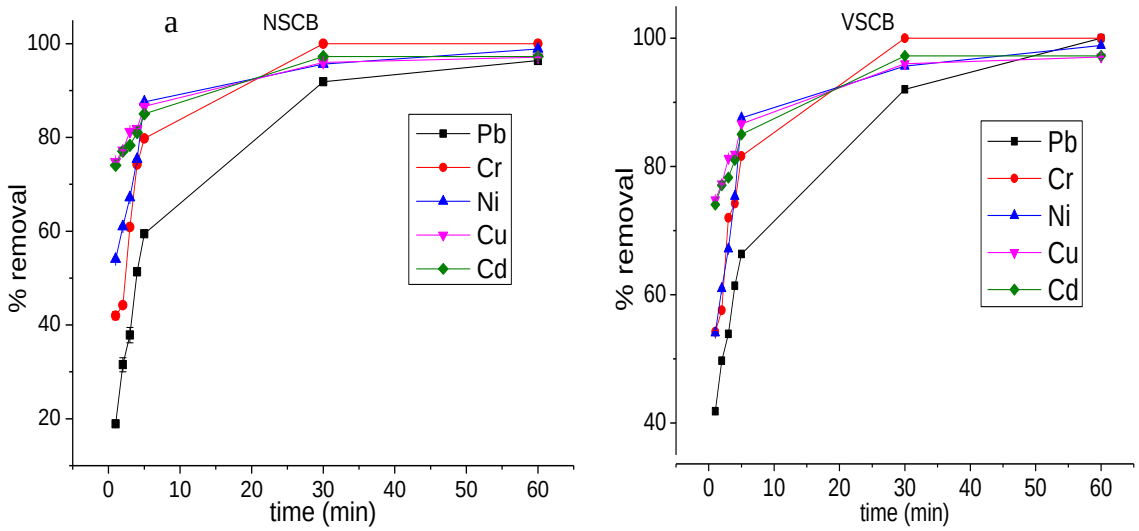

Figure 4: Effect of increasing contact time (Adsorbent dose 0.1 g, particle size 150 µm, temperature 20 °C) for (a) sugarcane bagasse and (b) valorised bagasse

4.2.5 Effect of pH

NSCB contains mainly cellulose (45%), hemi-cellulose (28%) and lignin (18%). This variation in the chemical composition, and consequently, number of functional groups makes NSCB show different efficiencies for removal of heavy-metal ions over a wide range of pH (Soliman *et al.*, 2011). This is quite clear as shown in Figure 5 (and Appendix E) for the uptake of the studied metal ions (Pb^{2+}, Cu^{2+}, Cr^{3+}, Cd^{2+}, Ni^{2+} and which were found to be dependent on pH (2.0–8.0) of the solutions. Hence , the pH of an aqueous solution is a vital factor in the adsorption of metal ions for it determines the surface properties of the adsorbent in terms of i) surface charges, ii) ionization of the functional groups and iii) degree of dissociation of functional groups present on active sites of adsorbents (Ezeonuegbu *et al.*, 2021). It can, therefore, be seen that as the pH was increased, the amount of metal bound also increased, with most of the binding of lead (II), chromium (III), copper (II), nickel (II) and cadmium (II) occurring between pH 4 and 6.

At low pH (pH ≤ 2) the removal efficiencies are low as the metal ions competed with the hydroxonium ions ($H_3O^{+)}$ for the active sites leading to protonation of these sites. This competition decreases as the pH is increased (Musumba *et al.*, 2020). This low adsorption efficiencies suggest that the adsorbed metal ions could be removed/or recovered by lowering the pH. Presumably because protons would displace the adsorbed heavy metal ions at low pH.

The maximum adsorption of Pb (97.43 %); Cr (96.23%) and Cu (96.40%) (Fig. 5), and Cd (96.64%), and Ni (97.26%) (Appendix--) occurred at pH of 6 (Fig. 5). After pH 6 there is a slight decrease in the amount of metal ion removed from the solution, which is attributed to precipitation of metal hydroxide complexes (Musumba *et al*., 2020; Ranaweera *et al*., 2023) by the equation.

$$M^{n+} + 2OH \rightarrow M(OH)_2$$

Subsequent studies were performed at pH 5.0.

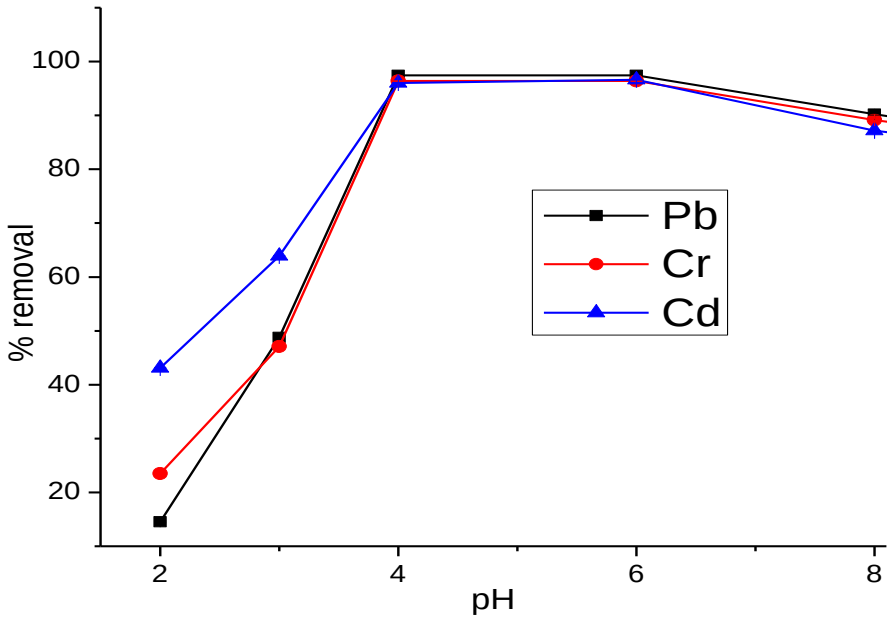

Figure 5: Effect of pH (0.1 g Adsorbent dose, 150 µm particle size, at 20 °C, shaken for 60 minutes at the appropriate pH with each of metal ion, independently)

4.2.6 Effect of metal ion concentration NSCB and VSCB

By increasing the initial concentrations of the metal ions from 2 to 60 mg/L, the removal efficiencies for the all the metals Pb, Cd and Cr (Figure 6), and Cu and Ni (in Appendix F) decreased for **NSCB**. At low concentrations (2 to 6 mg/L) the removal efficiency of Pb (II), Cd(II) and Cr(III) was 100%. The plausible explanation is that at low concentration of Pb (II), Cd(II) and Cr(III) ions there are enough active sites for adsorption, and also, less competition for the adsorption sites (Munene *et al*., 2020). Consequently, the adsorption efficiency was highest at low concentration. The same trend was followed at low concentration of the metal ions for the VSCB (also illustrated in appendix F). Furthermore, it follows that both normal sugarcane bagasse (NSCB) and valorised bagasse (VSCB) could

adsorb Pb(II), Cd(II), Cr(III), Cu(II) and Ni(II) ions from aqueous solutions of low concentration completely.

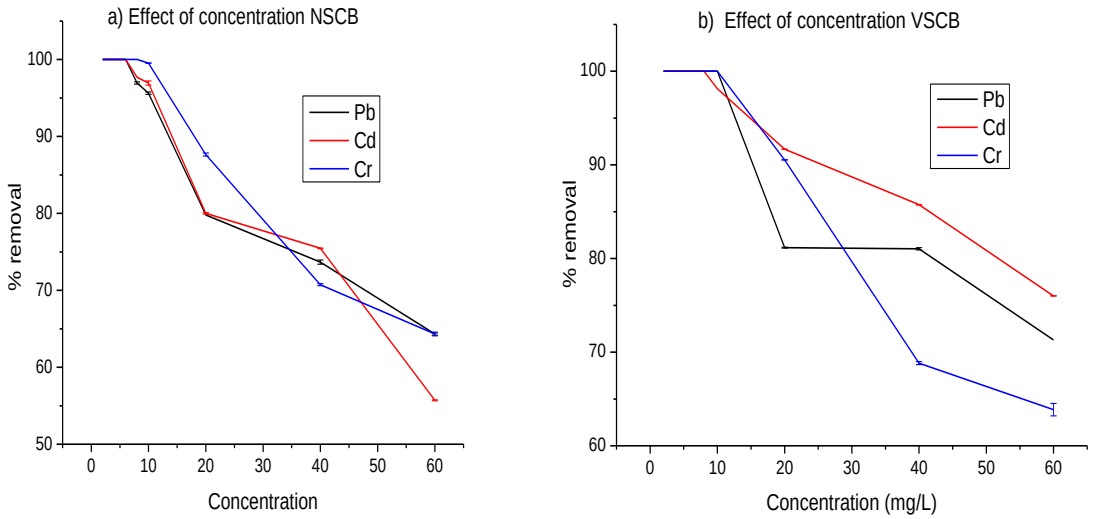

Figure 6: Removal of Cd(II), Pb(II) and Cr(III) from aqueous solution by (a) Normal sugarcane bagasse and (b) valorised bagasse under different initial concentration at 20 °C. (Adsorbent dose 0.1 g, particle size ≤150 µm, time 60 mins, and at pH 5)

Lead (Pb) removal efficiency decreased gradually from 99.48 % to 61.62%, Cd (97.71% to 55.77%), Cr (99.55% to 64.70%), Cu (96.92% to 30.83%) and Ni (96.67% to 74.95%) with increasing metal ions concentration from 8 mg/L to 60 mg/L. As explained by Tao *et al*. (2015) and Arshadi *et al*. (2014), the adsorption rate decreases as the initial concentration of the metal ion pollutants increase, indicating the saturation of the available active sites at higher concentration, beyond this point removal efficiency is diminished as further addition of adsorptive ions would not be expected to increase the amount adsorbed significantly. This behaviour is connected with the competitive diffusion process of the ions through the microchannel and pores, which lock the inlet of channel on the surface and prevent the metal ions to pass deeply inside the adsorbed material, *i.e*. the adsorption occurs on the surface only (Harripersadth *et al*., 2020).

4.2.7 Temperature optimisation

Effect of temperature on the removal of Pb^{2+} and Cd^{2+} in aqueous solution by NSCB and VSCB biomass was studied by varying the temperature between 25 and 60 ºC at the initial concentration of 20 mg/L, 0.1 g adsorbent dosage, pH 5.0 and contact time of 60 minutes.

The data presented in (Figures 7a, & b) shows that adsorption of metal ion by the NSCB adsorbent increased with increase in temperature from 20 °C to 60 °C, which is typical for the bio-sorption of most metal ions from their solution (Chakraborty *et al*., 2022). At 20^{o}C the percentage removal was 79.80%. As the temperature is increased there was gradual increase in percent removal and at 60 °C it was 99.39%. It was found that at higher temperatures the percentage removal was also higher. It was observed that an increase in temperature leads to an increase in removal of the metal ions. Which demonstrated that the adsorption process was facilitated by the higher temperatures (Freitas *et al.*, 2007) indicating that adsorption of the metals studied is an endothermic process.

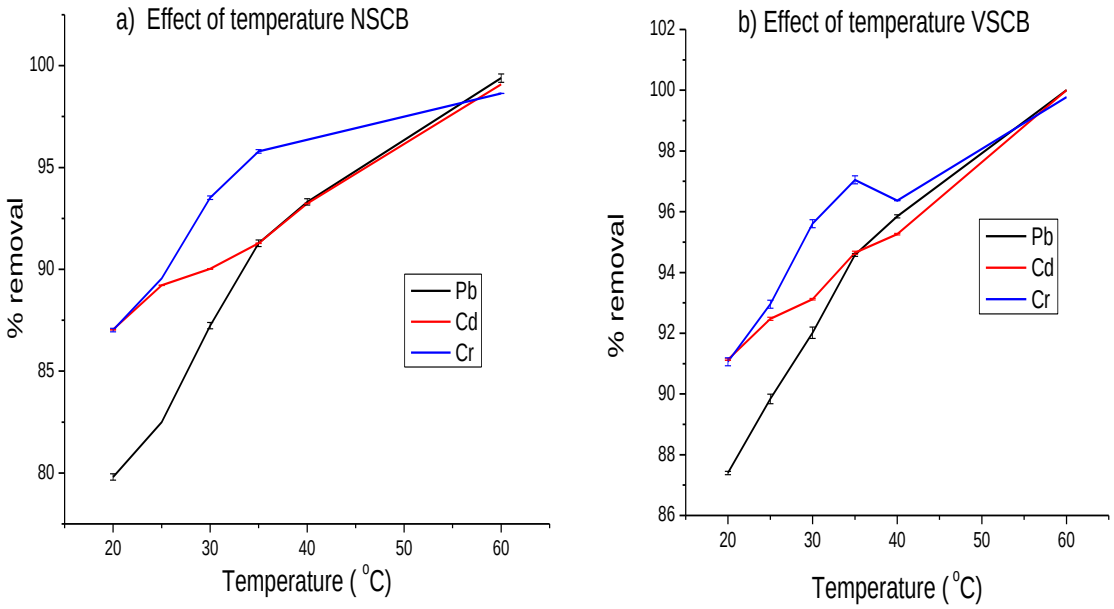

Figure 7: Variation of temperature on adsorption of heavy metals on (a) NSCB and (b) VSCB adsorbents (Adsorbent dose 0.1 g, particle size >150, 250< μm, shaking time 60mins at pH 5)

4.3 Kinetic data modelling

Kinetic data modelling results for lead when fitted in Lagergen pseudo 1st order kinetic model and pseudo 2nd order kinetic model are shown in Figure 8. It is evident from this figure that the pseudo-second-order kinetic model demonstrates higher R^2 value compared to the pseudo-first-order model for lead. The correlation coefficients for pseudo second order kinetics were higher than those of pseudo first order kinetics, suggesting that pseudo second kinetic model has better fit for experimental results.

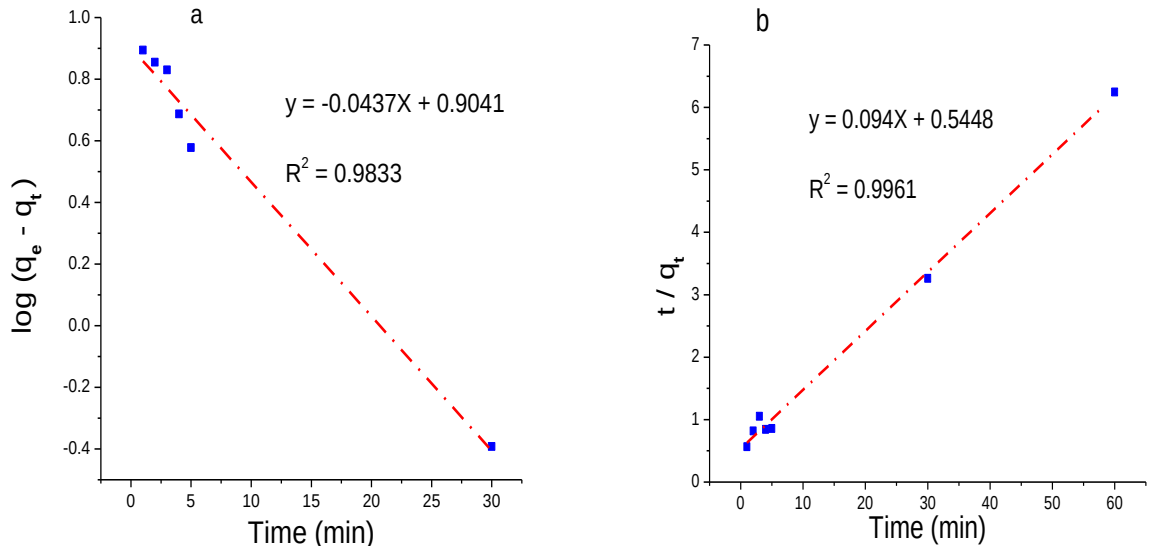

Figure 8: (a) Pseudo-first-order (b) Pseudo-second-order kinetic plots for sorption of lead ions

From kinetic parameters shown in Table 9, it is evident that VSCB generally exhibited higher pseudo-first-order rate constants for Pb^{2+}, Ni^{2+} and Cu^{2+} compared to NSCB, indicating a more rapid initial uptake of these metals. For Pb^{2+}, the K_1 value for VSCB (0.295) was significantly higher than that for SCB (0.101), suggesting that VSCB had a greater affinity or more active sites for Pb^{2+}. However, for Cd^{2+} and Cr^{3+}, SCB showed a higher K_1 value, i.e. Cr^{3+} (0.298 vs. 0.267).

The pseudo-second-order rate constants show that VSCB has higher K_2 values for $Pb^{2+,}$ Cd^{2+} and Ni^{2+} compared to NSCB, indicating a more efficient adsorption. Notably, for $Cd^{2+,}$ the K_2 value for VSCB (0.194) was significantly higher than that for SCB (0.094). However, for $Cr^{3+,}$ SCB had a much higher K_2 value (0.133) compared to VSCB (0.032). These results make VSCB a more effective adsorbent for the metals studied. The enhancement in kinetic parameters for VSCB might be attributed to increased surface area and greater porosity.

On comparing the adsorption capacities of NSCB and VSCB for various metal ions (Pb^{2+}, Cd^{2+}, Ni^{2+}, Cu^{2+}, and Cr^{3+}), using both pseudo-first-order and pseudo-second-order kinetics models, Pb^{2+} adsorption on VSCB shows a slightly higher capacity (8.260 mg/g) compared to NSCB (8.019 mg/g). This indicates a marginal improvement. Cd^{2+} adsorption on NSCB (4.509 mg/g) outperforms VSCB (2.426 mg/g), suggesting that the valorisation negatively affects the adsorption capacity for Cd^{2+}. Ni^{2+} adsorption on VSCB (5.976 mg/g) has a higher capacity than on NSCB (5.394 mg/g), showing improved performance. Cu^{2+} adsorption on VSCB (5.821 mg/g) significantly outperforms that of NSCB (3.047 mg/g), indicating a

substantial improvement. Cr^{3+} adsorption on VSCB (10.342 mg/g) shows a dramatically higher capacity compared to that on NSCB (5.131 mg/g), highlighting the effectiveness of valorisation as better technique for heavy metal waste management.

Table 9: Kinetic parameters for the adsorption of heavy metals by (a) Sugarcane Bagasse and (b) valorized sugarcane bagasse

Sugarcane bagasse	Pseudo-First-order model			Pseudo-Second-order model		
	k_1 (min^{-1})	q_1 (mg/g)	R^2	k_2 (mg g^{-1} min^{-1})	q_2 (mg/g)	R^2
Pb^{2+}	0.101	8.019	0.9833	0.016	10.638	0.9961
Cd^{2+}	0.176	4.509	0.9993	0.094	9.881	0.9998
Ni^{2+}	0.119	5.394	0.9179	0.045	9.960	0.9999
Cu^{2+}	0.107	3.047	0.9762	0.118	9.765	0.9999
Cr^{3+}	0.298	5.131	0.9858	0.133	10.101	0.9999
Valorised bagasse						
Pb^{2+}	0.295	8.260	0.8990	0.061	10.320	0.9994
Cd^{2+}	0.153	2.426	0.9302	0.194	9.911	0.9999
Ni^{2+}	0.187	5.976	0.9464	0.083	10.152	0.9998
Cr^{3+}	0.208	5.821	0.8801	0.120	16.807	0.9999
	0.267	10.342	0.8164	0.032	10.582	0.9984

4.4 Adsorption isotherms

The correlation coefficient for Freundlich was highest followed by Langmuir and lastly Dubinin-Radushchevik for lead and nickel. While Langmuir has a better fit for the experimental results for cadmium copper and chromium. Meaning that each model's performance can vary depending on the specific adsorbate (metal).

Freundlich isotherm, which is more versatile and suitable for heterogeneous surfaces, may show a better fit when adsorbing metals like lead and nickel, possibly due to their ability to form multiple weak interactions with the surface. Langmuir model may fit well for metals like cadmium, copper, and chromium if they form well-defined monolayers on the adsorbent

surface due to their specific chemical interactions or sizes. Results from isotherm studies are shown in Table 10.

Table 10: Isotherms for normal sugarcane bagasse and valorised sugarcane bagasse

	Isotherms		
NSCB	Freundlich R^2	Langmuir R^2	Dubinin-radushchevik R^2
Lead	0.9445	0.9380	0.0663
Nickel	0.9438	0.8834	0.0629
Cadmium	0.9693	0.9922	0.7595
Copper	0.9572	0.9778	0.7002
Chromium	0.9435	0.9512	0.0342
VSCB	Freundlich R^2	Langmuir R^2	Dubinin-radushchevik R^2
Lead	0.9810	0.9496	0.0309
Nickel	0.7982	0.7549	0.6064
Cadmium	0.9850	0.9748	0.7409
Copper	0.9669	0.9459	0.7019
Chromium	0.9279	0.9505	0.0222

Valorised adsorbents often have heterogeneous surfaces with various active sites and functional groups. The Freundlich isotherm, which is suitable for heterogeneous surfaces, may show a strong correlation for metals like lead, cadmium, copper, and nickel due to their ability to interact with multiple surface sites in different ways. It was observed that only chromium fitted well to Langmuir model for the valorised bagasse meaning that chromium to formed a well-defined monolayer on the valorised adsorbent surface. Isotherm parameters obtained from Freudlich and Langmuir isotherms are given in Table 11.

Table 11: Fitting of the parameters of the experimental results to Langmuir and Freundlich

Adsorbent	Adsorbate	Langmuir Isotherm				Freundlich Isotherm			
		q_{max} (mg/g)	K_L (L/mg)	R_L	R^2	K_f	n	1/n	R^2
SCB	Pb^{2+}	44.053	0.234	0.230	0.9392	11.939	2.804	0.357	0.9529
	Cu^{2+}	31.645	0.307	0.197	0.9771	11.665	3.899	0.257	0.9461
	Cd^{2+}	35.845	0.496	0.144	0.9922	13.359	3.362	0.297	0.9693
	Ni^{2+}	56.818	0.184	0.260	0.8228	12.331	2.339	0.428	0.9322
	Cr^{3+}	78.740	0.485	0.146	0.9512	17.624	4.852	0.206	0.9435
VSCB		q_{max} (mg/g)	K_L (L/mg)	R_L	R^2	K_f	n	1/n	R^2
	Pb^{2+}	45.871	0.459	0.152	0.9496	10.515	1.949	0.513	0.9810
	Cu^{2+}	47.393	0.257	0.219	0.9459	12.758	2.663	0.376	0.9669
	Cd^{2+}	51.020	0.490	0.145	0.9748	17.230	2.766	0.362	0.9850
	Ni^{2+}	51.282	0.243	0.226	0.7549	17.976	4.272	0.234	0.7980
	Cr^{3+}	38.022	0.595	0.126	0.9505	11.579	2.640	0.379	0.9279

The numbers of metal ions adsorbed on adsorbent surface by NSCB and VSCB are shown in Table 12.

Table 12: Number of molecules adsorbed

Metal ion	No. of molecules NSCB	No. of molecules VSCB
Pb^{2+}	1.27×10^{20}	1.33×10^{21}
Cu^{2+}	2.98×10^{21}	4.51×10^{20}
Cd^{2+}	1.92×10^{20}	2.74×10^{20}
Ni^{2+}	5.83×10^{20}	5.26×10^{20}
Cr^{3+}	9.12×10^{20}	4.40×10^{20}

4.5 Thermodynamic parameters

The Van't Hoff's plots and the Gibb's free energy equations were used to calculate the thermodynamic properties for NSCB and VSCB. The thermodynamic parameters for NSCB and VSCB obtained are shown in Table 13. The enthalpy change values (ΔH^o, NSCB) are as follows: Cr (49.451 kJ/mole), Ni (61.007 kJ/mole), Cd (57.867 kJ/mole), Pb (76.562 kJ/mole) and Cu (40.706 kJ/mole). The entropy (ΔS^o, NSCB) are as follows Cr (184.912 J/mole), Ni (218.209 J/mole), Cd (210.153 J/mole), Pb (269.681 J/mole) and Cu (149.269 J/mole). The Gibbs free energy (ΔG^o, NSCB) are as follows Cr (-5.652 kJ/mole), Ni (-4.019 kJ/mole), Cd (-4.758 kJ/mole), Pb (-3.802 kJ/mole) and Cu (-3.776 kJ/mole).

The enthalpy (ΔH^o, VSCB) values were respectively: Cr (74.840 kJ/mole), Ni (48.118 kJ/mole), Cd (96.359 kJ/mole), Pb (46.947 kJ/mole), and Cu (28.340 kJ/mole). These positive ΔH^o values indicate that the adsorption process was endothermic in nature. The entropy (ΔS^o, VSCB) values were also determined: Cr (272.284 J/mole), Ni (178.950 J/mole), Cd (344.241 J/mole), Pb (175.907 J/mole), and Cu (111.698 J/mole). The positive ΔS^o values suggest an increase in randomness at the solid-liquid interface during the adsorption process. This observation aligns with findings from other researchers such as Tegene (2013) who also reported positive ΔS^o values in adsorption studies. Additionally, the Gibbs free energy (ΔG^o, VSCB) values were: Cr (-6.3 kJ/mole), Ni (-5.209 kJ/mole), Cd (-6.225 kJ/mole), Pb (-5.473 kJ/mole), and Cu (-4.946 kJ/mole). These negative ΔG^o values indicate that the adsorption process was spontaneous.

Table 13: Thermodynamic parameters

	NSCB			**VSCB**		
	$\Delta G^{\#}$ kJmol^{-1}K^{-1}	$\Delta H^{\#}$ kJmol^{-1}	$\Delta S^{\#}$ Jmol^{-1}K^{-1}	$\Delta G^{\#}$ kJmol^{-1}K^{-1}	$\Delta H^{\#}$ kJmol^{-1}	$\Delta S^{\#}$ Jmol^{-1}K^{-1}
Cr^{2+}	-5.652	49.451	184.912	-6.300	74.840	272.284
Pb^{2+}	-3.802	76.562	269.681	-5.515	46.947	176.049
Ni^{2+}	-4.019	61.007	218.209	-5.210	48.117	178.950
Cd^{2+}	-4.758	57.867	210.153	-6.322	96.359	344.233
Cu^{2+}	-3.776	40.706	149.269	-4.946	28.340	111.698

In doing comparison, both NSCB and VSCB demonstrate endothermic and spontaneous adsorption processes with positive entropy changes, indicating increased randomness at the solid-liquid interface. However, VSCB generally shows higher enthalpy and entropy values, suggesting a stronger heat absorption requirement and greater randomness increase during the adsorption of certain metals. The more negative Gibbs free energy values for VSCB imply a more favourable and spontaneous adsorption process compared to NSCB.

In summary, both NSCB and VSCB are effective adsorbents for the removal of heavy metals from aqueous solutions, demonstrating endothermic and spontaneous adsorption processes with increased randomness at the solid-liquid interface. VSCB, however, tends to show slightly higher values of enthalpy and entropy changes, as well as more negative Gibbs free energy values, suggesting potentially more robust adsorption characteristics under the studied conditions.

4.6 Efficacy of the optimal conditions for removal of the heavy metals from industrial waters collected within Nakuru City

When the optimal conditions were applied to the water samples heavy metal analysis showed that the adsorbents were able to adsorb the metal ions analysed as shown in table 14.

Table 14: Efficacy of optimal conditions for removal of heavy metals from water samples

	Adsorbed metal ions (%)				
Wastewater	Cd	Cu	Cr	Ni	Pb
SCB Jua kali garage waste	50.00	92.59	87.95	79.10	94.78
Tannery	50.00	ND	47.20	ND	95.00
Portable water refilling plant	50.00	ND	ND	30	60.00
VSCB Jua kali garage waste	90.00	97.53	93.97	85.075	94.78
Tannery	50.00	ND	27.77	35.00	95.00
Portable water	50.00	ND	ND	68.75	40.00

refilling

plant

For garage waste, SCB demonstrated removal efficiency of 50% for Cd, 92.59% for Cu, 87.95% for Cr, 79.10% for Ni, and 94.78% for Pb. VSCB, however, showed an even higher removal efficiency, particularly for Cd (90.00%) and Cr (93.97%), indicating its superior adsorption capacity. The efficiency for Cu, Ni, and Pb was also slightly higher with VSCB, confirming its enhanced performance across most metals.

In the case of tannery waste, SCB showed a moderate removal efficiency with 50% for Cd, 47.20% for Cr, and 95.00% for Pb, but data for Cu and Ni were not detected (ND). VSCB maintained the same efficiency for Cd (50%) and Pb (95.00%), but showed a significantly lower removal rate for Cr (27.77%) and Ni (35.00%).

For portable water, SCB had a 50% removal rate for Cd, while the other metals showed were not detected either no data or low efficiency, with Ni at 30% and Pb at 60.00%. VSCB showed identical removal for Cd (50%) but improved significantly for Ni (68.75%). However, the removal efficiency for Pb decreased to 40.00% with VSCB. Levels of Cu and Cr were below detectable limits using NSCB and VSCB suggested that these metals were completely adsorbed. Generally VSCB outperformed SCB in removing heavy metals from garage waste, particularly for Cd, Cu, and Cr.

The lower removal percentages observed in certain instances can be attributed to the presence of competing ions in the wastewater, such as potassium (K), sodium (Na), magnesium (Mg), and calcium (Ca). These ions can interfere with the adsorption process by occupying active sites on the adsorbent materials, thereby reducing the availability of these sites for heavy metal ions. This competition is likely more pronounced in complex wastewater matrices, such as those from industrial sources, where a high concentration of various ions is typical *ie*. $K^{+}$and Ca^{2+} as well as chelating agents.

CHAPTER FIVE

CONCLUSIONS AND RECOMMENDATIONS

5.1 Conclusions

The work presented in this thesis sought to study heavy metals removal from Nakuru city industrial wastewaters using sugarcane bagasse and valorised bagasse as potential adsorbents in the removal of heavy metals (Pb, Cd, Cu, Ni and Cr).

i. From the results the lead levels were high except for three samples (sample 2, 3 and 6). Copper levels were within the permitted limits. Cadmium levels were high in samples 3,9,10 and 11. Nickel was high in samples 1, 7, 8, 10, 11 but was within permissible levels in sample 3 and was not detected in the rest of the samples. Chromium was high in four samples (1, 9, 10 and 11) while the rest were within permissible levels set by the Kenya bureau of standards (KEBs) for discharge into the environment at the time of this study.

ii. It was found that the best adsorbent mass used was 0.1 g and pH of 5. Particle size used was between 150 to 250 µm based on removal efficiency of Cd, Pb, Ni, Cr, Cu. Optimum contact time was 60minutes. Temperature used was 20 °C. For the adsorption isotherm models, for NSCB Pb^{2+} and Ni^{2+} showed better fitting for Freundlich isotherm while Cd^{2+}, Cu^{2+} and Cr^{3+} showed better fit for Langmuir isotherm model. For VSCB Pb^{2+}, Ni^{2+}, Cd^{2+}, Cu^{2+} had better fit for Freundlich isotherm while Cr^{3+} had better fit for Langmuir isotherm model. Characterization of NSCB and VSCB using Fourier transform infrared spectroscopy (FTIR) showed presence of the functional groups –OH, -C=O and C=C functional groups which played a key role in adsorption process.

iii. Thermodynamic properties are as follows: ΔH ranges from 28.340-74.840 $kJmol^{-1}$, ΔS ranges from 111.698-344.233 $Jmol^{-1}K^{-1}$ and ΔG ranges from -3.776 to -6.322 $kJmol^{-1}K^{-1}$ indicating spontaneous process. The negative values of ΔG^{o} indicating spontaneous adsorption. Kinetic properties of adsorption of the heavy metals on NSCB and VSCB showed that removal of Pb^{2+} , Cu^{2+}, Cd^{2+}, Ni^{2+} and Cr^{3+} followed pseudo second order rate equations as evidenced by R^2 values for both NSCB and VSCB.

iv. On studying the efficacy under the optimal conditions for removal of the heavy metals from real industrial waters collected within Nakuru City, it is demonstrated that the adsorbents were efficient in removal of heavy metals.

NSCB and VSCB demonstrated removal efficiencies ranging from 35-100% for heavy metal removal from wastewaters, with VSCB having higher removal rates than NSCB.

Overall this study has contributed in understanding of the optimum conditions, adsorption isotherms, thermodynamic and kinetics parameters when using sugarcane bagasse and valorised bagasse for removal of heavy metals from industrial wastewaters within Nakuru city. The sugarcane bagasse and valorised bagasse can therefore be used as efficient low-cost adsorbent materials.

5.2 Recommendations

The following recommendations were made:

i. To establish a systematic monitoring program to routinely measure the concentrations of heavy metals (Cd, Pb, Cr, Cu, Ni) in Nakuru industrial wastewaters and surface waters. This will provide baseline data and help in identifying trends and hotspots of contamination.

ii. It is recommended to further explore the scalability of these optimized conditions of NSCB in larger volume of industrial waste water and the effects on adsorption efficiency, adsorption isotherms, kinetics, and thermodynamic properties. This approach will ensure that the promising results obtained in controlled experiments translate effectively into practical solutions for heavy metal removal in large volume industrial wastewater.

iii. Valorised sugarcane bagasse (VSCB) has shown potential for enhanced adsorption. It is recommended to continue research on different modification techniques and their effects on adsorption efficiency, adsorption isotherms, kinetics, and thermodynamic properties.

iv. Based on laboratory findings on heavy metal removal from industrial waters collected within Nakuru City, it is recommended to design a pilot-scale treatment system and conduct pilot studies that can simulate real industrial operating conditions.

REFERENCES

Abate, G. Y., Alene, A. N., Habte, A. T., & Getahun, D. M. (2020). Adsorptive removal of malachite green dye from aqueous solution onto activated carbon of Catha edulis stem as a low-cost bio-adsorbent. *Environmental Systems Research, 9*(1), 1-13. https://doi.org/10.1186/s40068-020-00191-4

Abegunde, S. M., Idowu, K. S., Adejuwon, O. M., & Adeyemi-Adejolu, T. (2020). A review on the influence of chemical modification on the performance of adsorbents. *Resources, Environment and Sustainability*, *1*, 100001. https://doi.org/10.1016/j.resenv.2020.100001

Abdullah, N. H., Shameli, K., Abdullah, E. C., & Abdullah, L. C. (2019). Solid matrices for fabrication of magnetic iron oxide nanocomposites: synthesis, properties, and application for the adsorption of heavy metal ions and dyes. *Composites Part B: Engineering*, *162*, 538-568. https://doi.org/10.1016/j.compositesb.2018.12.075

Abdulrazak, S., Hussaini, K., & Sani, H. M. (2017). Evaluation of removal efficiency of heavy metals by low-cost activated carbon prepared from African palm fruit. *Applied Water Science, 7*(6), 3151-3155. https://doi.org/10.1007/s13201-016-0460-x

Adegoke, K. A., & Bello, O. S. (2015). Dye sequestration using agricultural wastes as adsorbents. *Water Resources and Industry, 12*, 8-24. https://doi.org/10.1016/j.wri.2015.09.002

Adeyemo, A. A., Adeoye, I. O., & Bello, O. S. (2012). Metal organic frameworks as adsorbents for dye adsorption: overview, prospects and future challenges. *Toxicological & Environmental Chemistry, 94*(10), 1846-1863. https://doi.org/10.1080/02772248.2012.744023

Agboola, O., Nwankwo, O. J., Akinyemi, F. A., Chukwuka, J. C., Ayeni, A. O., Popoola, P., & Sadiku, R. (2024). Adsorptive removal of Fe and Cd from the textile wastewater using ternary bio-adsorbent: adsorption, desorption, adsorption isotherms and kinetic studies. *Discover Sustainability, 5*(1), 312. https://doi.org/10.1007/s43621-024-00523-9

Ahamad, M. I., Yao, Z., Ren, L., Zhang, C., Li, T., Lu, H., ... & Feng, W. (2024). Impact of heavy metals on aquatic life and human health: a case study of River Ravi Pakistan. *Frontiers in Marine Science, 11*, 1374835. https://doi.org/10.3389/fmars.2024.1374835

Ahmed, H., Sobhy, N. A., Hefny, M. M., Abdel-Haleem, F. M., & El-Khateeb, M. A. (2023). Evaluation of Agrowaste Species for Removal of Heavy Metals from Synthetic Wastewater. *Journal of Environmental and Public Health, 2023*. https://doi.org/10.1155/2023/7419015

Al-Ghouti, M. A., & Da'ana, D. A. (2020). Guidelines for the use and interpretation of adsorption isotherm models: A review. *Journal of Hazardous Materials, 393,* 122383. https://doi.org/10.1016/j.jhazmat.2020.122383.

Al-Johani, H., & Salam, M. A. (2011). Kinetics and thermodynamic study of aniline adsorption by multi-walled carbon nanotubes from aqueous solution. *Journal of Colloid and Interface Science, 360*(2), 760-767. https://doi.org/10.1016/j.jcis.2011.04.097

Al-Harby, N. F., Albahly, E. F., & Mohamed, N. A. (2021). Kinetics, isotherm and thermodynamic studies for efficient adsorption of Congo Red dye from aqueous solution onto novel cyanoguanidine-modified chitosan adsorbent. *Polymers, 13*(24), 4446. https://doi.org/10.3390/polym13244446

Alkhaldi, H., Alharthi, S., Alharthi, S., AlGhamdi, H. A., AlZahrani, Y. M., Mahmoud, S. A., ... & Abaza, S. F. (2024). Sustainable polymeric adsorbents for adsorption-based water remediation and pathogen deactivation: a review. *RSC advances, 14*(45), 33143-33190. DOI: 10.1039/D4RA05269B

Aloo, P. A., Oyugi, D. O., Morara, G. N., & Owuor, M. A. (2013). Recent changes in fish communities of the equatorial Lake Naivasha, Kenya. *African Journal of Agricultural and Rural Development 13*(2), 058-066.

Amran, F., & Zaini, M. A. A. (2021). Valorization of Casuarina empty fruit-based activated carbons for dyes removal–activators, isotherm, kinetics and thermodynamics. *Surfaces and Interfaces, 25*, 101277. https://doi.org/10.1016/j.surfin.2021.101277

Anastopoulos, I., Bhatnagar, A., Bikiaris, D. N., & Kyzas, G. Z. (2017). Chitin adsorbents for toxic metals: a review. *International Journal of Molecular Sciences, 18*(1), 114. https://doi.org/10.3390/ijms18010114

Ankrah, A. F., Tokay, B., & Snape, C. E. (2022). Heavy metal removal from aqueous solutions using fly-ash derived zeolite NaP1. *International Journal of Environmental Research, 16*(2), 17. https://doi.org/10.1007/s41742-022-00395-9

Angon, P. B., Islam, M. S., Das, A., Anjum, N., Poudel, A., & Suchi, S. A. (2024). Sources, effects and present perspectives of heavy metals contamination: Soil, plants and human food chain. *Heliyon*, *10*(7).

Argun, M. E., Dursun, S., Ozdemir, C., and Karatas, M. (2007). Heavy metal adsorption by modified oak sawdust: Thermodynamics and kinetics. *Journal of Hazardous Materials*, *141*(1), 77-85. https://doi.org/10.1016/j.jhazmat.2006.06.095

Arora, N. K., & Mishra, I. (2022). Sustainable development goal 6: global water security. *Environmental Sustainability*, *5*(3), 271-275. https://doi.org/10.1007/s42398-022-00246-5

Arshadi, M., Amiri, M., & Mousavi, S. (2014). Kinetic, equilibrium and thermodynamic investigations of Ni (II), Cd (II), Cu (II) and Co (II) adsorption on barley straw ash. *Water Resources and Industry*, *6*, 1-17. https://doi.org/10.1016/j.wri.2014.06.001

Babatunde, K. A., Negash, B. M., Jufar, S. R., Ahmed, T. Y., & Mojid, M. R. (2022). Adsorption of gases on heterogeneous shale surfaces: A review. *Journal of Petroleum Science and Engineering*, *208*, 109466. https://doi.org/10.1016/j.petrol.2021.109466

Bakırcıoğlu, Y., Akman, S., Bıçak, N., & Şenkal, F. (2003). Determination of some trace heavy metals in some water samples by FAAS after their preconcentration using DETA. *Journal of Trace and Microprobe Techniques*, *21*(2), 239-248. https://doi.org/10.1081/TMA-120020259

Balali-Mood, M., Naseri, K., Tahergorabi, Z., Khazdair, M. R., and Sadeghi, M. (2021). Toxic mechanisms of five heavy metals: mercury, lead, chromium, cadmium, and arsenic. *Frontiers in Pharmacology*, *12*, 643972. https://doi.org/10.3389/fphar.2021.643972

Barakat, M. (2011). New trends in removing heavy metals from industrial wastewater. *Arabian Journal of Chemistry*, *4*(4), 361-377. https://doi.org/10.1016/j.arabjc.2010.07.019

Beyan, S. M., Prabhu, S. V., Ambio, T. A., & Gomadurai, C. (2022). A statistical modeling and optimization for Cr (VI) adsorption from aqueous media via teff straw-based activated carbon: isotherm, kinetics, and thermodynamic studies. *Adsorption Science & Technology, 2022*. https://doi.org/10.1155/2022/7998069

Bhatnagar, A., & Sillanpää, M. (2010). Utilization of agro-industrial and municipal waste materials as potential adsorbents for water treatment—a review. *Chemical Engineering Journal*, *157*(2-3), 277-296. https://doi.org/10.1016/j.cej.2010.01.007

Bullerjahn, J. T., & Hanson, S. M. (2024). Extracting thermodynamic properties from van't Hoff plots with emphasis on temperature-sensing ion channels. *Temperature*, *11*(1), 60-71. https://doi.org/10.1080/23328940.2023.2265962

Buxton, S., Garman, E., Heim, K. E., Lyons-Darden, T., Schlekat, C. E., Taylor, M. D., & Oller, A. R. (2019). Concise review of nickel human health toxicology and ecotoxicology. *Inorganics*, *7*(7), 89. https://doi.org/10.3390/inorganics7070089

Canton, H. (2021). United nations environment programme—unep. In *The Europa directory of international organizations 2021* (pp. 188-214). Routledge.

Chakraborty, R., Asthana, A., Singh, A. K., Jain, B., & Susan, A. B. H. (2022). Adsorption of heavy metal ions by various low-cost adsorbents: a review. *International Journal of Environmental Analytical Chemistry*, *102*(2), 342-379. https://doi.org/10.1080/03067319.2020.1722811

Chan, A. A., Buthiyappan, A., Raman, A. A. A., & Ibrahim, S. (2022). Recent advances on the coconut shell derived carbonaceous material for the removal of recalcitrant pollutants: a review. *Korean Journal of Chemical Engineering*, *39*(10), 2571-2593. https://doi.org/10.1007/s11814-022-1201-5

Chang, K. L., Hsieh, J. F., Ou, B. M., Chang, M. H., Hseih, W. Y., Lin, J. H., ... & Chen, S. T. (2012). Adsorption studies on the removal of an endocrine-disrupting compound (Bisphenol A) using activated carbon from rice straw agricultural waste. *Separation Science and Technology*, *47*(10), 1514-1521. https://doi.org/10.1080/01496395.2011.647212

Chen, X. (2015). Modeling of experimental adsorption isotherm data. *Information*, *6*(1), 14-22. https://doi.org/10.3390/info6010014

Chen, W., Yang, Y., Fu, K., Zhang, D., & Wang, Z. (2022). Progress in ICP-MS analysis of minerals and heavy metals in traditional medicine. *Frontiers in pharmacology*, *13*, 891273. https://doi.org/10.3389/fphar.2022.891273

Chien, S. W. C., Chen, S. H., & Li, C. J. (2018). Effect of soil pH and organic matter on the adsorption and desorption of pentachlorophenol. *Environmental Science and Pollution Research*, *25*(6), 5269-5279. https://doi.org/10.1007/s11356-017-9822-7

Chowdhury, S., Mishra, R., Saha, P., & Kushwaha, P. (2011). Adsorption thermodynamics, kinetics and isosteric heat of adsorption of malachite green onto

chemically modified rice husk. *Desalination, 265*(1), 159-168. https://doi.org/10.1016/j.desal.2010.07.047

Coetzee, J. J., Bansal, N., & Chirwa, E. (2020). Chromium in environment, its toxic effect from chromite-mining and ferrochrome industries, and its possible bioremediation. *Exposure and Health, 12*(1), 51-62. https://doi.org/10.1007/s12403-018-0284-z

Connor, R., Renata, A., Ortigara, C., Koncagül, E., Uhlenbrook, S., Lamizana-Diallo, B. M., Zadeh, S. M., Qadir, M., Kjellén, M., & Sjödin, J. (2017). The United Nations World Water Development Report 2017. Wastewater: The Untapped Resource. *The United Nations World Water Development Report*. https://wedocs.unep.org/20.500.11822/20448

Cutillas-Barreiro, L., Ansias-Manso, L., Fernández-Calviño, D., Arias-Estévez, M., Nóvoa-Muñoz, J. C., Fernández-Sanjurjo, M. J., ... & Núñez-Delgado, A. (2014). Pine bark as bio-adsorbent for Cd, Cu, Ni, Pb and Zn: Batch-type and stirred flow chamber experiments. *Journal of Environmental Management*, *144*, 258-264. https://doi.org/10.1016/j.jenvman.2014.06.008

Das, S., Sultana, K. W., Ndhlala, A. R., Mondal, M., & Chandra, I. (2023). Heavy metal pollution in the environment and its impact on health: exploring green technology for remediation. *Environmental health insights*, *17*, 11786302231201259. https://doi.org/10.1177/11786302231201259

Dawodu, F. A., Akpan, B. M., & Akpomie, K. G. (2020). Sequestered capture and desorption of hexavalent chromium from solution and textile wastewater onto low cost Heinsia crinita seed coat biomass. *Applied Water Science*, *10*(1), 1-15. https://doi.org/10.1007/s13201-019-1114-6

Demiral, H., & Gündüzoğlu, G. (2010). Removal of nitrate from aqueous solutions by activated carbon prepared from sugar beet bagasse. *Bioresource Technology, 101*(6), 1675-1680. https://doi.org/10.1016/j.biortech.2009.09.087

Deng, H., Yang, L., Tao, G., & Dai, J. (2009). Preparation and characterization of activated carbon from cotton stalk by microwave assisted chemical activation—application in methylene blue adsorption from aqueous solution. *Journal of Hazardous Materials, 166*(2), 1514-1521. https://doi.org/10.1016/j.jhazmat.2008.12.080

Deng, Y., Wang, M., Tian, T., Lin, S., Xu, P., Zhou, L., ... & Dai, Z. (2019). The effect of hexavalent chromium on the incidence and mortality of human cancers: a meta-

analysis based on published epidemiological cohort studies. *Frontiers in oncology*, *9*, 24.

De Rose, E., Bartucci, S., Bonaventura, C. P., Conte, G., Agostino, R. G., & Policicchio, A. (2023). Effects of activation temperature and time on porosity features of activated carbons derived from lemon peel and preliminary hydrogen adsorption tests. *Colloids and Surfaces A: Physicochemical and Engineering Aspects*, *672*, 131727. https://doi.org/10.1016/j.colsurfa.2023.131727

Dzyadevych, S., & Jaffrezic-Renault, N. (2014). Conductometric biosensors. *Biological Identification: DNA Amplification and Sequencing, Optical Sensing, Lab-On-Chip and Portable Systems*, 153. https://doi.org/10.1533/9780857099167.2.153

Eletta, O. A., Adeniyi, A. G., Ighalo, J. O., Onifade, D. V., & Ayandele, F. O. (2020). Valorisation of Cocoa (Theobroma cacao) pod husk as precursors for the production of adsorbents for water treatment. *Environmental Technology Reviews*, *9*(1), 20-36. https://doi.org/10.1080/21622515.2020.1730983

Emiliani, J., Oyarce, W. G. L., Salvatierra, L. M., Novo, L. A., & Pérez, L. M. (2021). Evaluation of cadmium bioaccumulation-related physiological effects in salvinia biloba: An insight towards its use as pollutant bioindicator in water reservoirs. *Plants*, *10*(12), 2679. https://doi.org/10.3390/plants10122679

Erdoğan, S., Önal, Y., Akmil-Başar, C., Bilmez-Erdemoğlu, S., Sarıcı-Özdemir, Ç., Köseoğlu, E., & Icduygu, G. (2005). Optimization of nickel adsorption from aqueous solution by using activated carbon prepared from waste apricot by chemical activation. *Applied Surface Science*, *252*(5), 1324-1331. https://doi.org/10.1016/j.apsusc.2005.02.089

Esilaba, F., Moturi, W. N., Mokua, M., & Mwanyika, T. (2020). Human health risk assessment of trace metals in the commonly consumed fish species in Nakuru Town, Kenya. *Environmental health insights*, *14*, 1178630220917128. doi: 10.1177/1178630220917128

Ezeonuegbu, B. A., Machido, D. A., Whong, C. M., Japhet, W. S., Alexiou, A., Elazab, S. T., ... & Batiha, G. E. S. (2021). Agricultural waste of sugarcane bagasse as efficient adsorbent for lead and nickel removal from untreated wastewater: Biosorption, equilibrium isotherms, kinetics and desorption studies. *Biotechnology Reports*, *30*, e00614. https://doi.org/10.1016/j.btre.2021.e00614

Ezzati, R., Ezzati, S., & Azizi, M. (2024). Exact solution of the Langmuir rate equation: New Insights into pseudo-first-order and pseudo-second-order kinetics models for adsorption. *Vacuum*, *220*, 112790. https://dx.doi.org/10.2139/ssrn.4589000

Freitas, A. F., Mendes, M. F., & Coelho, G. L. V. (2007). Thermodynamic study of fatty acids adsorption on different adsorbents. *The Journal of Chemical Thermodynamics*, *39*(7), 1027-1037. https://doi.org/10.1016/j.jct.2006.12.016

Fu, F., & Wang, Q. (2011). Removal of heavy metal ions from wastewaters: a review. *Journal of environmental management*, *92*(3), 407-418. https://doi.org/10.1016/j.jenvman.2010.11.011

García-Muñoz, J., Fernández Casado, D., Portillo-Moreno, Á., Míguez-Santiyán, M. D. P., Soler Rodríguez, F., López-Beceiro, A., ... & Pérez-López, M. (2025). First study of heavy metals analysis in hair and oxidative status of European Otters (Lutra lutra) from Southwestern Europe. *Ecotoxicology*, 1-17. https://doi.org/10.1007/s10646-025-02911-x

Gao, X., Guo, C., Hao, J., Zhao, Z., Long, H., & Li, M. (2020). Adsorption of heavy metal ions by sodium alginate based adsorbent-a review and new perspectives. *International Journal of Biological Macromolecules*, *164*, 4423-4434. https://doi.org/10.1016/j.ijbiomac.2020.09.046

Genchi, G., Carocci, A., Lauria, G., Sinicropi, M. S., & Catalano, A. (2020). Nickel: Human health and environmental toxicology. *International Journal of Environmental Research and Public Health, 17*(3), 679. https://doi.org/10.3390/ijerph17030679

Gezahegn, A. M., Feyessa, F. F., Tekeste, E. A., & Beyene, E. M. (2021). Chromium laden soil, water, and vegetables nearby tanning industries: speciation and spatial distribution. *Journal of Chemistry*, *2021*(1), 5531349. https://doi.org/10.1155/2021/5531349

Ghosh, N., Sen, S., Biswas, G., Saxena, A., & Haldar, P. K. (2023). Adsorption and desorption study of reusable magnetic iron oxide nanoparticles modified with Justicia adhatoda leaf extract for the removal of textile dye and antibiotic. *Water, Air, & Soil Pollution*, *234*(3), 202. https://doi.org/10.1007/s00267-022-01716-6

Giacomin, H., Unno, M., Eichbauer, K., & Atkins, C. (2019). Automotive wastes. *Water Environment Research*, *91*(10), 1223-1228. https://doi.org/10.1002/wer.1217

Githaiga, K. B., Njuguna, S. M., Gituru, R. W., & Yan, X. (2021). Water quality assessment, multivariate analysis and human health risks of heavy metals in eight

major lakes in Kenya. *Journal of Environmental Management*, *297*, 113410. https://doi.org/10.1016/j.jenvman.2021.113410

Gkika, D. A., Tolkou, A. K., Katsoyiannis, I. A., & Kyzas, G. Z. (2025). The adsorption-desorption-regeneration pathway to a circular economy: the role of waste-derived adsorbents on chromium removal. *Separation and Purification Technology*, 132996. https://doi.org/10.1016/j.seppur.2025.132996

Gull, A., Dar, A. A.,& Sharma, M. (2018). Effects of heavy metals on the health of pregnant women and fetus: a review. *International Journal of Theoretical & Applied Sciences, 10*(1), 01-09. ISSN No. (Online): 2249-3247

Gupta, V. K., Jain, C. K., Ali, I., Sharma, M., & Saini, V. K. (2003). Removal of cadmium & nickel from wastewater using bagasse fly ash—a sugar industry waste. *Water research*, *37*(16), 4038-4044. https://doi.org/10.1016/S0043-1354 (03)00292-6

Gusmão, K. A. G., Gurgel, L. V. A., Melo, T. M. S., & Gil, L. F. (2012). Application of succinylated sugarcane bagasse as adsorbent to remove methylene blue and gentian violet from aqueous solutions–kinetic and equilibrium studies. *Dyes and Pigments*, *92*(3), 967-974. https://doi.org/10.1016/j.dyepig.2011.09.005

Heidarinejad, Z., Dehghani, M. H., Heidari, M., Javedan, G., Ali, I., & Sillanpää, M. (2020). Methods for preparation and activation of activated carbon: a review. *Environmental Chemistry Letters*, *18*, 393-415. https://doi.org/10.1007/s10311-019-00955-0

Hettiarachchi, H., & Ardakanian, R. (Eds.). (2018). *Safe use of wastewater in agriculture: From concept to implementation*. Springer.

Hijab, M. S. (2017). *Equilibrium Studies for Malachite Green-Dye Removal Using Modified Date Pits*. Hamad Bin Khalifa University (Qatar). https://doi.org/10.1016/j.cej.2018.10.138

Hong, M., Yu, L., Wang, Y., Zhang, J., Chen, Z., Dong, L., & Li, R. (2019). Heavy metal adsorption with zeolites: The role of hierarchical pore architecture. *Chemical Engineering Journal*, *359*, 363-372. https://doi.org/10.1016/j.cej.2018.11.087

Hu, Q., & Zhang, Z. (2019). Application of Dubinin–Radushkevich isotherm model at the solid/solution interface: A theoretical analysis. *Journal of Molecular Liquids*, *277*, 646-648. https://doi.org/10.1016/j.molliq.2019.01.005

Huang, D., Wu, J., Wang, L., Liu, X., Meng, J., Tang, X., Tang, C., & Xu, J. (2019). Novel insight into adsorption and co-adsorption of heavy metal ions and an

organic pollutant by magnetic graphene nanomaterials in water. *Chemical Engineering Journal*, *358*, 1399-1409. https://doi.org/10.1016/j.cej.2018.10.138

Ibrahim, F., Halttunen, T., Tahvonen, R., & Salminen, S. (2006). Probiotic bacteria as potential detoxification tools: assessing their heavy metal binding isotherms. *Canadian Journal of Microbiology*, *52*(9), 877-885. https://doi.org/10.1139/w06-043

Jaishankar, M., Tseten, T., Anbalagan, N., Mathew, B. B., & Beeregowda, K. N. (2014). Toxicity, mechanism and health effects of some heavy metals. *Interdisciplinary toxicology*, *7*(2), 60. doi: 10.2478/intox-2014-0009

Järup, L. (2003). Hazards of heavy metal contamination. *British Medical Bulletin*, *68*(1), 167-182. https://doi.org/10.1093/bmb/ldg032

Kassim, N. A., Ghazali, S. A. I. S. M., Bohari, F. L., & Abidin, N. A. Z. (2022). Assessment of heavy metals in wastewater plant effluent and lake water by using atomic absorption spectrophotometry. *Materials Today: Proceedings*, *66*, 3961-3964. https://doi.org/10.1016/j.matpr.2022.04.671

Kheddo, A., Rhyman, L., Elzagheid, M. I., Jeetah, P., & Ramasami, P. (2020). Adsorption of synthetic dyed wastewater using activated carbon from rice husk. *SN Applied Sciences*, *2*(12), 2170. https://doi.org/10.1007/s42452-020-03922-5

Lawtae, P., & Tangsathitkulchai, C. (2021). The use of high surface area mesoporous-activated carbon from longan seed biomass for increasing capacity and kinetics of methylene blue adsorption from aqueous solution. *Molecules*, *26*(21), 6521. doi: 10.3390/molecules26216521

Li, X., Sun, F., Qu, Z., Feng, Y., Li, Y., Yang, C., ... & Zhao, G. (2024). Selective pore regulation of activated carbon using trace carbonate-assisted catalytic activation: Revealing the effect of cation catalysis on pore topology. *Chemical Engineering Journal*, *481*, 148626. https://doi.org/10.1016/j.cej.2024.148626

Kalavathy, M. H., Karthikeyan, T., Rajgopal, S., & Miranda, L. R. (2005). Kinetic and isotherm studies of Cu (II) adsorption onto H_3PO_4-activated rubber wood sawdust. *Journal of Colloid and Interface Science*, *292*(2), 354-362. https://doi.org/10.1016/j.jcis.2005.05.087

Kallel, F., Chaari, F., Bouaziz, F., Bettaieb, F., Ghorbel, R., & Chaabouni, S. E. (2016). Sorption and desorption characteristics for the removal of a toxic dye, methylene blue from aqueous solution by a low cost agricultural by-product. *Journal of Molecular Liquids*, *219*, 279-288. https://doi.org/10.1016/j.molliq.2016.03.024

Karić, N., Maia, A. S., Teodorović, A., Atanasova, N., Langergraber, G., Crini, G., ... & Đolić, M. (2022). Bio-waste valorisation: Agricultural wastes as biosorbents for removal of (in) organic pollutants in wastewater treatment. *Chemical Engineering Journal Advances*, *9*, 100239. https://doi.org/10.1016/j.ceja.2021.100239

Khalid, N., Rizvi, Z. F., Yousaf, N., Khan, S. M., Noman, A., Aqeel, M., ... & Rafique, A. (2021). Rising metals concentration in the environment: a response to effluents of leather industries in Sialkot. *Bulletin of Environmental Contamination and Toxicology*, *106*, 493-500. https://doi.org/10.1007/s00128-021-03111-z

Khan, M. I., Zafar, S., Khan, M. A., Buzdar, A. R., & Prapamonthon, P. (2017). Adsorption kinetic, equilibrium and thermodynamic study for the removal of Congo Red from aqueous solution. *Desalination and Water Treatment*, *98*, 294-305. doi:10.5004/dwt.2017.21609

Khan, S. R., Sharma, B., Chawla, P. A., & Bhatia, R. (2022). Inductively coupled plasma optical emission spectrometry (ICP-OES): a powerful analytical technique for elemental analysis. *Food Analytical Methods*, 1-23. https://doi.org/10.1007/s12161-021-02148-4

Kharrazi, S. M., Mirghaffari, N., Dastgerdi, M. M., & Soleimani, M. (2020). A novel post-modification of powdered activated carbon prepared from lignocellulosic waste through thermal tension treatment to enhance the porosity and heavy metals adsorption. *Powder Technology*, *366*, 358-368. https://doi.org/10.1016/j.powtec.2020.01.065

Kibet, K., Nthiga, E. W., & Ollengo, M. A. (2023). Removal of Cd^{2+} and Cr^{3+} ions from Aqueous Solution by Modified Polypropylene Plastic Waste: Equilibrium Study. *Asian Journal of Research in Chemistry,* 16(5), 349-357. DOI: 10.52711/0974-4150.2023.00056

Kishor, R., Purchase, D., Saratale, G. D., Saratale, R. G., Ferreira, L. F. R., Bilal, M., ... & Bharagava, R. N. (2021). Ecotoxicological and health concerns of persistent coloring pollutants of textile industry wastewater and treatment approaches for environmental safety. *Journal of Environmental Chemical Engineering*, *9*(2), 105012. https://doi.org/10.1016/j.jece.2020.105012

Krishnan, K. A., & Anirudhan, T. (2003). Removal of cadmium (II) from aqueous solutions by steam-activated sulphurised carbon prepared from sugar-cane bagasse pith: Kinetics and equilibrium studies. *Water Sa, 29*(2), 147-156. https://doi.org/10.4314/wsa.v29i2.4849

Kumar, A., Kumar, A., MMS, C.-P., Chaturvedi, A. K., Shabnam, A. A., Subrahmanyam, G., Mondal, R., Gupta, D. K., Malyan, S. K., & Kumar, S. S. (2020). Lead toxicity: health hazards, influence on food chain, and sustainable remediation approaches. *International Journal of Environmental Research and Public Health, 17*(7), 2179. https://doi.org/10.3390/ijerph17072179

Kumar, P. S., Ramakrishnan, K., Kirupha, S. D., & Sivanesan, S. (2010). Thermodynamic and kinetic studies of cadmium adsorption from aqueous solution onto rice husk. *Brazilian Journal of Chemical Engineering, 27*(2), 347-355. https://doi.org/10.1590/S0104-66322010000200013

Kumar, P. S., Korving, L., Keesman, K. J., van Loosdrecht, M. C., & Witkamp, G. J. (2019). Effect of pore size distribution and particle size of porous metal oxides on phosphate adsorption capacity and kinetics. *Chemical Engineering Journal, 358*, 160-169. https://doi.org/10.1016/j.cej.2018.09.202

Laxmi, V., & Kaushik, G. (2020). Toxicity of hexavalent chromium in environment, health threats, and its bioremediation and detoxification from tannery wastewater for environmental safety. *Bioremediation of Industrial Waste for Environmental Safety: volume I: industrial waste and its management*, 223-243. https://doi.org/10.1007/978-981-13-1891-7_11

Legrouri, K., Khouya, E., Ezzine, M., Hannache, H., Denoyel, R., Pallier, R., & Naslain, R. (2005). Production of activated carbon from a new precursor molasses by activation with sulphuric acid. *Journal of hazardous materials, 118*(1), 259-263. https://doi.org/10.1016/j.jhazmat.2004.11.004

Li, X., Zhang, L., Yang, Z., Wang, P., Yan, Y., & Ran, J. (2020). Adsorption materials for volatile organic compounds (VOCs) and the key factors for VOCs adsorption process: A review. *Separation and Purification Technology, 235*, 116213. https://doi.org/10.1016/j.seppur.2019.116213

Liu, H., Probst, A., & Liao, B. (2005). Metal contamination of soils and crops affected by the Chenzhou lead/zinc mine spill (Hunan, China). *Science of the Total Environment, 339*(1-3), 153-166. https://doi.org/10.1016/j.scitotenv.2004.07.030

Liu, S. (2015). Cooperative adsorption on solid surfaces. *Journal of Colloid and Interface Science, 450*, 224-238. https://doi.org/10.1016/j.jcis.2015.03.013

Mabuza, M., Premlall, K., & Daramola, M. O. (2022). Modelling and thermodynamic properties of pure CO2 and flue gas sorption data on South African coals using Langmuir, Freundlich, Temkin, and extended Langmuir isotherm models.

International Journal of Coal Science & Technology, *9*(1), 1-15. https://doi.org/10.1007/s40789-022-00515-y

Maddodi, S. A., Alalwan, H. A., Alminshid, A. H., & Abbas, M. N. (2020). Isotherm and computational fluid dynamics analysis of nickel ion adsorption from aqueous solution using activated carbon. *South African Journal of Chemical Engineering*, *32*, 5-12.https://doi.org/10.1016/j.sajce.2020.01.002

Mahamadi, C. (2011). Water hyacinth as a biosorbent: A review. *African Journal of Environmental Science and Technology*, *5*(13), 1137-1145.https://doi.org/10.5897/AJESTX11.007

Makoni, F. S., Thekisoe, O. M., & Mbati, P. A. (2016). Urban wastewater for sustainable urban agriculture and water management in developing countries. In *Sustainable water management in urban environments* (pp. 265-293). Cham: Springer International Publishing.

Mariska, S., Lin, J. L., Tuyet, T. T. A., Hai, N. D., & Chao, H. P. (2024). Adsorption of methyl blue, dichromate, and copper on ettringite under various pH values. *Applied Water Science*, *14*(5), 95. https://doi.org/10.1007/s13201-024-02161-y

Mavura, W., & Wangila, P. (2003). The pollution status of Lake Nakuru, Kenya: heavy metals and pesticide residues, 1999/2000. *African Journal of Aquatic Science, 28*(1), 13-18. https://doi.org/10.2989/16085914.2003.9626594

Moreno, J. C., Gómez, R., & Giraldo, L. (2010). Removal of Mn, Fe, Ni and Cu ions from wastewater using cow bone charcoal. *Materials, 3*(1), 452-466. https://doi.org/10.3390/ma3010452

Nantongo, M. F. (2021). *Levels of Selected Water Quality Parameters, Heavy Metals and Pesticide Residues in Water, Sediments and Nile Tilapia of Lake Nakuru, Kenya.* Egerton University. http://41.89.96.81:8080/xmlui/handle/123456789/2775

Nantongo, M. F., Edebe, J., Otachi, E. O., & Kipkemboi, J. (2024). Assessment of the status of selected heavy metals in water, sediments and a fish species (Oreochromis niloticus) of commercial value in Lake Nakuru with a focus on human health risks. *Lakes & Reservoirs: Research & Management*, *29*(1), e12452. https://doi.org/10.1111/lre.12452

Ndetei, R., & Muhandiki, V. S. (2005). Mortalities of lesser flamingos in Kenyan Rift Valley saline lakes and the implications for sustainable management of the lakes. *Lakes & Reservoirs: Research & Management, 10*(1), 51-58. https://doi.org/10.1111/j.1440-1770.2005.00255.x

Nduka, J. K., Kelle, H. I., & Amuka, J. O. (2019). Health risk assessment of cadmium, chromium and nickel from car paint dust from used automobiles at auto-panel workshops in Nigeria. *Toxicology Reports, 6,* 449-456. https://doi.org/10.1016/j.toxrep.2019.05.007

Ochieng, E., Lalah, J., & Wandiga, S. (2007). Analysis of heavy metals in water and surface sediment in five rift valley lakes in Kenya for assessment of recent increase in anthropogenic activities. *Bulletin of Environmental Contamination and Toxicology, 79*(5), 570-576. https://doi.org/10.1007/s00128-007-9286-4

Oladimeji, T. E., Oyedemi, M., Emetere, M. E., Agboola, O., Adeoye, J. B., & Odunlami, O. A. (2024). Review on the impact of heavy metals from industrial wastewater effluent and removal technologies. *Heliyon*, *10*(23)

Olawale, A. S., Ajayi, O. A., Olakunle, M. S., Ityokumbul, M. T., & Adefila, S. S. (2015). Preparation of phosphoric acid activated carbons from Canarium Schweinfurthii Nutshell and its role in methylene blue adsorption. *Preparation of phosphoric acid activated carbons from Canarium Schweinfurthii Nutshell and its role in methylene blue adsorption, 6*(2), 1-6. DOI: 10.5897/JCEMS2015.0219

Omran, A. R., Baiee, M. A., Juda, S. A., Salman, J. M., & AlKaim, A. F. (2016). Removal of Congo red dye from aqueous solution using a new adsorbent surface developed from aquatic plant (*Phragmites australis*). *International Journal of ChemTech Research*, *9*(4), 334-342.

Onchieku, J., Chikamai, B., & Rao, M. (2012). Optimum parameters for the formulation of charcoal briquettes using bagasse and clay as binder. *European Journal of Sustainable Development, 1*(3), 477-492. https://doi.org/10.14207/ejsd.2012.v1n3p477

Oribayo, O., Olaleye, O. O., Akinyanju, A. S., Omoloja, K. O., & Williams, S. O. (2020). Coconut shell-based activated carbon as adsorbent for the removal of dye from aqueous solution: equilibrium, kinetics, and thermodynamic studies. *Nigerian Journal of Technology*, *39*(4), 1076-1084. http://dx.doi.org/10.4314/njt.v39i4.14

Oves, M., Saghir Khan, M., Huda Qari, A., Nadeen Felemban, M., & Almeelbi, T. (2016). Heavy metals: biological importance and detoxification strategies. *J Bioremed Biodeg, 7*(334), 2. http://dx.doi.org/10.4172/2155-6199.1000334

Poljak, M., Zgorelec, Ž., Kisić, I., Kuharić, Ž., & Perčin, A. (2024). Comparison of AAS, ICP-MS, and pXRF Performance for Copper Analysis in Agricultural Soils.

Journal of Central European Agriculture, *25*(2), 580-587. https://doi.org/10.5513/JCEA01/25.2.4279

Qasem, N. A., Mohammed, R. H., & Lawal, D. U. (2021). Removal of heavy metal ions from wastewater: a comprehensive and critical review. *Npj Clean Water*, *4*(1), 36. https://doi.org/10.1038/s41545-021-00127-0

Qi, X., Tong, X., Pan, W., Zeng, Q., You, S., & Shen, J. (2021). Recent advances in polysaccharide-based adsorbents for wastewater treatment. *Journal of Cleaner Production*, *315*, 128221. https://doi.org/10.1016/j.jclepro.2021.128221

Radulescu, C., Dulama, I., Stihi, C., Ionita, I., Chilian, A., Necula, C., & Chelarescu, E. D. (2014). Determination of heavy metal levels in water and therapeutic mud by atomic absorption spectrometry. *Rom. Journ. Phys*, *59*(9-10), 1057.

Raj, K., & Das, A. P. (2023). Lead pollution: Impact on environment and human health and approach for a sustainable solution. *Environmental Chemistry and Ecotoxicology*, *5*, 79-85. https://doi.org/10.1016/j.enceco.2023.02.001

Raj, V., Chauhan, M. S., & Pal, S. L. (2022). Potential of sugarcane bagasse in remediation of heavy metals: A review. *Chemosphere*, *307*, 135825. https://doi.org/10.1016/j.chemosphere.2022.135825.

Rajeshkumar, S., & Li, X. (2018). Bioaccumulation of heavy metals in fish species from the Meiliang Bay, Taihu Lake, China. *Toxicology reports*, *5*, 288-295. https://doi.org/10.1016/j.toxrep.2018.01.007

Ramadhani, P., Chaidir, Z., Zilfa, Z., Tomi, Z. B., Rahmiarti, D., & Zein, R. (2020). Shrimp shell (Metapenaeus monoceros) waste as a low-cost adsorbent for metanil yellow dye removal in aqueous solution. *Desalination and Water Treatment*, *197*, 413-423. https://doi.org/10.5004/dwt.2020.25963

Rehman, M., Liu, L., Wang, Q., Saleem, M. H., Bashir, S., Ullah, S., & Peng, D. (2019). Copper environmental toxicology, recent advances, and future outlook: a review. *Environmental Science and Pollution Research*, *26*(18), 18003-18016. https://doi.org/10.1007/s11356-019-05073-6

Ren, X., Wang, J., Yu, J., Song, B., Feng, H., Shen, M., ... & Wang, J. (2021). Waste valorization: transforming the fishbone biowaste into biochar as an efficient persulfate catalyst for degradation of organic pollutant. *Journal of Cleaner Production*, *291*, 125225. https://doi.org/10.1016/j.jclepro.2020.125225

Sahmoune, M. N. (2019). Evaluation of thermodynamic parameters for adsorption of heavy metals by green adsorbents. *Environmental Chemistry Letters*, *17*(2), 697-704. https://doi.org/10.1007/s10311-018-00819-z

Sahu, S., Pahi, S., Tripathy, S., Singh, S. K., Behera, A., Sahu, U. K., & Patel, R. K. (2020). Adsorption of methylene blue on chemically modified lychee seed biochar: Dynamic, equilibrium, and thermodynamic study. *Journal of Molecular Liquids*, *315*, 113743. https://doi.org/10.1016/j.molliq.2020.113743

Saleem, J., Shahid, U. B., Hijab, M., Mackey, H., & McKay, G. (2019). Production and applications of activated carbons as adsorbents from olive stones. *Biomass Conversion and Biorefinery*, *9*(4), 775-802. https://doi.org/10.1007/s13399-019-00473-7

Saleh, T. A. (2022). Kinetic models and thermodynamics of adsorption processes: classification. In *Interface Science and Technology* (Vol. 34, pp. 65-97). Elsevier. https://doi.org/10.1016/B978-0-12-849876-7.00003-8

Sharma, J. N., Pattadar, D. K., Mainali, B. P., & Zamborini, F. P. (2018). Size determination of metal nanoparticles based on electrochemically measured surface-area-to-volume ratios. *Analytical Chemistry*, *90*(15), 9308-9314. https://doi.org/10.1021/acs.analch em.8b01905

Sharma, R., Agrawal, P. R., Kumar, R., & Gupta, G. (2021). Current scenario of heavy metal contamination in water. *Contamination of Water*, 49-64. https://doi.org/10.1016/B978-0-12-824058-8.00010-4

Simonin, J. P. (2016). On the comparison of pseudo-first order and pseudo-second order rate laws in the modeling of adsorption kinetics. *Chemical Engineering Journal*, *300*, 254-263. https://doi.org/10.1016/j.cej.2016.04.079

Song, C., Wu, S., Cheng, M., Tao, P., Shao, M., & Gao, G. (2013). Adsorption studies of coconut shell carbons prepared by KOH activation for removal of lead (II) from aqueous solutions. *Sustainability*, *6*(1), 86-98. https://doi.org/10.3390/su6010086

Rodríguez-Díaz, J. M., García, J. O. P., Sánchez, L. R. B., da Silva, M. G. C., da Silva, V. L., & Arteaga-Pérez, L. E. (2015). Comprehensive characterization of sugarcane bagasse ash for its use as an adsorbent. *Bioenergy Research*, *8*, 1885-1895. https://doi.org/10.1007/s12155-015-9646-6

Russakova, A. V., Altynbaeva, L. S., Barsbay, M., Zheltov, D. A., Zdorovets, M. V., & Mashentseva, A. A. (2021). Kinetic and isotherm study of as (Iii) removal from

aqueous solution by pet track-etched membranes loaded with copper microtubes. *Membranes*, *11*(2), 116.

Tan, I., Hameed, B., & Ahmad, A. (2007). Equilibrium and kinetic studies on basic dye adsorption by oil palm fibre activated carbon. *Chemical Engineering Journal*, *127*(1), 111-119. https://doi.org/10.1016/j.cej.2006.09.010

Taylor, A. A., Tsuji, J. S., Garry, M. R., McArdle, M. E., Goodfellow, W. L., Adams, W. J., & Menzie, C. A. (2020). Critical review of exposure and effects: implications for setting regulatory health criteria for ingested copper. *Environmental Management*, *65*(1), 131-159. https://doi.org/10.1007/s00267-019-01234-y

Tchounwou, P. B., Yedjou, C. G., Patlolla, A. K., & Sutton, D. J. (2012). Heavy metal toxicity and the environment *Molecular, Clinical and Environmental Toxicology* (pp. 133-164): Springer. https://doi.org/10.1007/978-3-7643-8340-4_6

Tong, Y., McNamara, P. J., & Mayer, B. K. (2019). Adsorption of organic micropollutants onto biochar: a review of relevant kinetics, mechanisms and equilibrium. *Environmental Science: Water Research & Technology*, *5*(5), 821-838.

Tripathi, N. (2013). Cationic and anionic dye adsorption by agricultural solid wastes: A comprehensive review. *Journal of Applied Chemistry*, *5*, 91-108.

Trotta, V., Baaloudj, O., & Brienza, M. (2024). Risks associated with wastewater reuse in agriculture: investigating the effects of contaminants in soil, plants, and insects. *Frontiers in Environmental Science*, *12*, 1358842. doi: 10.3389/fenvs.2024.1358842

Umeh, A. C., Hassan, M., Egbuatu, M., Zeng, Z., Al Amin, M., Samarasinghe, C., & Naidu, R. (2023). Multicomponent PFAS sorption and desorption in common commercial adsorbents: Kinetics, isotherm, adsorbent dose, pH, and index ion and ionic strength effects. *Science of the Total Environment*, *904*, 166568. https://doi.org/10.1016/j.scitotenv.2023.166568

Ungureanu, Elena Loredana, & Gabriel Mustatea. "Toxicity of heavy metals." *Environmental Impact and Remediation of Heavy Metals*. IntechOpen, 2022. DOI: 10.5772/intechopen.102441

Van Acker, T., Theiner, S., Bolea-Fernandez, E., Vanhaecke, F., & Koellensperger, G. (2023). Inductively coupled plasma mass spectrometry. *Nature Reviews Methods Primers*, *3*(1), 52. https://doi.org/10.1038/s43586-023-00235-w

Vera, L. M., Bermejo, D., Uguña, M. F., Garcia, N., Flores, M., & González, E. (2019). Fixed bed column modeling of lead (II) and cadmium (II) ions biosorption on sugarcane bagasse. *Environmental Engineering Research*, *24*(1), 31-37. https://doi.org/10.4491/eer.2018.042

Vijayalakshmi, K., Devi, B. M., Latha, S., Gomathi, T., Sudha, P., Venkatesan, J., & Anil, S. (2017). Batch adsorption and desorption studies on the removal of lead (II) from aqueous solution using nanochitosan/sodium alginate/microcrystalline cellulose beads. *International Journal of Biological Macromolecules, 104*, 1483-1494. https://doi.org/10.1016/j.ijbiomac.2017.04.120

Wang, J., & Guo, X. (2022). Rethinking of the intraparticle diffusion adsorption kinetics model: Interpretation, solving methods and applications. *Chemosphere*, *309*, 136732. https://doi.org/10.1016/j.chemosphere.2022.136732

Water, U. N. (2018). Sustainable Development Goal 6 synthesis report on water and sanitation. *Published by the United Nations New York, New York, 10017*.

WHO. (2011). Guidelines for drinking-water quality. *WHO chronicle*, *38*(4), 104-108.

Wuana, R. A., & Okieimen, F. E. (2011). Heavy metals in contaminated soils: a review of sources, chemistry, risks and best available strategies for remediation. *Isrn Ecology, 2011*. https://doi.org/10.5402/2011/402647

Yadav, S. P. S., Bhandari, S., Bhatta, D., Poudel, A., Bhattarai, S., Yadav, P., ... & Oli, B. (2023). Biochar application: A sustainable approach to improve soil health. *Journal of Agriculture and Food Research*, *11*, 100498. https://doi.org/10.1016/j.jafr.2023.100498

Yang, X., Wan, Y., Zheng, Y., He, F., Yu, Z., Huang, J., & Gao, B. (2019). Surface functional groups of carbon-based adsorbents and their roles in the removal of heavy metals from aqueous solutions: a critical review. *Chemical Engineering Journal*, *366*, 608-621.https://doi.org/10.1016/j.cej.2019.02.119

Yang, Y., Wei, L., Cui, L., Zhang, M., & Wang, J. (2017). Profiles and risk assessment of heavy metals in Great Rift Lakes, Kenya. *CLEAN–Soil, Air, Water, 45*(3), 1600825.https://doi.org/10.1002/clen.201600825

Yuh-Shan, H. (2004). Citation review of Lagergren kinetic rate equation on adsorption reactions. *Scientometrics*, *59*(1), 171-177. https://doi.org/10.1023/b:scie.0000013305.99473.cf

Yunus, Z. M., Al-Gheethi, A., Othman, N., Hamdan, R., & Ruslan, N. N. (2022). Advanced methods for activated carbon from agriculture wastes; a comprehensive

review. *International Journal of Environmental Analytical Chemistry*, *102*(1), 134-158. https://doi.org/10.1080/03067319.2020.1717477

Zhu, S., Khan, M. A., Wang, F., Bano, Z., & Xia, M. (2020). Rapid removal of toxic metals Cu^{2+} and Pb^{2+} by amino trimethylene phosphonic acid intercalated layered double hydroxide: A combined experimental and DFT study. *Chemical Engineering Journal*, *392*, 123711. https://doi.org/10.1016/j.cej.2019.123711

Zhou, X., Yu, X., Maimaitiniyazi, R., Zhang, X., & Qu, Q. (2024). Discussion on the thermodynamic calculation and adsorption spontaneity re Ofudje et al.(2023). *Heliyon*, *10*(8). https://doi.org/10.1016/j.heliyon.2024.e28188

Zolotov, Y. A., Malofeeva, G., Petrukhin, O., & Timerbaev, A. (1987). New methods for preconcentration and determination of heavy metals in natural water. *Pure and Applied Chemistry*, *59*(4), 497-504. https://doi.org/10.1351/pac198759040497

APPENDICES

Appendix A: Calibration curves

Appendix A1: Calibration curve for lead

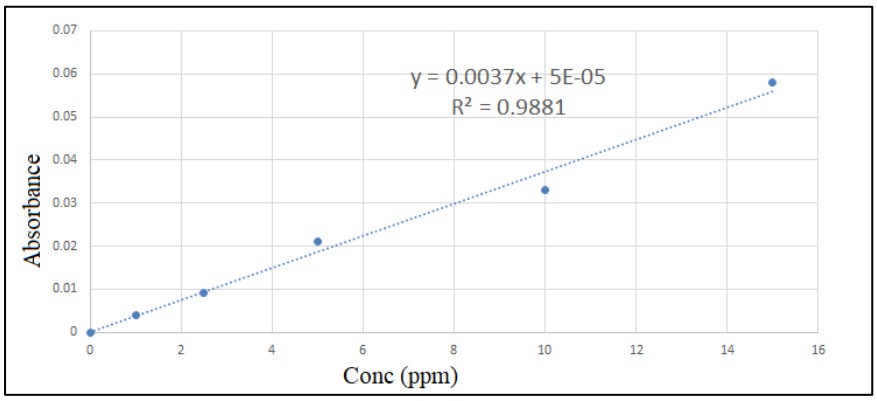

Appendix A2: Calibration curve for nickel

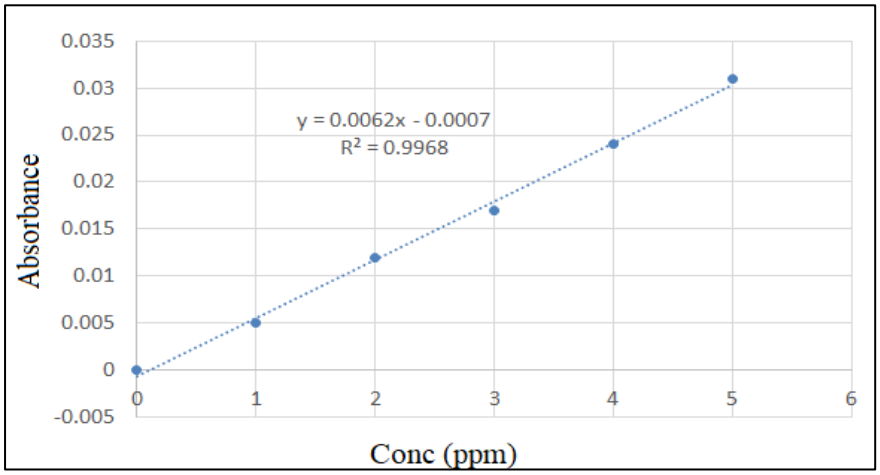

Appendix A3: Calibration curve for copper

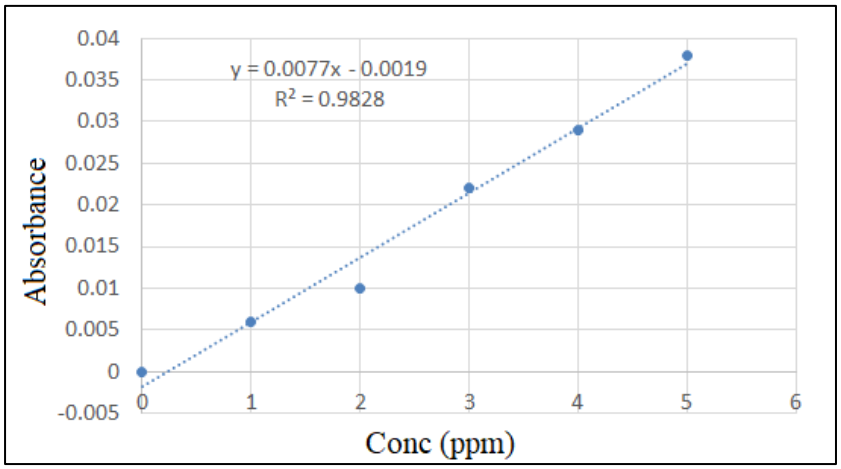

Appendix A4: Calibration curve for cadmium

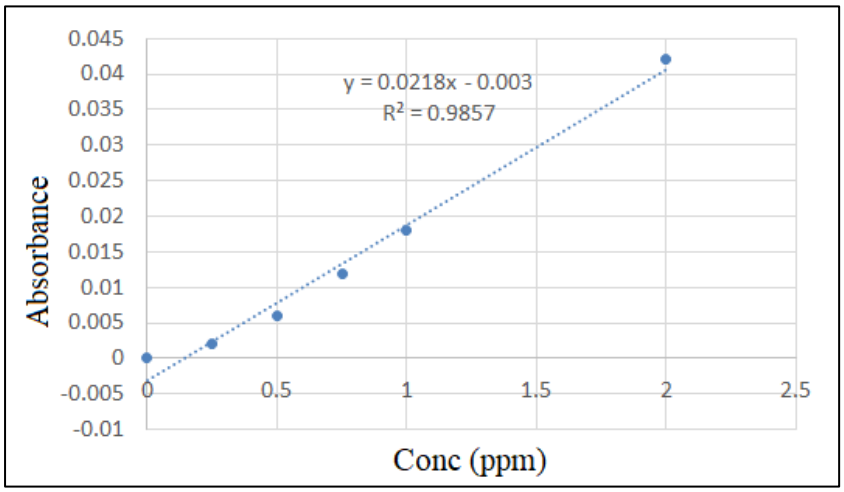

Appendix A5: Calibration curve for chromium

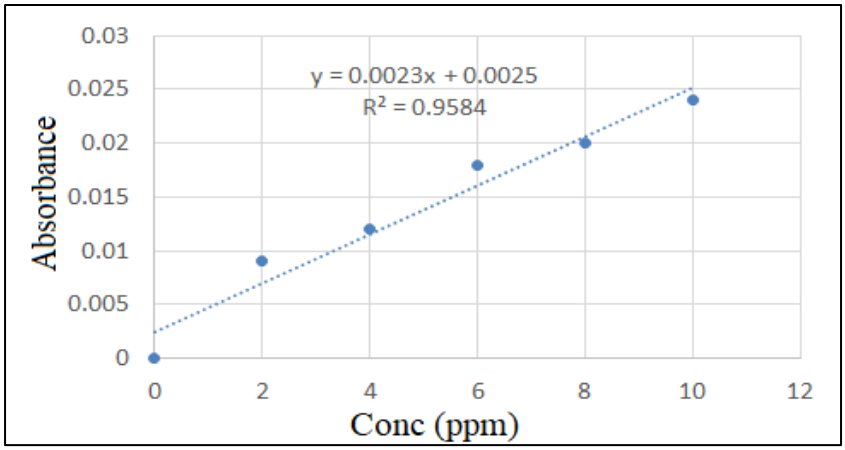

Appendix B: Concentration of heavy metals in wastewaters

Lead	Run1	Run 2	Run3	mean	SD	Pb mean ± SD
Sample 1	0.016	0.020	0.024	0.020	0.004	0.02 ± 0.004
Sample 2	0.011	0.010	0.009	0.010	0.001	0.010 ± 0.001
Sample 3	0.000	0.000	0.000	0.000	0.000	0
Sample 4	0.120	0.080	0.100	0.100	0.020	0.100 ± 0.020
Sample 5	0.035	0.033	0.031	0.033	0.002	0.033 ± 0.002
Sample 6	0.000	0.000	0.000	0.000	0.000	0
Sample 7	0.110	0.100	0.090	0.100	0.010	0.100 ± 0.01
Sample 8	0.036	0.033	0.030	0.033	0.003	0.033 ± 0.003

Sample 9	1.044	1.066	1.022	1.044	0.022	1.044 ± 0.022
Sample 10	1.149	1.151	1.150	1.150	0.001	1.150 ± 0.001
Sample 11	2.204	2.200	2.202	2.202	0.002	2.202 ± 0.002

Copper	Run1	Run 2	Run3	mean	SD	Cu mean ± SD
Sample 1	0.020	0.020	0.020	0.020	0.000	0.020 ± 0
Sample 2	0.009	0.011	0.010	0.010	0.001	0.010 ± 0.001
Sample 3	0.000	0.000	0.000	0.000	0.000	0
Sample 4	0.008	0.010	0.012	0.010	0.002	0.010 ± 0.002
Sample 5	0.004	0.008	0.006	0.006	0.002	0.006 ± 0.002
Sample 6	0.001	0.004	0.007	0.004	0.003	0.004 ± 0.003
Sample 7	0.001	0.001	0.001	0.001	0.000	0.001 ± 0
Sample 8	0.002	0.006	0.004	0.004	0.002	0.004 ± 0.002
Sample 9	0.002	0.001	0.003	0.002	0.001	0.002 ± 0.001
Sample 10	0.820	0.800	0.810	0.810	0.010	0.810 ± 0.010
Sample 11	0.002	0.002	0.002	0.002	0.000	0.002 ± 0

Cadmium	Run1	Run 2	Run3	mean	SD	Cd mean ± SD
Sample 1	0.021	0.019	0.020	0.020	0.001	0.020 ± 0.001
Sample 2	0.017	0.020	0.023	0.020	0.003	0.020 ± 0.003
Sample 3	0.076	0.096	0.116	0.096	0.020	0.096 ± 0.020
Sample 4	0.020	0.020	0.020	0.020	0.000	0.020 ± 0.000
Sample 5	0.007	0.007	0.007	0.007	0.000	0.007 ± 0.000
Sample 6	0.000	0.000	0.000	0.000	0.000	0
Sample 7	0.020	0.016	0.024	0.020	0.004	0.020 ± 0.004
Sample 8	0.022	0.015	0.029	0.022	0.007	0.022 ± 0.007
Sample 9	0.051	0.057	0.063	0.057	0.006	0.057 ± 0.006
Sample 10	0.091	0.100	0.109	0.100	0.009	0.100 ± 0.009
Sample 11	0.086	0.079	0.093	0.086	0.007	0.086 ± 0.007

Nickel	Run1	Run 2	Run3	mean	SD	Ni mean ± SD
Sample 1	0.190	0.190	0.220	0.200	0.017	0.200 ± 0.017

Sample 2	ND	ND	ND	ND	ND	ND
Sample 3	0.024	0.018	0.030	0.024	0.006	0.024 ± 0.006
Sample 4	ND	ND	ND	ND	ND	ND
Sample 5	ND	ND	ND	ND	ND	ND
Sample 6	ND	ND	ND	ND	ND	ND
Sample 7	0.316	0.320	0.324	0.320	0.004	0.320 ± 0.004
Sample 8	0.119	0.119	0.119	0.119	0.000	0.119 ± 0.000
Sample 9	ND	ND	ND	ND	ND	ND
Sample 10	0.664	0.670	0.676	0.670	0.006	0.670 ± 0.006
Sample 11	0.327	0.355	0.341	0.341	0.014	0.341 ± 0.014

Chromium	Run1	Run 2	Run3	mean	SD	Cr mean ± SD
Sample 1	8.010	11.870	9.940	9.940	1.930	9.940 ± 1.930
Sample 2	0.005	0.007	0.009	0.007	0.002	0.007 ± 0.002
Sample 3	0.037	0.043	0.055	0.045	0.009	0.045 ± 0.009
Sample 4	0.011	0.015	0.007	0.011	0.004	0.011 ± 0.004
Sample 5	0.045	0.045	0.045	0.045	0.000	0.045 ± 0.000
Sample 6	ND	ND	ND	ND	-	ND
Sample 7	0.003	0.004	0.005	0.004	0.001	0.004 ± 0.001
Sample 8	ND	ND	ND	ND	-	ND
Sample 9	0.487	0.217	0.340	0.348	0.135	0.348 ± 0.135
Sample 10	0.617	0.660	0.715	0.664	0.049	0.664 ± 0.049
Sample 11	0.426	0.291	0.555	0.424	0.132	0.424 ± 0.132

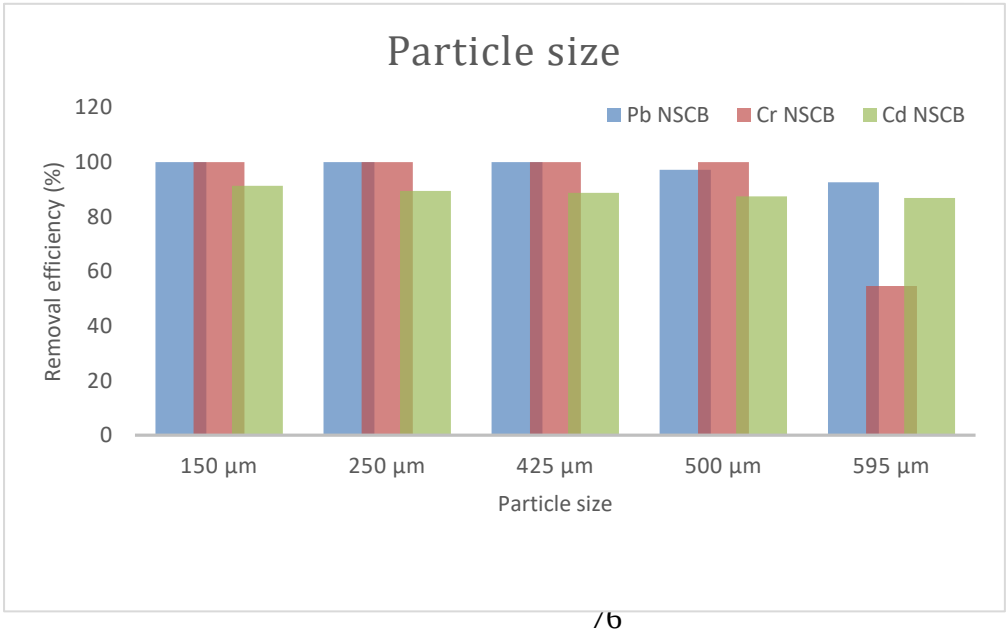

Appendix C: Adsorbent dosage

Adsorbent dose NSCB Mass(g)	% removal Pb	Cd	Cu	Ni	Cr
0.05	42.75	61.63	59.29	58.05	42.19
0.1	63.11	73.42	70.32	73.15	62.42
0.3	80.89	79.05	73.8	76.23	67.96
0.5	85.33	86.07	74.89	77.44	71.92
0.7	92	88.89	79.46	82.68	74.55
0.9	94.22	90.29	81.74	85.59	77.16
1.2	94.44	91.7	84.9	88.13	79.73
1.5	96.44	95.92	89.89	93.37	86.67
2	96.44	97.33	92.94	95.46	91.92

Adsorbent dose VSCB Mass(g)	% removal Pb	Cd	Cu	Ni	Cr
0.05	55.58	80.119	88.935	83.0115	59.066
0.1	94.67	95.446	98.448	98.7525	93.63
0.3	99.89	100	100	100	98.3
0.5	100	100	100	100	100
0.7	100	100	100	100	100
0.9	100	100	100	100	100
1.2	100	100	100	100	100
1.5	100	100	100	100	100
2	100	100	100	100	100

Appendix D: Particle size

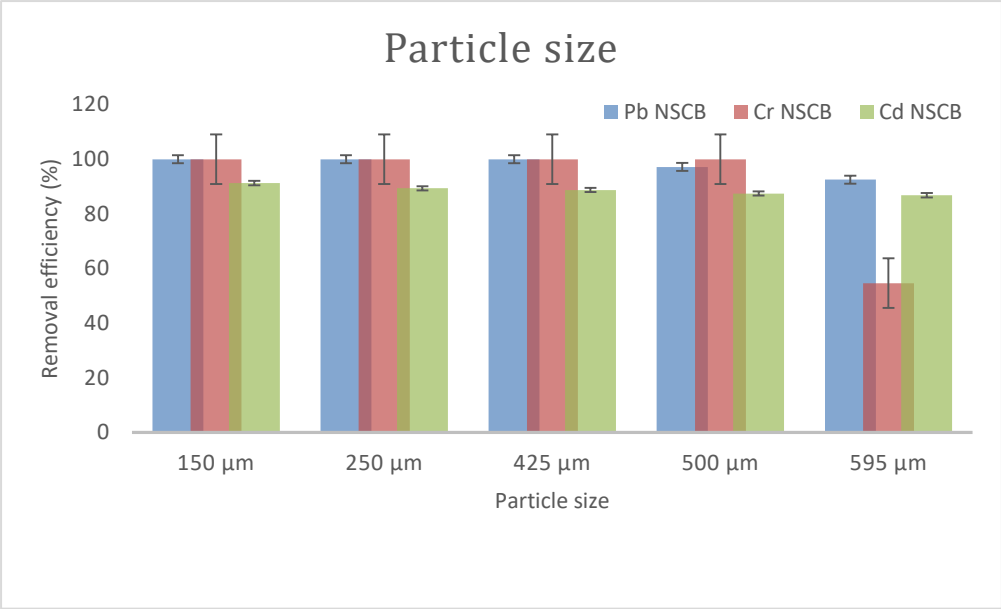

	Particle size NSCB	run1	run2	run3	ave. conc	% removal
Pb 5ppm	150 µm	ND	ND	ND	ND	100.00
	250µm	ND	ND	ND	ND	100.00
	425 µm	ND	ND	ND	ND	100.00
	500µm	0.1395	0.1395	0.1395	0.1395	97.21
	595µm	0.3721	0.3721	0.3721	0.3721	92.56
Cr 2.5ppm	150 µm	ND	ND	ND	0	100.00
	250µm	ND	ND	ND	0	100.00
	425 µm	ND	ND	ND	0	100.00
	500µm	ND	ND	ND	ND	100.00
	595µm	1.1333	1.1333	1.1333	1.1333	54.67
Cu 2ppm	150 µm	0.0123	0.0123	0.0123	0.0123	99.39
	250µm	0.0736	0.0736	0.0736	0.0736	96.32

	425 µm	0.0736	0.0736	0.0736	0.0736	96.32
	500µm	0.1963	0.1963	0.1350	0.1759	91.21
	595µm	0.1963	0.1963	0.1963	0.1963	90.18
Cd 1.5ppm	150 µm	0.1400	0.1400	0.1114	0.1305	91.30
	250µm	0.1400	0.1686	0.1686	0.1590	89.40
	425 µm	0.1686	0.1686	0.1686	0.1686	88.76
	500µm	0.1971	0.1686	0.1971	0.1876	87.49
	595µm	0.1971	0.1971	0.1971	0.1971	86.86
Ni 3ppm	150 µm	0.0159	0.0159	0.0159	0.0159	99.47
	250µm	0.1746	0.1746	0.1746	0.1746	94.18
	425 µm	0.1746	0.1746	0.1746	0.1746	94.18
	500µm	0.3333	0.3333	0.1746	0.2804	90.65
	595µm	0.4921	0.4921	0.4921	0.4921	83.60
Particle size VSCB	150-250 µm					

	Time (mins) NSCB	abs 1	abs 2	abs 3	ave.conc	%removal
Pb 10ppm	1	0.031	0.030	0.029	8.108	18.919
	2	0.028	0.028	0.019	6.847	24.459
	3	0.027	0.026	0.016	6.216	28.514
	4	0.018	0.021	0.015	4.865	47.432
	5	0.016	0.015	0.014	4.054	58.243
	30	0.003	0.003	0.003	0.811	92.027
	60	0.001	0.002	0.001	0.270	96.396
Ni	1	0.042	0.040	0.040	6.672	32.742

10ppm	2	0.037	0.038	0.037	6.134	38.656
	3	0.029	0.030	0.029	4.844	51.559
	4	0.022	0.021	0.021	3.554	64.462
	5	0.011	0.010	0.011	1.833	81.667
	30	0.003	0.003	0.002	0.543	94.570
	60	0.002	0.002	0.002	0.435	95.645
Cd	1	0.079	0.079	0.080	3.761	62.232
10ppm	2	0.075	0.074	0.074	3.532	64.526
	3	0.065	0.065	0.066	3.165	68.654
	4	0.055	0.052	0.053	2.569	74.159
	5	0.046	0.045	0.045	2.202	77.829
	30	0.005	0.004	0.005	0.352	96.483
	60	0.004	0.004	0.004	0.321	96.789
Cr	1	0.017	0.017	0.018	3.909	60.909
10ppm	2	0.012	0.012	0.012	2.773	72.273
	3	0.009	0.009	0.009	2.091	79.091
	4	0.008	0.007	0.008	1.750	82.500
	5	0.005	0.005	0.005	1.182	88.182
	30	0.000	0.000	0.00	0.045	99.545
	60	0.000	0.000	0.00	0.045	99.545
Cu	1	0.025	0.025	0.024	3.450	65.498
10ppm	2	0.021	0.022	0.023	3.104	69.961
	3	0.019	0.019	0.020	2.758	72.424
	4	0.017	0.018	0.018	2.541	74.589
	5	0.011	0.010	0.011	1.632	83.896
	30	0.002	0.002	0.002	0.506	94.935
	60	0.001	0.001	0.001	0.377	96.234

	Time (mins)					
	VSCB	abs 1	abs 2	abs 3	ave.conc	%removal
Pb	1	0.021	0.023	0.021	5.898	41.022
10ppm	2	0.018	0.019	0.019	4.874	51.261
	3	0.018	0.017	0.016	4.761	52.387

	4	0.013	0.015	0.015	3.715	62.855
	5	0.011	0.013	0.014	3.117	68.829
	30	0.003	0.003	0.003	0.797	92.027
	60	ND	ND	ND	0.000	100.000
Ni	1	0.028	0.028	0.027	4.596	54.043
10ppm	2	0.025	0.022	0.024	3.905	60.952
	3	0.019	0.020	0.019	3.285	67.151
	4	0.015	0.014	0.015	2.464	75.363
	5	0.007	0.007	0.008	1.242	87.581
	30	0.002	0.002	0.002	0.435	95.645
	60	0.001	0.001	0.000	0.113	98.871
Cd	1	0.053	0.054	0.054	2.594	74.057
10ppm	2	0.047	0.047	0.047	2.294	77.064
	3	0.043	0.046	0.044	2.171	78.278
	4	0.037	0.040	0.038	1.896	81.040
	5	0.029	0.030	0.030	1.498	85.015
	30	0.003	0.003	0.003	0.257	97.248
	60	0.003	0.003	0.003	0.275	97.248
Cr	1	0.011	0.011	0.012	4.578	54.222
10ppm	2	0.010	0.010	0.011	4.244	57.556
	3	0.006	0.006	0.006	2.800	72.000
	4	0.006	0.005	0.005	2.578	74.222
	5	0.003	0.003	0.003	1.837	81.630
	30	Nd	Nd	Nd	0.000	100.000
	60	Nd	Nd	Nd	0.000	100.000
Cu	1	0.018	0.017	0.018	2.463	74.795
10ppm	2	0.016	0.015	0.016	2.220	77.264
	3	0.013	0.012	0.013	1.854	81.281
	4	0.012	0.012	0.012	1.793	81.886
	5	0.008	0.008	0.009	1.305	86.643
	30	0.001	0.001	0.001	0.451	96.017
	60	0.001	0.000	0.000	0.390	97.100

Appendix E: pH

Effect of pH on adsorption of heavy metals on NSCB

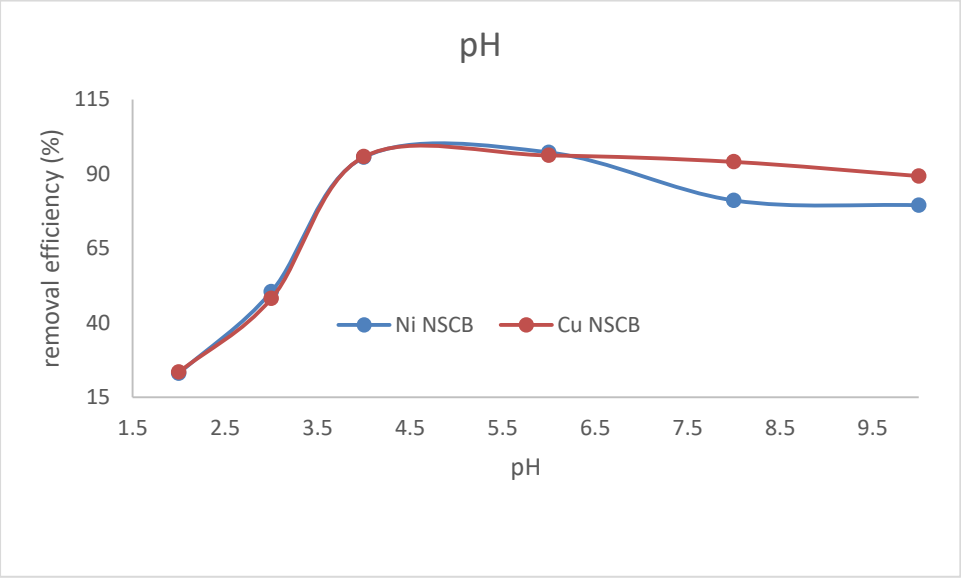

	pH NSCB	run1	run2	run3	Ave conc	% removal
Pb 10ppm	2	0.032	0.031	0.032	8.545	14.550
	3	0.019	0.019	0.019	5.122	48.784
	4	0.001	0.001	0.001	0.257	97.432
	6	0.001	0.001	0.001	0.257	97.432

	8	0.004	0.004	0.003	0.977	90.225
	10	0.006	0.005	0.005	1.423	83.530
Ni 10ppm	2	0.047	0.046	0.046	5.075	23.065
	3	0.030	0.032	0.031	3.409	50.484
	4	0.002	0.002	0.002	0.290	95.645
	6	0.001	0.002	0.002	0.237	97.258
	8	0.011	0.010	0.011	1.833	81.129
	10	0.012	0.011	0.012	4.190	79.516
Cd 10ppm	2	0.120	0.122	0.121	5.688	43.119
	3	0.076	0.075	0.076	3.609	63.914
	4	0.005	0.006	0.006	0.398	96.024
	6	0.004	0.004	0.005	0.336	96.636
	8	0.025	0.025	0.025	1.284	87.156
	10	0.036	0.037	0.037	1.820	81.881
Cr 10ppm	2	0.022	0.023	0.021	8.478	15.217
	3	0.015	0.014	0.015	5.290	47.101
	4	0.003	0.003	0.004	0.362	96.377
	6	0.004	0.003	0.003	0.362	96.377
	8	0.005	0.006	0.004	1.087	89.130
	10	0.007	0.006	0.006	1.667	83.333
Cu 10ppm	2	0.058	0.056	0.057	7.649	23.506
	3	0.039	0.037	0.038	5.182	48.182
	4	0.002	0.001	0.001	0.420	95.801
	6	0.001	0.001	0.001	0.377	96.234
	8	0.003	0.002	0.003	0.593	94.069

10	0.006	0.006	0.007	1.069	89.307

pH
VSC
B

pH 5 was used for all.

Appendix F: Concentration

Effect of concentration on adsorption of heavy metals

	Concentration NSCB	2	4	6	8	10	20	40	60
Pb (mg/L)	Run1	ND	ND	ND	0.257	0.257	4.041	10.257	21.878
	Run2	ND	ND	ND	0.000	0.527	4.041	10.257	21.878
	Run3	ND	ND	ND	0.000	0.527	4.041	10.527	21.608
	Average conc (c_t)	0	0	0	0.086	0.437	4.041	10.527	21.788
	% removal Lead	100	100	100	98.930	95.631	79.797	73.682	63.686
Cd (mg/L)	Run1	ND	ND	ND	0.183	0.321	3.073	9.817	26.560
	Run2	ND	ND	ND	0.183	0.321	3.028	9.862	26.514
	Run3	ND	ND	ND	0.183	0.275	2.890	9.771	26.651
	Average conc	0	0	0	0.183	0.306	2.997	9.817	26.575

	(c_t)								
	% removal cadmium	100	100	100	97.706	96.946	85.015	75.459	55.708
Cu (mg/L)	Run1	ND	ND	ND	0.247	0.377	5.052	15.052	30.766
	Run2	ND	ND	ND	0.247	0.377	5.182	14.792	30.896
	Run3	ND	ND	ND	0.247	0.377	5.052	14.879	30.810
	Average conc (c_t)	0	0	0	0.247	0.377	5.117	14.92	30.83
	% removal copper	100	100	100	96.916	96.234	74.40	62.803	48.62
Ni (mg/L)	Run1	ND	ND	ND	0.274	0.435	3.500	8.500	15.113
	Run2	ND	ND	ND	0.274	0.435	3.661	8.500	15.113
	Run3	ND	ND	ND	0.274	0.435	3.823	8.339	15.059
	Average conc (c_t)	0	0	0	0.274	0.489	3.661	8.446	15.059
	% removal nickel	100	100	100	96.573	95.108	81.694	78.884	74.901
Cr (mg/L)	Run1	ND	ND	ND	ND	0.045	2.241	11.786	21.034

	Run2	ND	ND	ND	ND	0.045	2.586	11.548	20.575
	Run3	ND	ND	ND	ND	0.045	2.586	11.706	20.805
	Average conc (c_t)	0	0	0	0	0.045	2.471	11.706	20.805
	% removal chromium	100	100	100	100	99.545	87.644	70.734	64.326
	Concentration VSCB	2	4	6	8	10	20	40	60
Pb (mg/L)	Run 1	ND	ND	ND	ND	ND	4.1452	7.532	16.081
	Run 2	ND	ND	ND	ND	ND	3.500	7.693	17.778
	Run3	ND	ND	ND	ND	ND	3.661	7.532	17.780
	Average conc ct	0	0	0	0	0	3.769	7.586	17.213
	% removal Lead	100	100	100	100	100	81.156	81.030	71.312
Cd (mg/L)	Run 1	ND	ND	ND	ND	0.185	1.677	5.662	14.313
	Run 2	ND	ND	ND	ND	0.185	1.652	5.688	14.289
	Run3	ND	ND	ND	ND	0.170	1.572	5.751	14.591
	Average conc (c_t)	0	0	0	0	0.185	1.665	5.70	14.398
	% removal cadmium	100	100	100	100	98.150	91.676	85.75	76.004
Cu (mg/L	Run 1	ND	ND	ND	ND	0.451	3.337	8.866	19.264

)									
	Run 2	ND	ND	ND	ND	0.329	3.226	9.435	19.060
	Run 3	ND	ND	ND	ND	0.392	3.226	9.182	19.060
	Average conc (c_t)	0	0	0	0	0.391	3.282	9.161	19.160
	% removal copper	100	100	100	100	96.093	83.588	77.100	68.120
Ni (mg/L)	Run 1	ND	ND	ND	ND	0.053	3.982	8.661	15.035
	Run 2	ND	ND	ND	ND	0.053	3.982	8.718	15.035
	Run 3	ND	ND	ND	ND	0.053	3.883	8.690	15.035
	Average conc (c_t)	0	0	0	0	0.053	3.895	8.689	15.035
	% removal nickel	100	100	100	100	99.474	80.255	78.280	74.942
Cr (mg/L)	Run1	ND	ND	ND	ND	ND	1.522	12.390	22.826
	Run2	ND	ND	ND	ND	ND	1.957	12.356	22.391
	Run 3	ND	ND	ND	ND	ND	1.087	12.830	20.652
	Average conc (c_t)	0	0	0	0	0	1.522	12.680	21.957
	% removal chromium	100	100	100	100	100	90.535	68.833	63.852

Appendix G: Temperature

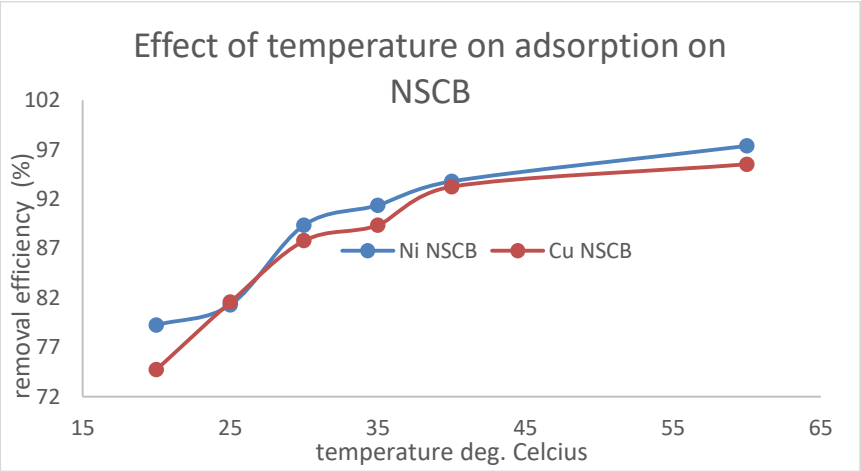

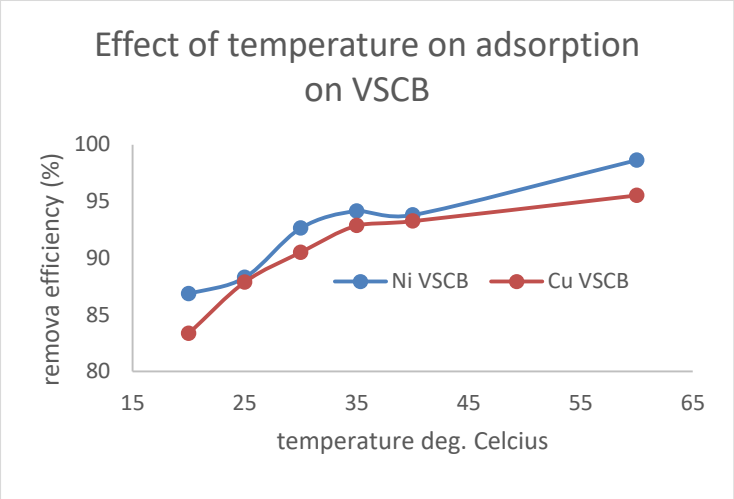

	Temp (^{0}C) NSCB	20	25	30	35	40	60
Cr 20ppm	Run1	0.012	0.009	0.005	0.004	0.003	0.001
	Run2	0.011	0.009	0.006	0.003	0.003	0.001
	Run3						

	Ave conc	2.659	2.091	1.295	0.841	0.727	0.273
	% removal chromium	86.71	89.55	93.52	95.79	96.36	98.64
Cd 20ppm	Run1	0.053	0.043	0.040	0.030	0.027	0.001
	Run2	0.054	0.045	0.041	0.032	0.026	0.001
	Ave conc	2.592	2.156	1.995	1.560	1.353	0.183
	% removal Cadmium	87.04	89.22	90.02	92.20	93.23	99.08
Ni 20ppm	Run1	0.025	0.022	0.013	0.010	0.007	0.001
	Run2	0.025	0.023	0.012	0.010	0.007	0.001
	Ave conc	4.145	3.747	2.129	1.726	1.242	0.274
	% removal nickel	79.25	81.290	89.36	91.37	93.79	97.38
Pb 20ppm	Run1	0.015	0.013	0.009	0.007	0.005	0.001
	Run2	0.015	0.013	0.010	0.006	0.005	0.000
	Ave conc	4.041	3.500	2.554	1.743	1.338	0.122
	% removal lead	79.80	82.50	87.23	91.28	93.31	99.39
Cu	Run1	0.037	0.027	0.020	0.015	0.008	0.005
	Run2	0.037	0.026	0.020	0.014	0.009	0.005
	Ave conc	5.052	3.688	2.844	2.130	1.351	0.896
	% removal copper	74.74	81.56	87.78	89.35	93.25	95.52
	Temp (^{0}C) VSCB	20	25	30	35	40	60
Cr 20ppm	Run1	0.007	0.006	0.003	0.003	0.003	0.000
	Run2	0.008	0.006	0.004	0.002	0.003	0.000
	Conc 1	1.712	1.409	0.803	0.668	0.727	0.045

	Conc 2	1.864	1.409	0.955	0.512	0.727	0.045
	Ave conc	1.788	1.409	0.879	0.590	0.727	0.045
	% removal chromium	91.061	92.955	95.606	97.049	96.364	99.773
Cd 20ppm	Run1	0.035	0.030	0.027	0.021	0.018	ND
	Run2	0.036	0.030	0.027	0.020	0.017	ND
	Conc 1	1.758	1.496	1.361	1.086	0.963	0.000
	Conc 2	1.789	1.514	1.391	1.055	0.933	0.000
	Ave conc	1.774	1.505	1.376	1.070	0.948	0.000
	% removal Cadmium	91.131	92.476	93.119	94.648	95.260	100.000
Pb 20ppm	Run1	0.009	0.008	0.006	0.004	0.003	ND
	Run2	0.009	0.007	0.006	0.004	0.003	ND
	Conc 1	2.520	2.196	1.507	1.169	0.831	0.000
	Conc 2	2.520	1.868	1.686	1.000	0.831	0.000
	Ave conc	2.520	2.032	1.597	1.084	0.831	0.000
	% removal lead	87.399	89.839	92.017	94.578	95.845	100
Ni 20ppm	Run1	0.016	0.014	0.008	0.007	0.007	0.001
	Run2	0.016	0.014	0.009	0.006	0.007	0.001
	Conc 1	2.633	2.359	1.423	1.222	1.242	0.274
	Conc 2	2.633	2.331	1.524	1.121	1.242	0.274
	Ave conc	2.633	2.345	1.474	1.171	1.242	0.274
	% removal nickel	86.835	88.277	92.631	94.143	93.790	98.629

Cu 20ppm	Run1	0.023	0.017	0.013	0.0088	0.008	0.005
	Run2	0.024	0.017	0.012	0.0094	0.009	0.005
	Conc 1	3.250	2.398	1.978	1.393	1.286	0.896
	Conc 2	3.408	2.454	1.821	1.464	1.416	0.896
	Ave conc	3.329	2.426	1.900	1.428	1.351	0.896
	% removal copper	83.355	87.871	90.502	92.858	93.247	95.520

Appendix H: Kinetic data

NSCB	Time (min)	C_t	C_e	q_t	q_e	Log q_e	q_e-q_t	log(q_e-q_t)	t/q_t
Pb	1	8.365	0.392	1.635	9.608	0.983	7.973	0.902	0.612
	2	7.554	0.392	2.446	9.608	0.983	7.162	0.855	0.818
	3	7.149	0.392	2.851	9.608	0.983	6.757	0.830	1.052
	4	5.257	0.392	4.743	9.608	0.983	4.865	0.687	0.843
	5	4.176	0.392	5.824	9.608	0.983	3.784	0.578	0.858
	30	0.797	0.392	9.203	9.608	0.983	0.405	-0.392	3.260
	60	0.392	0.392	9.608	9.608	0.983	0.000	-	6.245
Ni	1	6.7258	0.4355	3.2742	9.5645	0.9807	6.2903	0.7987	0.3054
	2	6.1613	0.4355	3.8387	9.5645	0.9807	5.7258	0.7578	0.5210
	3	4.8710	0.4355	5.1290	9.5645	0.9807	4.4355	0.6469	0.5849
	4	3.5806	0.4355	6.4194	9.5645	0.9807	3.1451	0.4976	0.6231
	5	1.8065	0.4355	8.1935	9.5645	0.9807	1.3710	0.1370	0.6102
	30	0.5968	0.4355	9.4032	9.5645	0.9807	0.1613	-0.7924	3.1904
	60	0.4355	0.4355	9.5645	9.5645	0.9807	0.0000	-	6.2732
Cd	1	3.7615	0.3211	6.2385	9.6789	0.9858	3.4404	0.5366	0.1603
	2	3.5550	0.3211	6.4450	9.6789	0.9858	3.2339	0.5097	0.3103
	3	3.1193	0.3211	6.8807	9.6789	0.9858	2.7982	0.4469	0.4360
	4	2.5917	0.3211	7.4083	9.6789	0.9858	2.2706	0.3561	0.5399

	5	2.2248	0.3211	7.7752	9.6789	0.9858	1.9037	0.2796	0.6431
	30	0.3440	0.3211	9.6560	9.6789	0.9858	0.0229	-1.6395	3.1069
	60	0.3211	0.3211	9.6789	9.6789	0.9858	0.0000	-	6.1991
Cu	1	3.494	0.377	6.506	9.623	0.983	3.117	0.494	0.154
	2	3.039	0.377	6.961	9.623	0.983	2.662	0.425	0.287
	3	2.714	0.377	7.286	9.623	0.983	2.337	0.369	0.412
	4	2.519	0.377	7.481	9.623	0.983	2.142	0.331	0.535
	5	1.610	0.377	8.390	9.623	0.983	1.233	0.091	0.596
	30	0.506	0.377	9.494	9.623	0.983	0.129	-0.888	3.160
	60	0.377	0.377	9.623	9.623	0.983	0.000	-	6.235
Cr	1	3.9091	0.046	6.091	9.955	0.998	3.864	0.5870	0.164
	2	2.7727	0.046	7.227	9.955	0.998	2.728	0.4358	0.277
	3	2.0909	0.046	7.909	9.955	0.998	2.046	0.3109	0.379
	4	1.7500	0.046	8.250	9.955	0.998	1.705	0.2317	0.485
	5	1.1439	0.046	8.856	9.955	0.998	1.099	0.0410	0.565
	30	0.0455	0.046	9.955	9.955	0.998	0.000	-	3.014
	60	0.0455	0.046	9.955	9.955	0.998	0.000	-	6.027

VSCB	Time (min)	C_t	C_e	q_t	q_e	Log qe	qe-qt	log(qe-qt)	t/q_t
Pb	1	5.309	0.000	4.691	10.000	1.000	5.309	0.725	0.213
	2	4.715	0.000	5.285	10.000	1.000	4.715	0.673	0.378
	3	4.299	0.000	5.701	10.000	1.000	4.299	0.633	0.526
	4	2.593	0.000	7.407	10.000	1.000	2.593	0.414	0.540
	5	1.632	0.000	8.368	10.000	1.000	1.632	0.213	0.597
	30	0.000	0.000	10.000	10.000	1.000	0.000	-	3.000
	60	0.000	0.000	10.000	10.000	1.000	0.000	-	6.000
Ni	1	4.7895	0.0526	5.2105	9.974	0.9989	4.7369	0.6755	0.1919
	2	4.0000	0.0526	6.0000	9.974	0.9989	3.9474	0.5963	0.3333
	3	3.2982	0.0526	6.7018	9.974	0.9989	3.2456	0.5113	0.4476
	4	2.4211	0.0526	7.5789	9.974	0.9989	2.3685	0.3745	0.5278
	5	1.1053	0.0526	8.8947	9.974	0.9989	1.0527	0.0223	0.5621

	30	0.2281	0.0526	9.7719	9.974	0.9989	0.1755	-0.7558	3.0700
	60	0.0526	0.0526	9.9474	9.974	0.9989	0.0000	-4.5006	6.0317
Cu	1	7.585	3.282	12.415	16.719	1.223	4.304	0.634	0.081
	2	6.661	3.282	13.339	16.719	1.223	3.380	0.529	0.150
	3	6.793	3.282	13.207	16.719	1.223	3.511	0.545	0.227
	4	4.439	3.282	15.561	16.719	1.223	1.158	0.064	0.257
	5	3.988	3.282	16.012	16.719	1.223	0.706	-0.151	0.312
	30	3.697	3.282	16.303	16.719	1.223	0.416	-0.381	1.840
	60	3.282	3.282	16.718	16.719	1.223	0.000	-5.391	3.589
Cd	1	2.1927	0.1850	7.8073	9.8150	0.9919	2.0077	0.302707	0.1281
	2	1.9306	0.1850	8.0694	9.8150	0.9919	1.7456	0.241956	0.2479
	3	1.8298	0.1850	8.1702	9.8150	0.9919	1.6448	0.216123	0.3672
	4	1.5879	0.1850	8.4121	9.8150	0.9919	1.4029	0.147027	0.4755
	5	1.2250	0.1850	8.7750	9.8150	0.9919	1.0400	0.017033	0.5698
	30	0.1850	0.1850	9.8150	9.8150	0.9919	0.0000	-	3.0565
	60	0.1850	0.1850	9.8150	9.8150	0.9919	0.0000	-	6.1131
Cr	1	7.244	0.000	2.756	10.000	1.000	7.244	0.860	0.363
	2	5.884	0.000	4.116	10.000	1.000	5.884	0.770	0.486
	3	5.036	0.000	4.964	10.000	1.000	5.036	0.702	0.604
	4	4.745	0.000	5.255	10.000	1.000	4.745	0.676	0.761
	5	2.126	0.000	7.874	10.000	1.000	2.126	0.328	0.635
	30	0.000	0.000	10.000	10.000	1.000	0.000	-	3.000
	60	0.000	0.000	10.000	10.000	1.000	0.000	-	6.000

Appendix I: Removal efficiency (%) and amount adsorbed (q)

				Removal efficiency (%)		Amount adsorbed (q) in mg/g	
	$C_{initial}$ (mg/L)	C_{NSCB} (mg/L)	C_{VSCB} (mg/L)	NSCB	VSCB	NSCB	VSCB
Ni	10	0.435	0.053	95.650	99.470	9.565	9.947
	20	3.581	3.895	82.095	80.525	16.419	16.105
	40	8.5	8.689	78.750	78.278	31.500	31.311
	60	15.032	15.035	74.947	74.942	44.968	44.965
Cu	10	0.376	0.390	96.240	96.100	9.624	9.610
	20	5.117	3.282	74.415	83.590	14.883	16.718
	40	14.792	9.150	63.020	77.125	25.208	30.850
	60	30.831	19.162	48.615	68.063	29.169	40.838
Cr	10	0.045	0.000	99.550	100.000	9.955	10.000

20	2.3182	1.893	88.409	90.535	17.682	18.107
40	11.977	12.467	70.058	68.833	28.023	27.533
60	21.409	21.689	64.318	63.852	38.591	38.311

Appendix J: Isotherms data

NSCB	Conc ppm	qe	Ce	1/qe	1/ce	log qe	log ce	ln qe	ε^2
Pb							-		
	10	9.203	0.392	0.109	2.552	0.964	0.407	2.219	9402777.25
	20	15.959	4.041	0.063	0.247	1.203	0.606	2.770	286233.00
	40	29.608	10.392	0.034	0.096	1.471	1.017	3.388	49409.00
	60	38.122	21.878	0.026	0.046	1.581	1.340	3.641	11692.00
Ni							-		
	10	9.565	0.435	0.105	2.296	0.981	0.361	2.258	8328004
	20	16.419	3.581	0.061	0.279	1.215	0.554	2.798	355078
	40	31.500	8.500	0.032	0.118	1.498	0.929	3.450	72413
	60	44.968	15.032	0.022	0.067	1.653	1.177	3.806	24279
Cu	10	9.623	0.376	0.104	2.655	0.983	-0.42	2.264	9833588.5
	20	14.883	5.117	0.067	0.195	1.173	0.709	2.700	186516.57
	40	25.207	14.792	0.039	0.067	1.402	1.170	3.227	25048.13
	60	29.169	30.831	0.0343	0.032	1.465	1.489	3.373	5963.848
Cd	10	9.679	0.321	0.103	3.114	0.986	-0.49	2.269	11710908
	20	16.9495	3.0505	0.0590	0.327	1.229	0.484	2.830	470575.22
	40	30.1605	9.8394	0.0332	0.102	1.479	0.993	3.406	54838.927
	60	33.4633	26.536	0.0299	0.037	1.524	1.424	3.510	8009.3593
Cr							-		
	10	9.955	0.045	0.100	22.00	0.998	1.342	2.298	12198.55
	20	17.6818	2.3182	0.05655	0.431	1.247	0.361	2.873	57546382
	40	28.0227	11.977	0.03568	0.083	1.447	1.078	3.333	752850
	60	38.590	21.409	0.02591	0.046	1.586	1.331	3.653	37638.47
VSCB	Conc ppm	qe	ce	1/qe	1/ce	log qe	log ce	ln qe	ε^2
Pb	10	10.000	0.000	0.100	-	1.000	-	2.303	-
	20	17.430	2.570	0.057	0.389	1.241	0.410	2.858	632348

	40	32.716	7.284	0.031	0.137	1.515	0.862	3.488	96873
	60	42.222	17.778	0.024	0.056	1.626	1.250	3.743	17530
Ni	10	9.947	0.053	0.101	19.00	0.998	-1.28	2.297	52530558
	20	16.105	3.895	0.062	0.257	1.207	0.590	2.779	305710
	40	31.311	8.689	0.032	0.115	1.496	0.939	3.444	69452
	60	44.965	15.035	0.022	0.067	1.653	1.177	3.806	24270
Cu	10	9.610	0.390	0.104	2.563	0.983	-0.41	2.263	9447779
	20	16.718	3.282	0.060	0.305	1.223	0.516	2.817	414168
	40	30.850	9.150	0.032	0.109	1.489	0.961	3.429	62964
	60	40.838	19.162	0.024	0.052	1.611	1.282	3.710	15147
Cd	10	9.815	0.185	0.102	5.405	0.992	-0.73	2.284	20188142
	20	18.335	1.665	0.055	0.601	1.263	0.221	2.909	1295321
	40	34.325	5.675	0.029	0.176	1.536	0.754	3.536	154173
	60	45.699	14.301	0.022	0.070	1.660	1.155	3.822	26739
Cr	10	10.000	0.000	0.100	-	1.000	-	2.303	-
	20	18.107	1.893	0.055	0.528	1.258	0.287	2.896	1053030
	40	27.533	12.467	0.036	0.080	1.440	1.096	3.315	34848.18
	60	38.311	21.689	0.026	0.046	1.583	1.336	3.646	11892.74

Appendix K: Thermodynamic data

VSCB	Temp (^{0}C)	20	25	30	35	40	60
	Temp (K)	293	298	303	308	313	333
Cr	Ave conc (C_e)	2.656	2.091	1.295	0.841	0.727	0.273
	q_e	17.344	17.909	18.705	19.159	19.273	19.727
	K_c	6.530	8.565	14.444	22.781	26.510	72.260
	K_c / T	0.0223	0.02874	0.04767	0.0739	0.0846	0.2169
	1/ T	0.0034	0.003	0.0033	0.0032	0.00325	0.00303
	ln K_c	1.876425	2.147	2.670	3.125	3.277	4.280
	ln Kc / T	0.006404	0.0072	0.0088	0.0101	0.0105	0.0128
Cd	Ave conc (C_e)	2.952	2.156	1.995	1.56	1.353	0.183
	q_e	17.048	17.844	18.005	18.44	18.647	19.817

	K_c	5.775	8.276	9.025	11.820	13.782	108.289
	K_c / T	0.019	0.027	0.0297	0.0383	0.0440	0.325
	1/ T	0.0034	0.0033	0.0033	0.0032	0.0032	0.00303
	ln K_c	1.753	2.113	2.200	2.469	2.623	4.684
	ln Kc / T	0.0059	0.0071	0.0072	0.0080	0.0083	0.014
Ni	Ave conc (C_e)	4.145	3.747	2.129	1.726	1.242	0.274
	q_e	15.855	16.253	17.871	18.274	18.758	19.726
	K_c	3.825	4.337	8.394	10.587	15.103	71.992
	K_c / T	0.0130	0.0146	0.027	0.034	0.048	0.216
	1/ T	0.003	0.003	0.0033	0.003	0.003	0.003
	ln K_c	1.341	1.467	2.127	2.359	2.714	4.276
	ln Kc / T	0.00479	0.00492	0.00702	0.00766	0.00867	0.01284
Pb	Ave conc (C_e)	4.041	3.5	2.554	1.743	1.338	0.122
	q_e	15.959	16.5	17.446	18.257	18.662	19.878
	K_c	3.949	4.714	6.830	10.474	13.947	162.934
	K_c / T	0.013	0.015	0.022	0.034	0.044	0.489
	1/ T	0.0034	0.0036	0.0033	0.0032	0.0031	0.0030
	ln K_c	1.373	1.550	1.921	2.348	2.635	5.093
	ln Kc / T	0.013	0.015	0.022	0.034	0.044	0.489
Cu	Ave conc (C_e)	5.052	3.688	2.844	2.13	1.351	0.896
	q_e	14.948	16.312	17.156	17.870	18.649	19.104
	K_c	2.958	4.422	6.032	8.389	13.803	21.321
	K_c / T	0.585	1.199	2.121	3.938	10.217	23.796
	1/ T	0.0034	0.0033	0.0033	0.0032	0.0031	0.0030
	ln K_c	1.084	1.486	1.797	2.127	2.624	3.059
	ln Kc / T	0.0037	0.0049	0.0059	0.0069	0.0083	0.0091

Cr	ΔH = -(-slope) x R	49.451 $KJmol^{-1}K^{-1}$
	ΔS = intercept x R	184.911 $Jmol^{-1}K^{-1}$
	$\Delta G = \Delta Ho - T\Delta S$	-5.652.00 $KJmol^{-1}K^{-1}$
Cd	ΔH = -(slope) x R	57.867 $KJmol^{-1}K^{-1}$
	ΔS = intercept x R	210.153 $Jmol^{-1}K^{-1}$
	$\Delta G = \Delta H^o - T\Delta S^o$	-4.758 $KJmol^{-1}K^{-1}$
Ni	ΔH = -(slope) x R	61.007 $KJmol^{-1}K^{-1}$
	ΔS = intercept x R	218.209 $Jmol^{-1}K^{-1}$
	$\Delta G = \Delta H^o - T\Delta S^o$	-4.019 $KJmol^{-1}K^{-1}$
Pb	ΔH = -(slope) x R	76.652 $KJmol^{-1}K^{-1}$
	ΔS = intercept x R	269.681 $Jmol^{-1}K^{-1}$
	$\Delta G = \Delta Ho - T\Delta S)$	-3.802 $KJmol^{-1}K^{-1}$
Cu	ΔH = -(slope) x R	28.340 $KJmol^{-1}K^{-1}$
	ΔS = intercept x R	111.698 $Jmol^{-1}K^{-1}$
	$\Delta G = \Delta Ho - T\Delta S)$	-61.626 $KJmol^{-1}K^{-1}$

VSCB	Temp (^0C)	20	25	30	35	40	60
	Temp (K)	293	298	303	308	313	333
Cr	Ave conc (C_e)	1.788	1.409	0.879	0.590	0.727	0.045
	q_e	18.212	18.591	19.121	19.410	19.273	19.955
	K_c	10.186	13.194	21.753	32.898	26.510	443.444
	K_c / T	0.035	0.044	0.072	0.107	0.085	1.332
	1/ T	0.003	0.003	0.003	0.003	0.003	0.003
	ln K_c	2.321	2.580	3.080	3.493	3.278	6.095
	ln Kc / T	-3.359	-3.117	-2.634	-2.237	-2.469	0.286
Cd	Ave conc (C_e)	1.774	1.505	1.376	1.070	0.095	0.000
	q_e	18.226	18.495	18.624	18.930	19.905	20.000
	K_c	10.276	12.292	13.533	17.686	209.968	-
	K_c / T	0.035	0.041	0.045	0.057	0.671	-
	1/ T	0.003	0.003	0.003	0.003	0.003	0.003
	ln K_c	2.330	2.509	2.605	2.873	5.347	-
	ln Kc / T	-3.350	-3.188	-3.109	-2.857	-0.399	-
Ni	Ave conc (C_e)	2.633	2.345	1.474	1.171	1.242	0.274

	q_e	17.367	17.655	18.526	18.829	18.758	19.726
	K_c	6.596	7.529	12.569	16.079	15.103	71.993
	K_c / T	0.023	0.025	0.041	0.052	0.048	0.216
	1/ T	0.003	0.003	0.003	0.003	0.003	0.003
	ln K_c	1.886	2.019	2.531	2.778	2.715	4.277
	ln Kc / T	-3.794	-3.678	-3.183	-2.953	-3.031	-1.532
Pb	Ave conc (C_e)	2.520	2.032	1.597	1.084	0.831	0.000
	q_e	17.480	17.968	18.403	18.916	19.169	20.000
	K_c	6.937	8.843	11.523	17.450	23.067	#DIV/0
	K_c / T	0.024	0.030	0.038	0.057	0.074	#DIV/0
	1/ T	0.003	0.003	0.003	0.003	0.003	0.003
	ln K_c	1.937	2.180	2.444	2.859	3.138	#DIV/0
	ln Kc / T	-3.743	-3.518	-3.269	-2.871	-2.608	#DIV/0
Cu	Ave conc (C_e)	3.329	2.426	1.9	1.428	1.351	0.896
	q_e	16.671	17.574	18.100	18.572	18.649	19.104
	K_c	5.008	7.244	9.526	13.006	13.804	21.321
	K_c / T	0.017	0.024	0.031	0.042	0.044	0.064
	1/ T	0.003	0.003	0.003	0.003	0.003	0.003
	ln K_c	1.611	1.980	2.254	2.565	2.625	3.060
	ln Kc / T	0.017	0.024	0.031	0.042	0.044	0.064

Cr	ΔH = -(-slope) x R	74.831 $KJmol^{-1}K^{-1}$
	ΔS = intercept x R	272.284 $Jmol^{-1}K^{-1}$
	$\Delta G = \Delta Ho - T\Delta S$	-155.00 $KJmol^{-1}K^{-1}$
Cd	ΔH = -(slope) x R	96.359 $KJmol^{-1}K^{-1}$
	ΔS = intercept x R	344.233 $Jmol^{-1}K^{-1}$
	$\Delta G = \Delta H^o - T\Delta S^o$	-198.941 $KJmol^{-1}K^{-1}$
Ni	ΔH = -(slope) x R	48.117 $KJmol^{-1}K^{-1}$
	ΔS = intercept x R	178.950 $Jmol^{-1}K^{-1}$
	$\Delta G = \Delta H^o - T\Delta S^o$	-101.445 $KJmol^{-1}K^{-1}$
Pb	ΔH = -(slope) x R	46.947 $KJmol^{-1}K^{-1}$

	ΔS = intercept x R	176.049 $Jmol^{-1}K^{-1}$
	$\Delta G = \Delta Ho - T\Delta S)$	-99.409 $KJmol^{-1}K^{-1}$
Cu	ΔH = -(slope) x R	28.340 $KJmol^{-1}K^{-1}$
	ΔS = intercept x R	111.698 $Jmol^{-1}K^{-1}$
	$\Delta G = \Delta Ho - T\Delta S)$	-61.626 $KJmol^{-1}K^{-1}$

Appendix L: FTIR Analyses

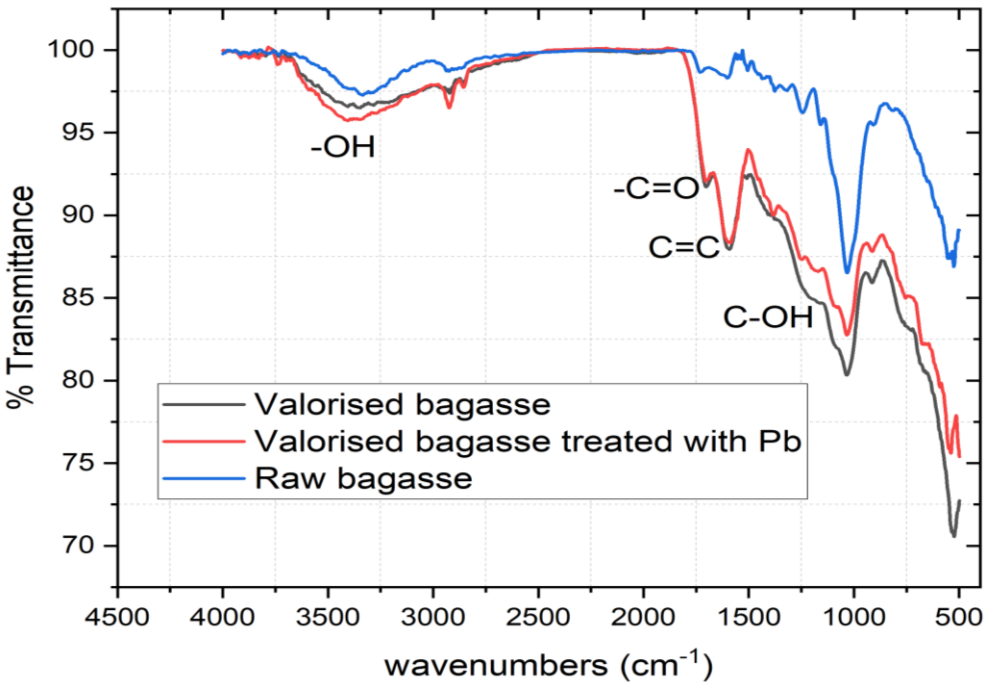

Table: raw bagasse

Raw SCB			
	-OH	-C=O	C=C
	3334	Hump at 1700	1600-1500
Cu,	3336	1727	
Cd,	3344		1610
Pb,	3344	shrank	1601
Cr,	3731, 3351	shrank	1615,1515
Ni,	3351	shrank	1626

Observation. There was a high frequency shift (from initial value of -OH 3336, -C=O 1700 and C=C 1500) . Showing that the metal was attached to the raw SCB through O-H or carboxylate, carbonyl and C=C aromatic groups.

Table.. Valorised bagasse

Valorised SCB

	-OH	-C=O	C=C
	3796,3733,3404,3346	1702	1591, 1509
Cu	3860,3383	1705	1597
Pb	3866, 3379	1705	1584
Cr	3860,3387	1705	1597
Cd	, 3866, 3378	Consumed	1579
Ni	3846, 3741,3380	1705	1596

Observation. There was high frequency shift (from 3796 to values above 3800) indicating adsorption took place mainly via O-H or carboxylate, carbonyl and C=C aromatic groups.

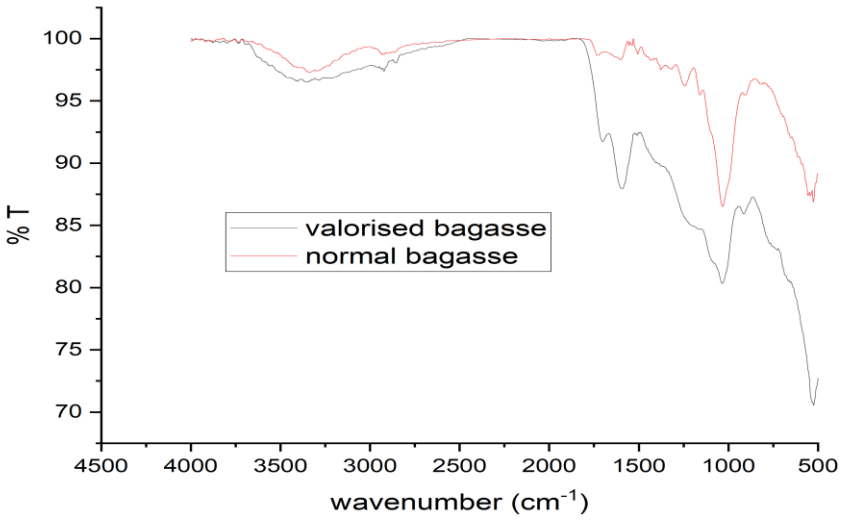

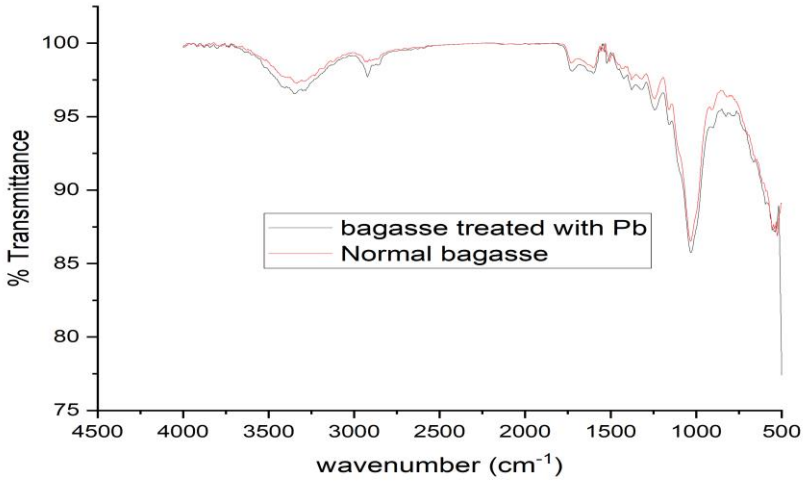
% Transmittance
100
95
90
85
80
75
4500
4000
3500
3000
2500
2000
1500
1000
500
wavenumber (cm-1)
bagasse treated with Pb
Normal bagasse

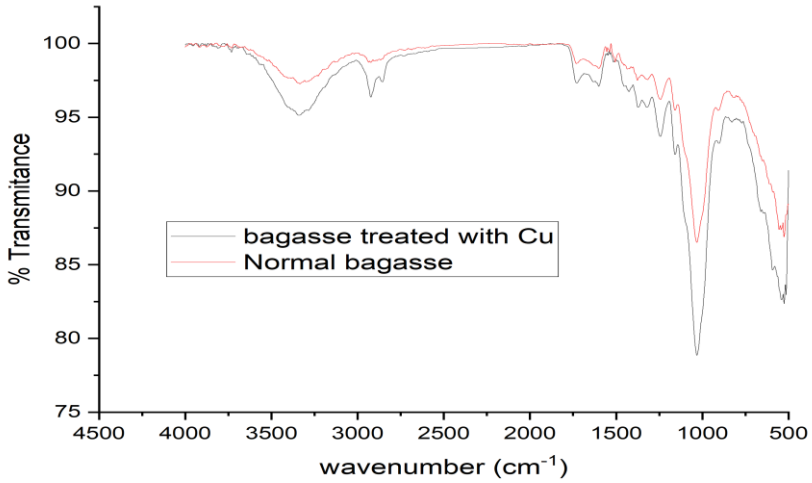
% Transmitance
100
95
90
85
80
75
4500
4000
3500
3000
2500
2000
1500
1000
500
wavenumber (cm-1)
bagasse treated with Cu
Normal bagasse

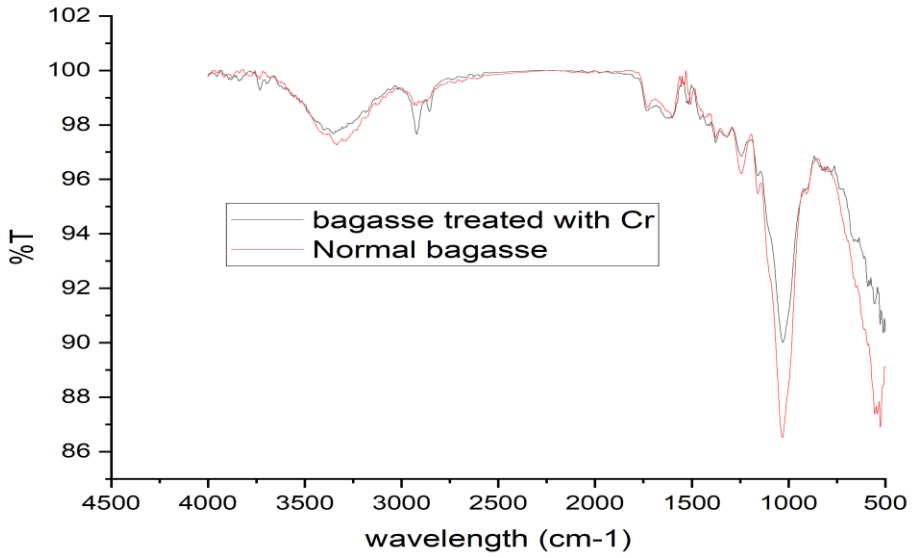
%T
wavelength (cm-1)
bagasse treated with Cr
Normal bagasse

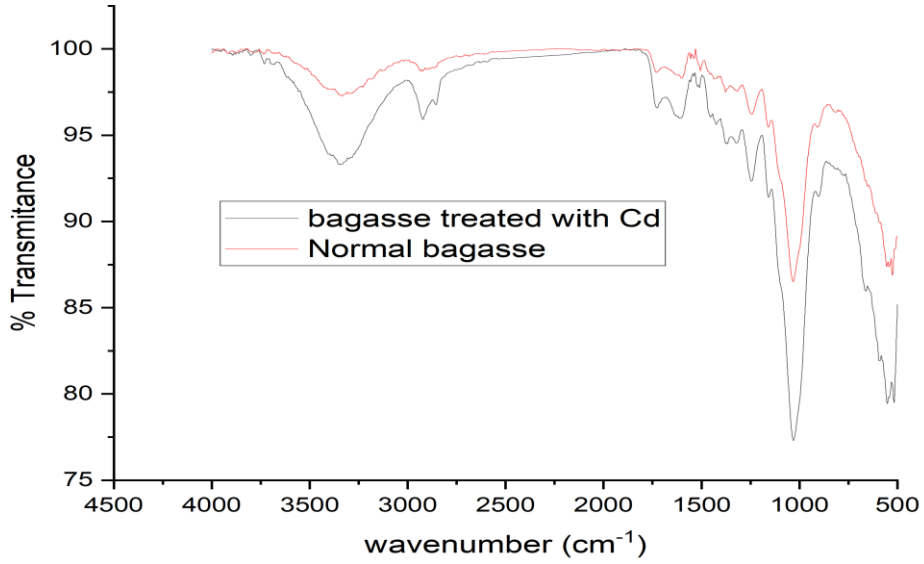
% Transmitance
wavenumber (cm-1)
bagasse treated with Cd
Normal bagasse

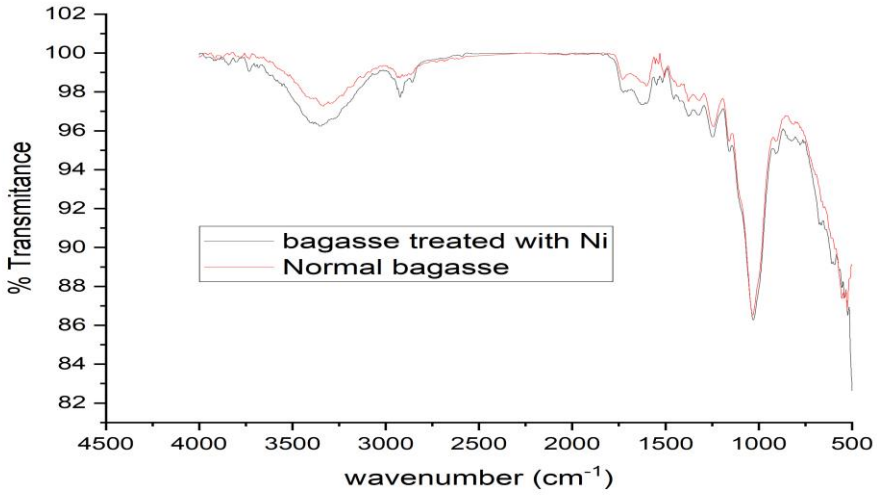
% Transmitance
wavenumber (cm-1)
bagasse treated with Ni
Normal bagasse

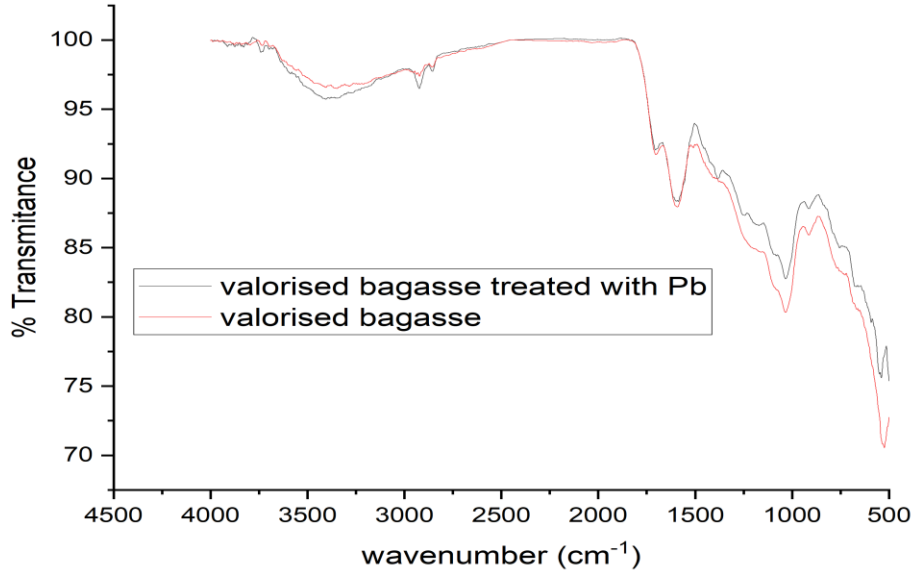
% Transmitance
wavenumber (cm-1)
valorised bagasse treated with Pb
valorised bagasse

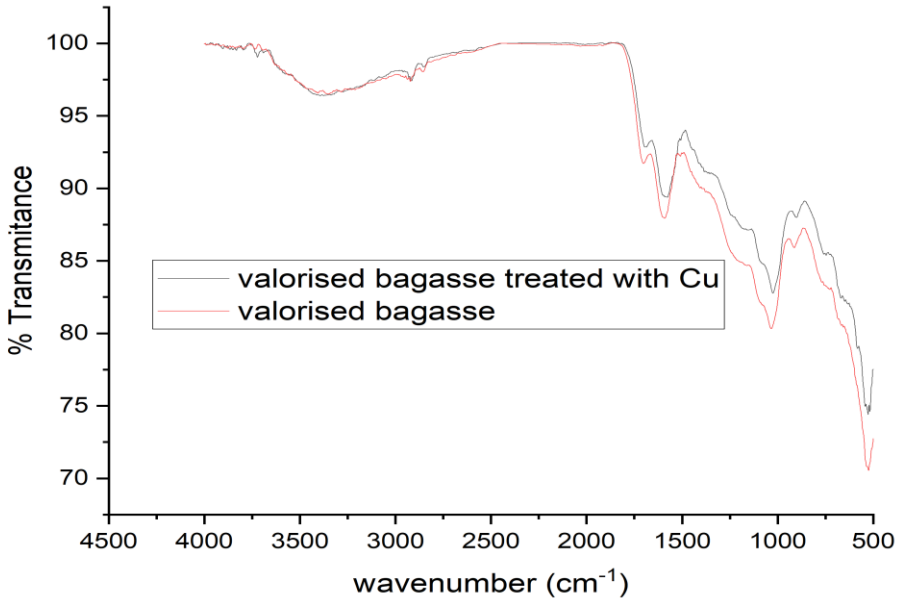
% Transmitance
100
95
90
85
80
75
70
4500
4000
3500
3000
2500
2000
1500
1000
500
wavenumber (cm-1)
valorised bagasse treated with Cu
valorised bagasse

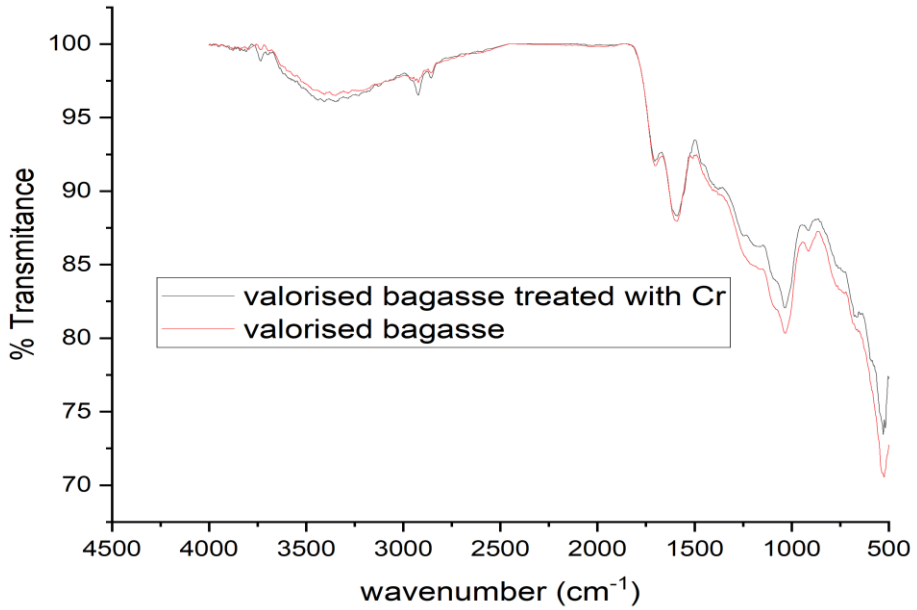
% Transmitance
100
95
90
85
80
75
70
4500
4000
3500
3000
2500
2000
1500
1000
500
wavenumber (cm-1)
valorised bagasse treated with Cr
valorised bagasse

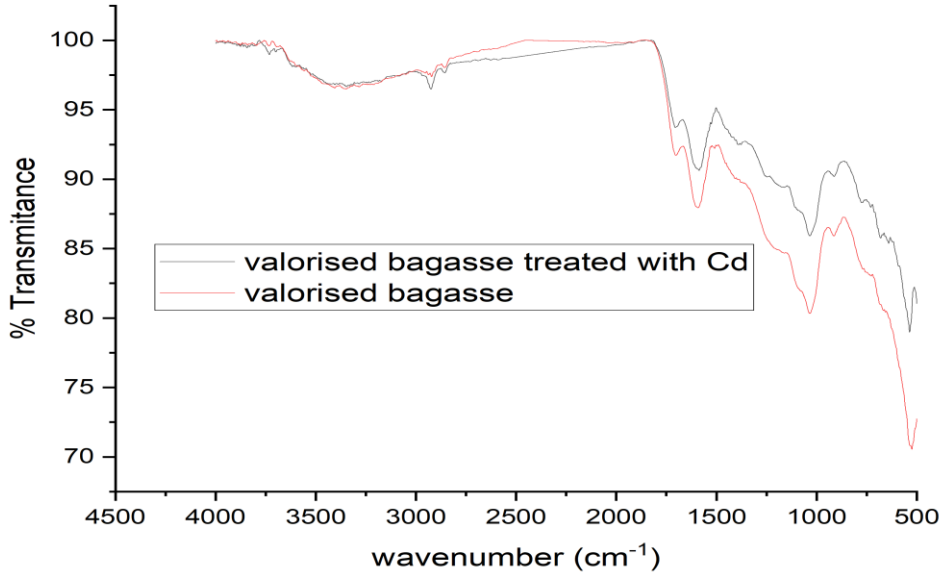
% Transmitance
wavenumber (cm-1)
valorised bagasse treated with Cd
valorised bagasse

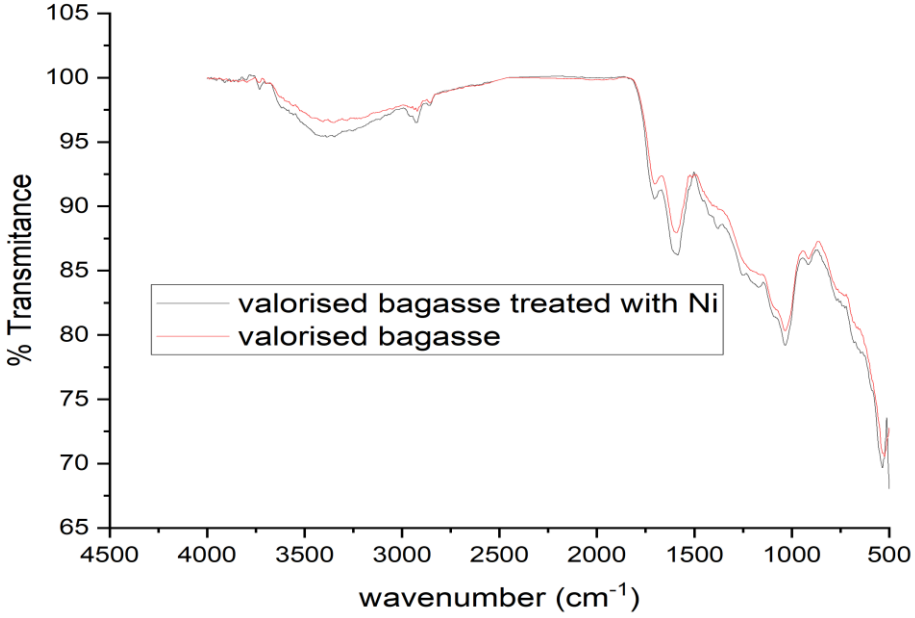
% Transmitance
wavenumber (cm-1)
valorised bagasse treated with Ni
valorised bagasse

Appendix M: Plots for kinetic studies for NSCB and VSCB

Appendix M1: (a) Pseudo-first-order (b) Pseudo-second-order kinetic plots for sorption of lead ions on NSCB

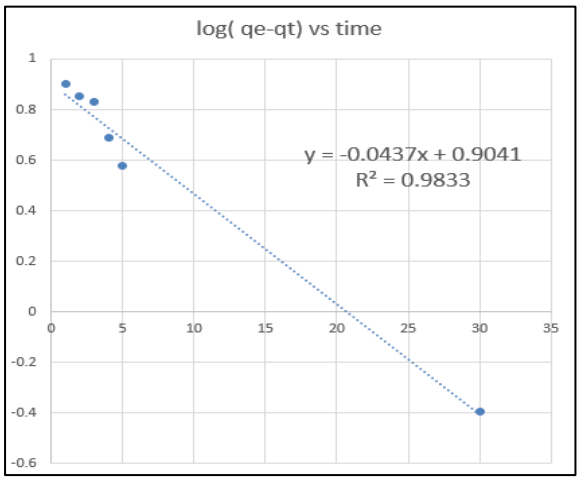

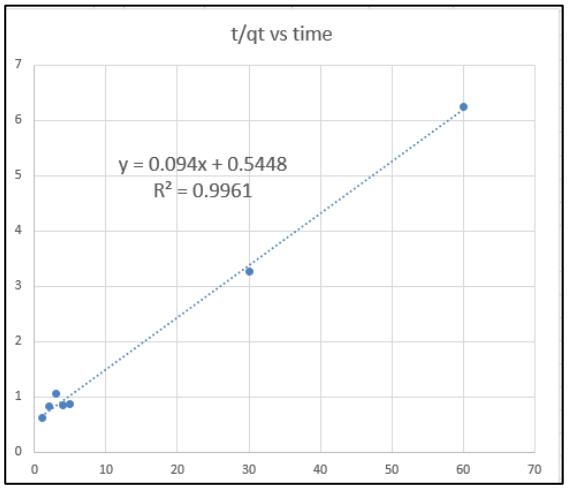

Appendix M2: Nickel (a) Pseudo-first-order (b) Pseudo-second-order kinetic plots for sorption of nickel ions NSCB

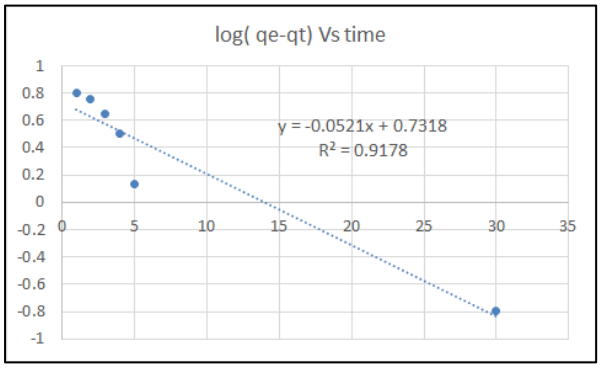

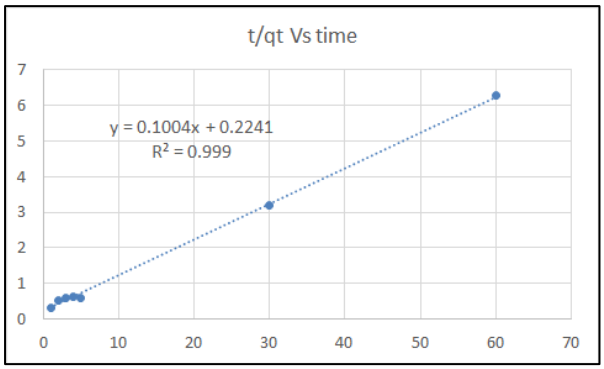

Appendix M3: (a) Pseudo-first-order (b) Pseudo-second-order kinetic plots for sorption of Cadmium on NSCB

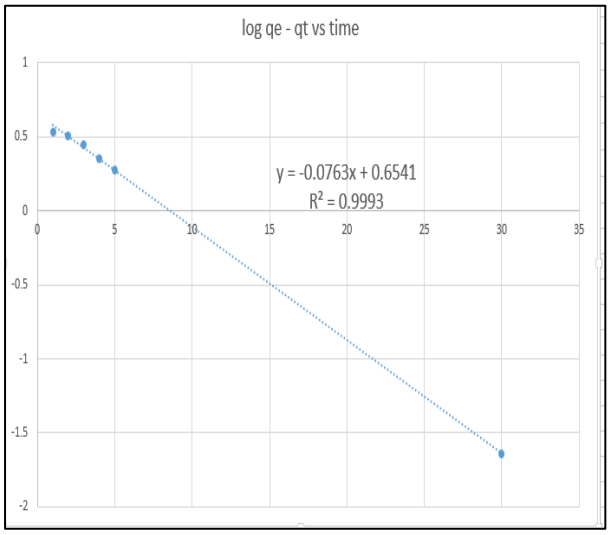

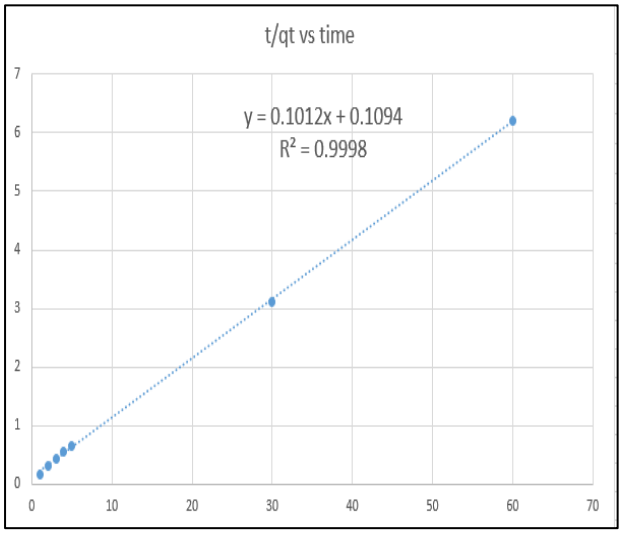

Appendix M4: (a) Pseudo-first-order (b) Pseudo-second-order kinetic plots for sorption of Copper ions on NSCB

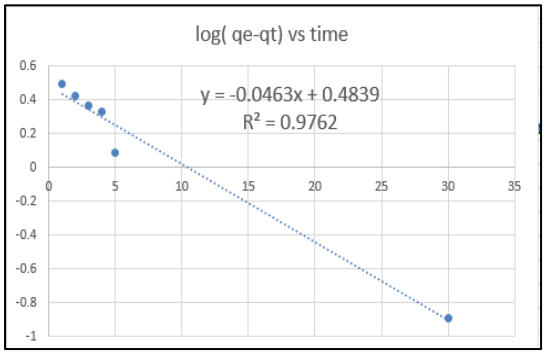

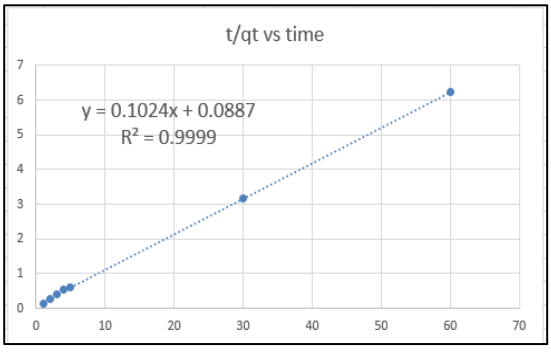

Appendix M5: (a) Pseudo-first-order (b) Pseudo-second-order kinetic plots for sorption of Chromium ions on NSCB

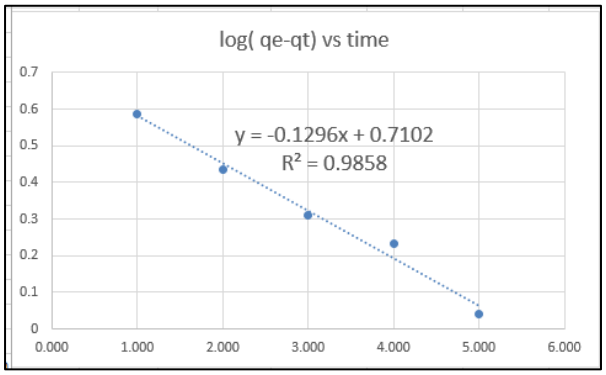

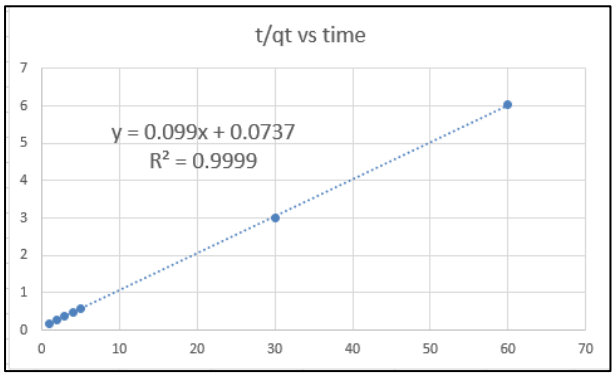

Appendix M6: (a) Pseudo-first-order (b) Pseudo-second-order kinetic plots for sorption of lead ions on VSCB

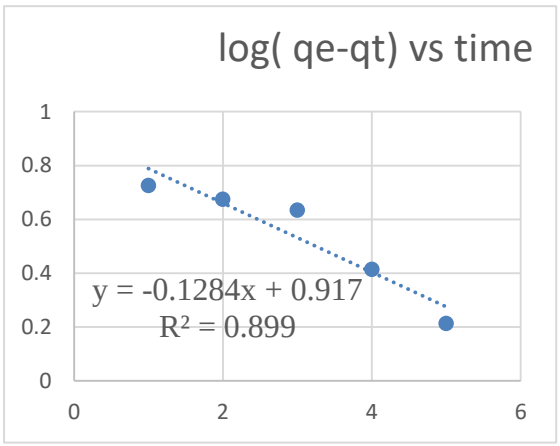

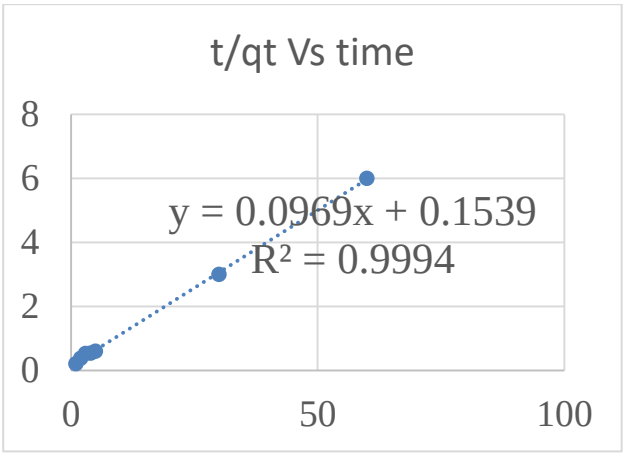

Appendix M7: (a) Pseudo-first-order (b) Pseudo-second-order kinetic plots for sorption of nickel ionsVSCB

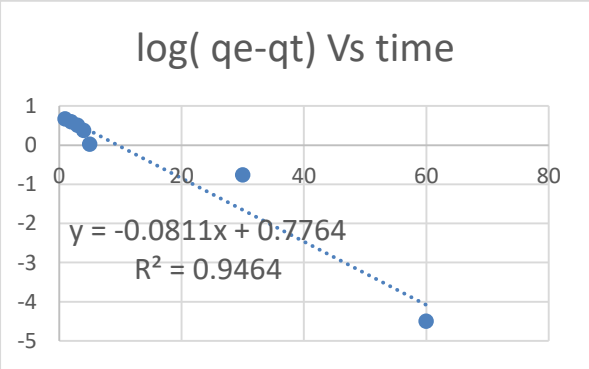

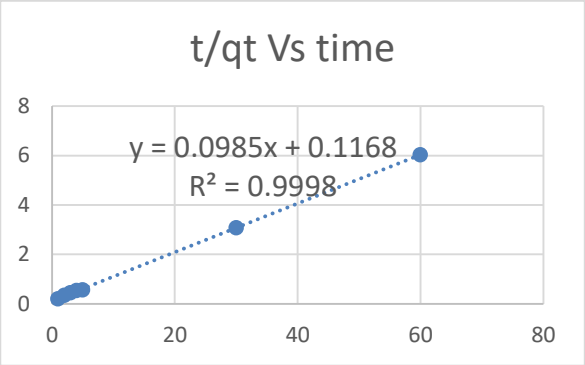

Appendix M8: (a) Pseudo-first-order (b) Pseudo-second-order kinetic plots for sorption of Cadmium on VSCB

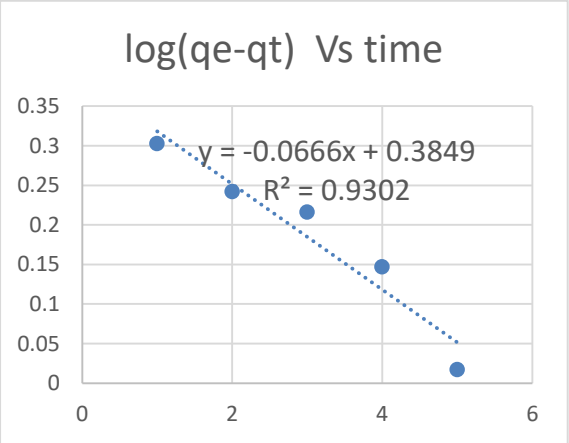

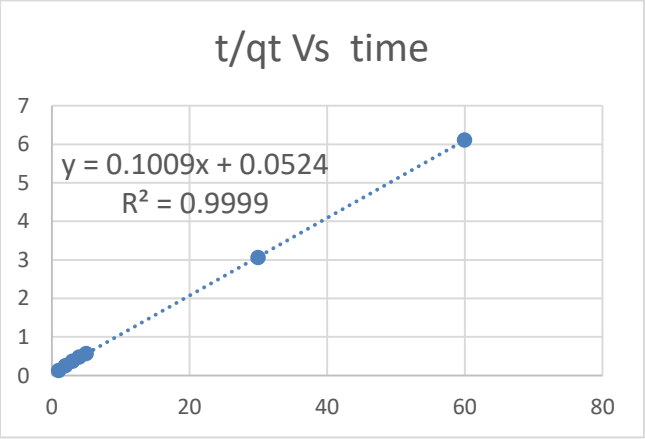

Appendix M9: (a) Pseudo-first-order (b) Pseudo-second-order kinetic plots for sorption of Copper ions on VSCB

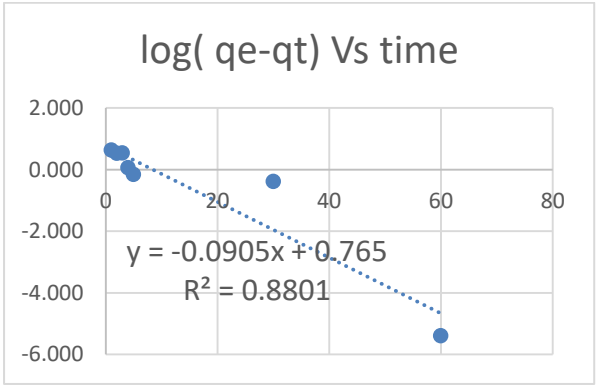

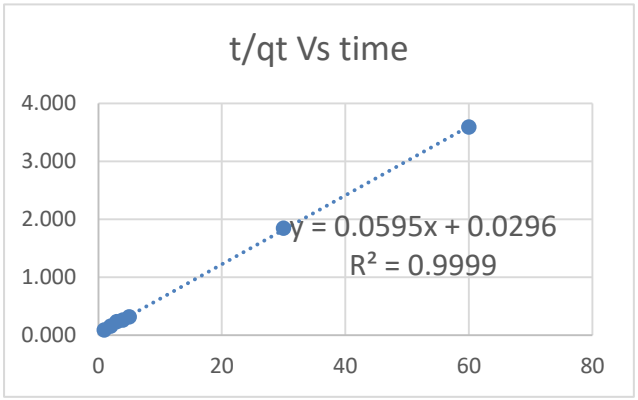

Appendix M10: (a) Pseudo-first-order (b) Pseudo-second-order kinetic plots for sorption of Chromium ions on VSCB

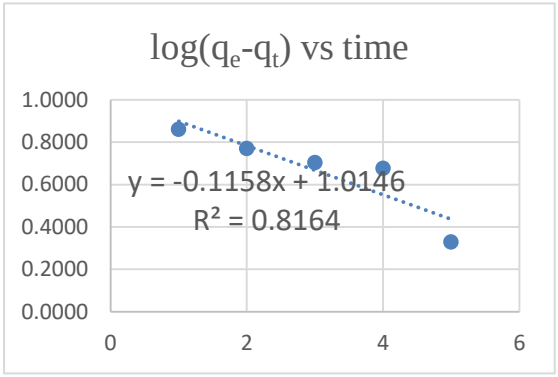

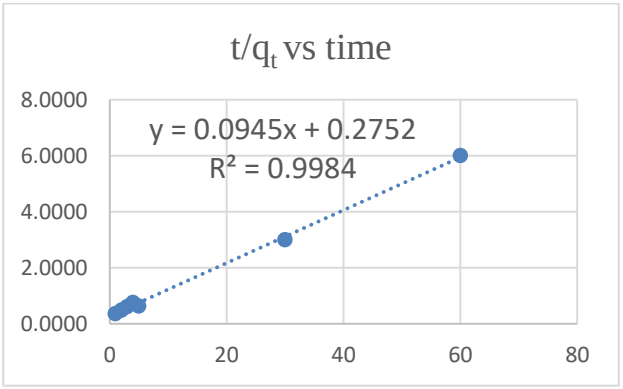

Appendix N: Isotherm plots for NSCB and VSCB

Appendix N1: (a) Langmuir, (b) freundlich and, (c) dubinin-radushchevik plots for sorption of lead ions on NSCB

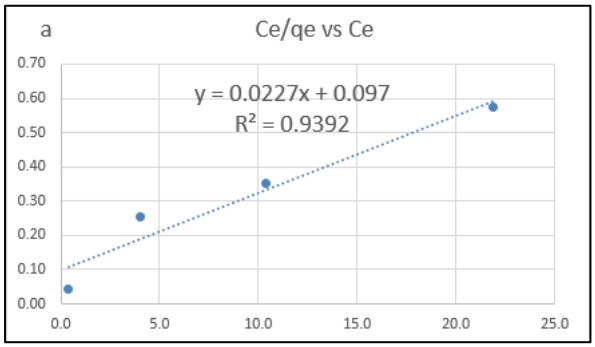

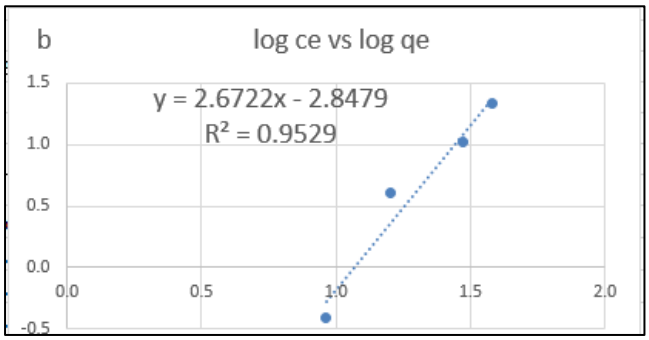

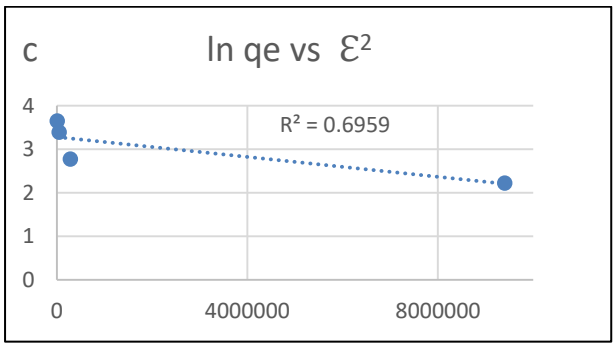

Appendix N2: (a) Langmuir, (b) freundlich and, (c) dubinin-radushchevik plots for sorption of nickel ions on NSCB

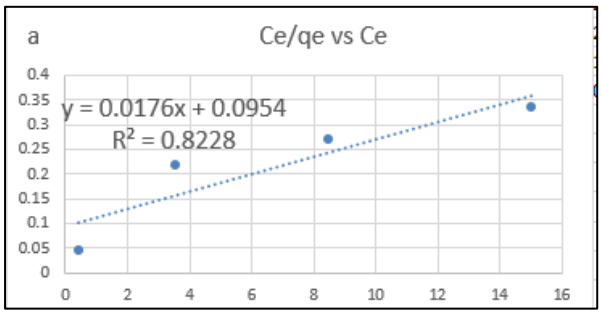

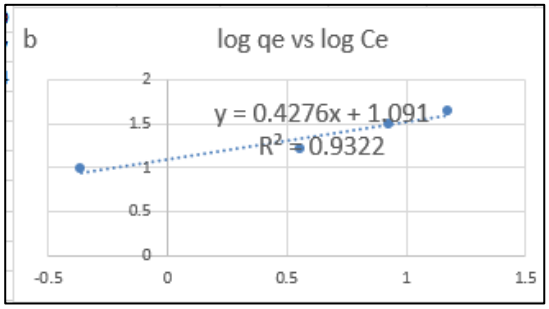

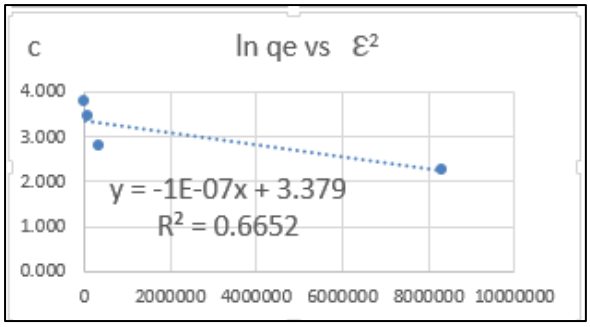

Appendix N3: (a) Langmuir, (b) freundlich and, (c) dubinin-radushchevik plots for sorption of copper ions on NSCB

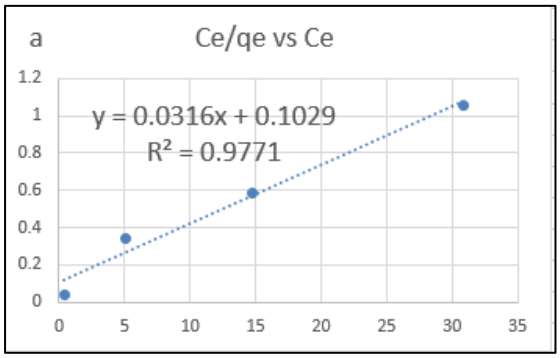

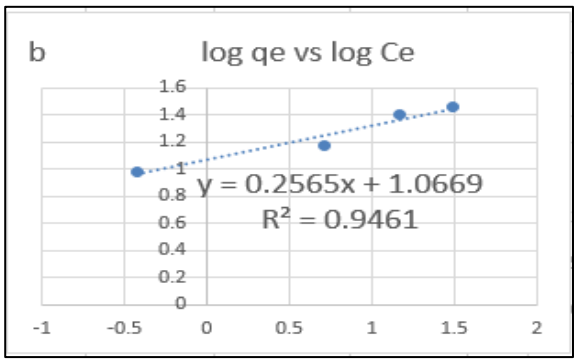

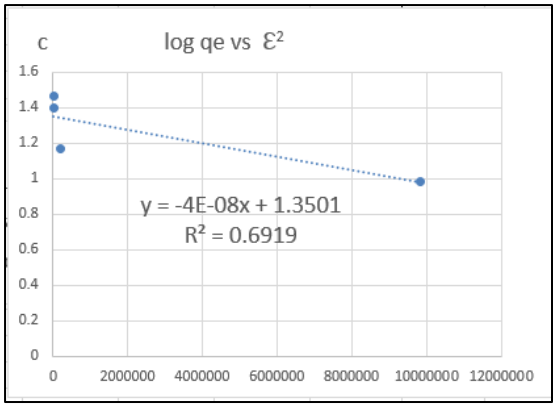

Appendix N4: (a) Langmuir, (b) freundlich and, (c) dubinin-radushchevik plots for sorption of cadmium ions on NSCB

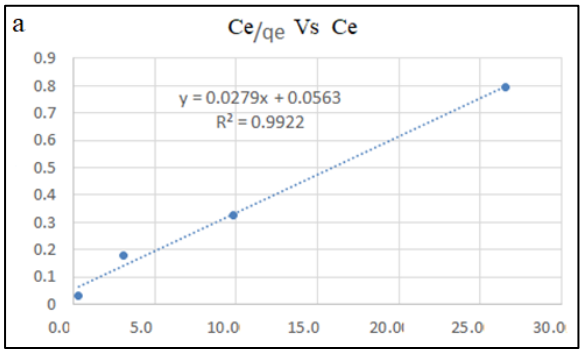

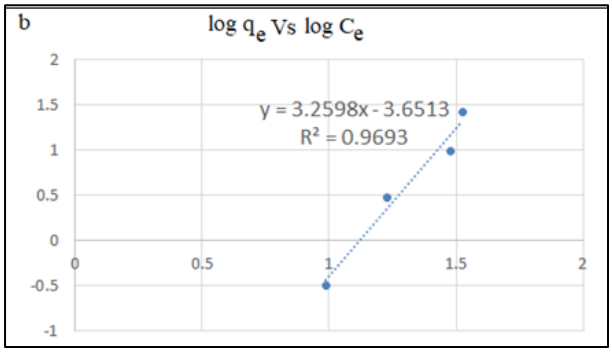

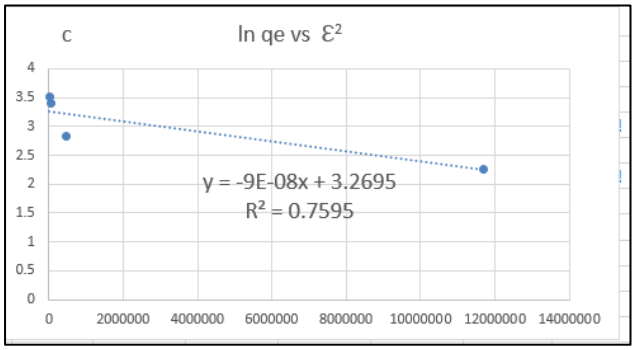

Appendix N5: (a) Langmuir, (b) freundlich and, (c) dubinin-radushchevik plots for sorption of chromium ions on NSCB

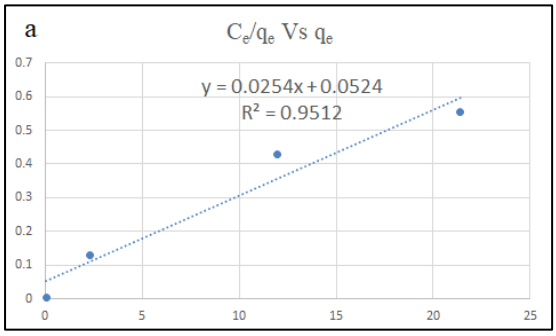

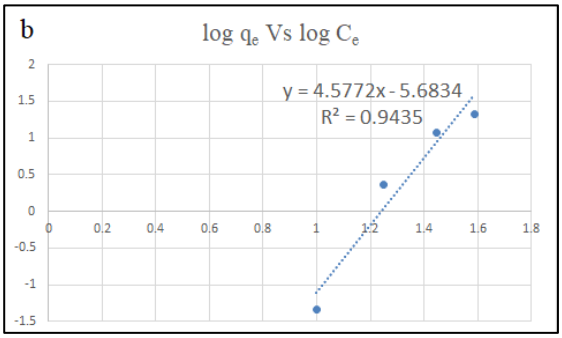

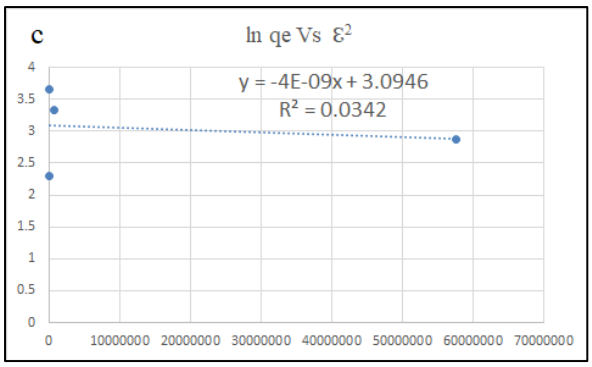

Appendix N6: (a) Langmuir, (b) freundlich and, (c) dubinin-radushchevik plots for sorption of lead ions on VSCB

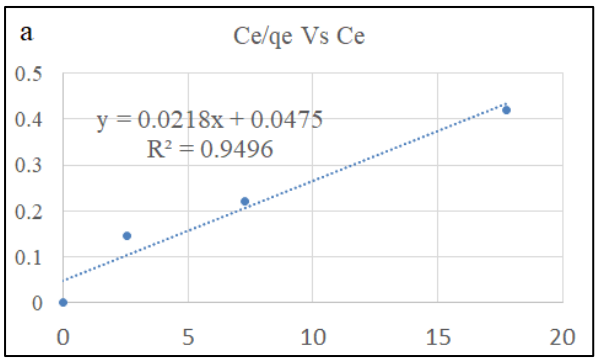

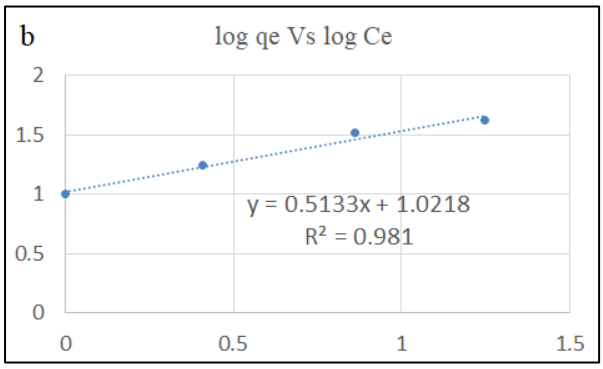

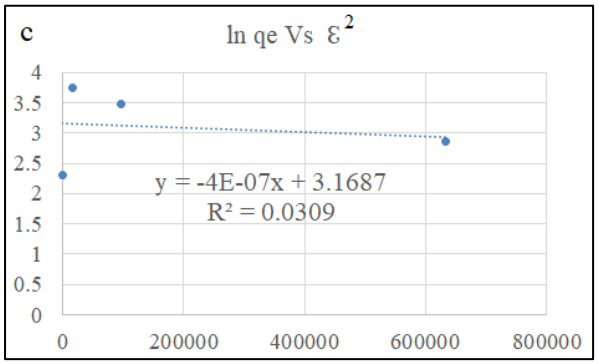

Appendix N7: (a) Langmuir, (b) freundlich and, (c) dubinin-radushchevik plots for sorption of nickel ions on VSCB

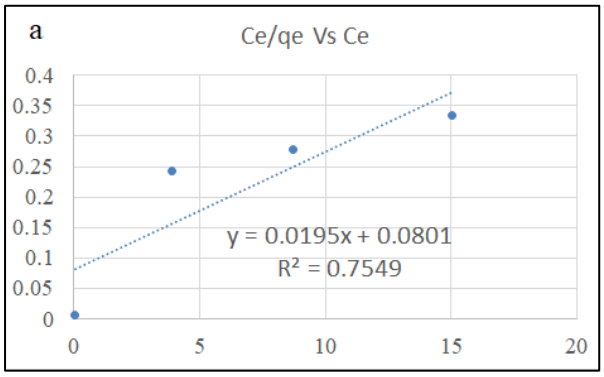

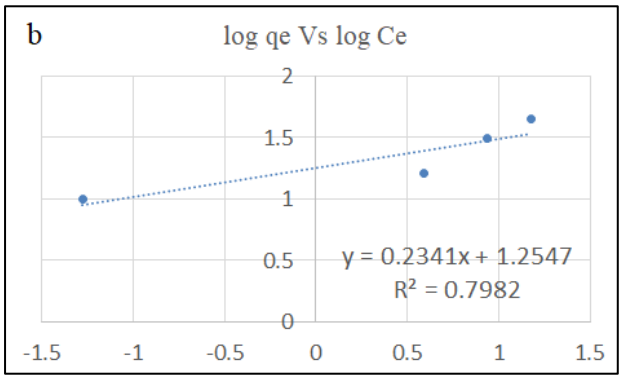

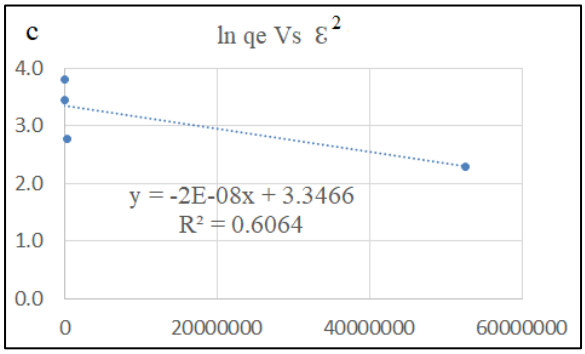

Appendix N8: (a) Langmuir, (b) freundlich and, (c) dubinin-radushchevik plots for sorption of copper ions on VSCB

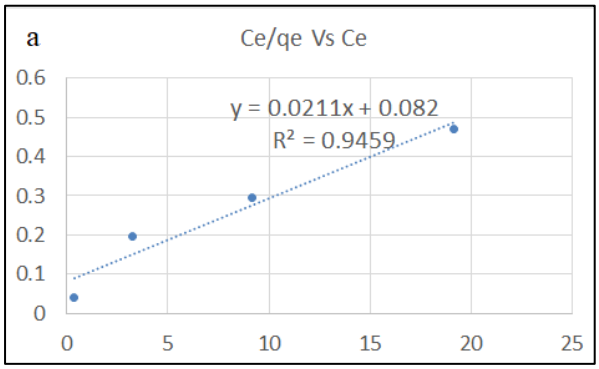

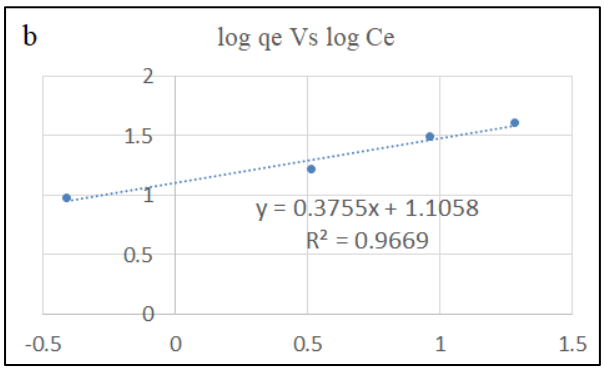

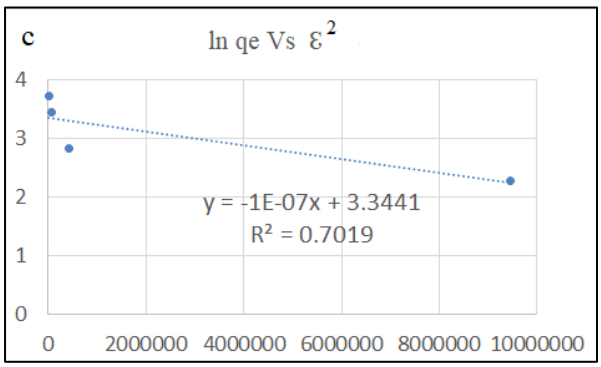

Appendix N9: (a) Langmuir, (b) freundlich and, (c) dubinin-radushchevik plots for sorption of cadmium ions on VSCB

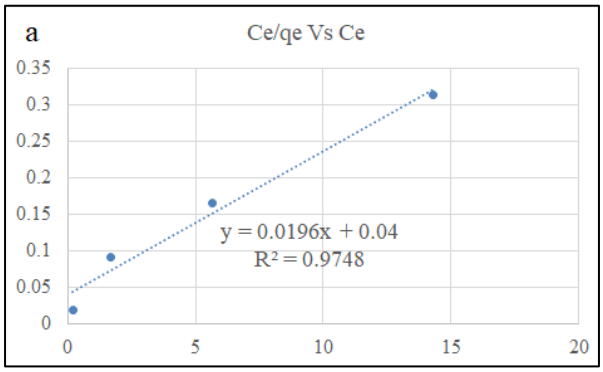

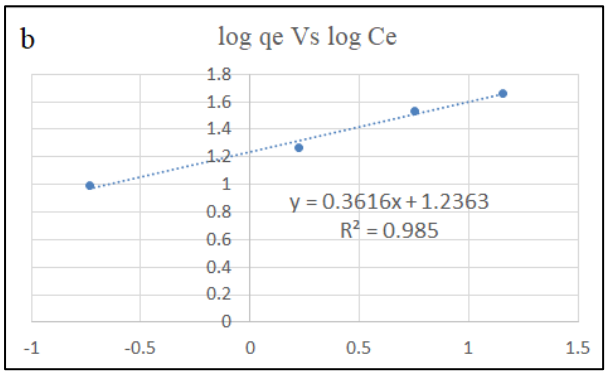

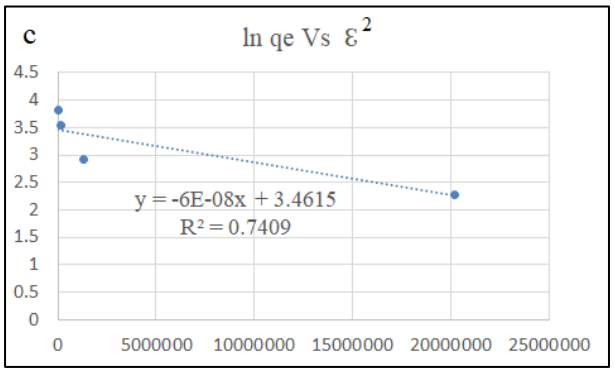

Appendix N10: (a) Langmuir, (b) freundlich and, (c) dubinin-radushchevik plots for sorption of cadmium ions on VSCB

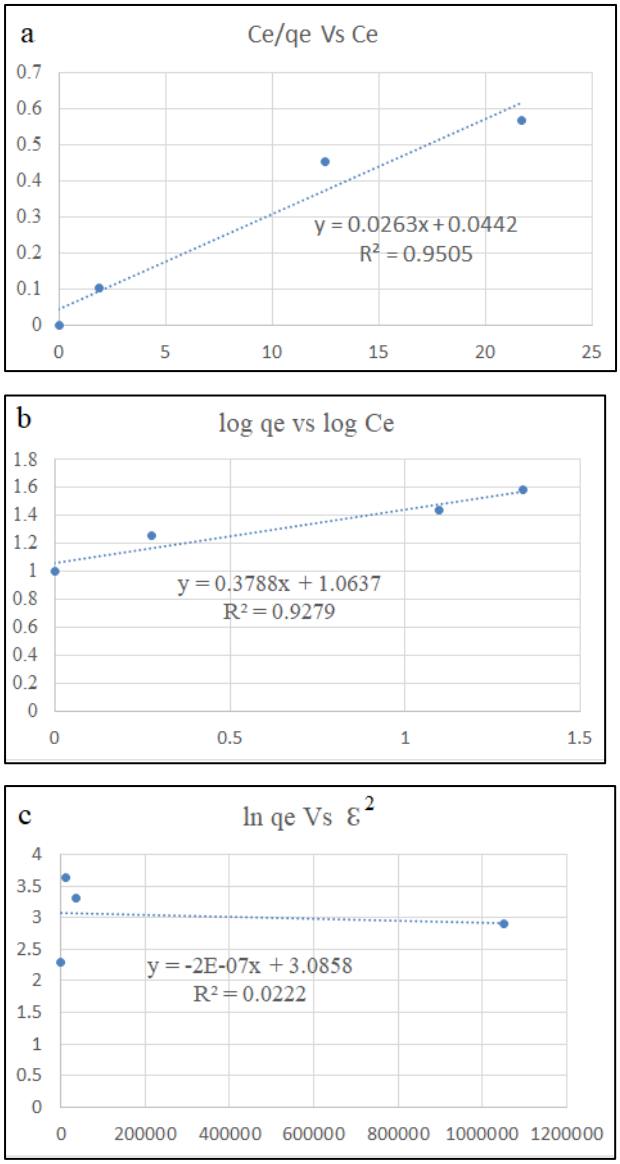

Appendix O: Research permit

REPUBLIC OF KENYA

NATIONAL COMMISSION FOR SCIENCE,TECHNOLOGY & INNOVATION

Ref No: **490148**

Date of Issue: **04/October/2022**

RESEARCH LICENSE

This is to Certify that Mr.. Ezekiel kipkorir langat of Egerton University, has been licensed to conduct research in Nakuru on the topic: Optimization of thermodynamic and kinetic properties for removal of heavy metals from Nakuru industrial wasterwaters using sugarcane bagasse for the period ending : 04/October/2023.

License No: **NACOSTI/P/22/20631**

490148

Applicant Identification Number

Director General
NATIONAL COMMISSION FOR SCIENCE,TECHNOLOGY & INNOVATION

Verification QR Code

NOTE: This is a computer generated License. To verify the authenticity of this document, Scan the QR Code using QR scanner application.

Appendix P: Publication

Asian Journal of Applied Chemistry Research

Volume 15, Issue 4, Page 276-293, 2024; Article no.AJACR.124544
ISSN: 2582-0273

Sugarcane Bagasse Based Adsorbents and their Adsorption Efficacy on Removal of Heavy Metals from Nakuru Industrial Wastewater: Optimization, Kinetic and Thermodynamic Aspects

Ezekiel Kipkorir Lang'at [a*], Josiah Ouma Omolo [a] and Peter Olengo Ongoma [a]

[a] Department of Chemistry, Egerton University, P.O. Box 536 - 20115 Egerton, Kenya.

Authors' contributions

This work was carried out in collaboration among all authors. Authors EKL, JOO and POO they contributed to the development of the project, experimental design and writing. All authors read and approved the final manuscript.

Article Information

DOI: https://doi.org/10.9734/ajacr/2024/v15i4311

Open Peer Review History:
This journal follows the Advanced Open Peer Review policy. Identity of the Reviewers, Editor(s) and additional Reviewers, peer review comments, different versions of the manuscript, comments of the editors, etc are available here: https://www.sdiarticle5.com/review-history/124544

Original Research Article

Received: 05/08/2024
Accepted: 07/10/2024
Published: 21/10/2024

ABSTRACT

Currently, researchers are seeking to reduce heavy metal contamination from the environment, using agricultural waste materials like rice husk, groundnuts shells among others. The study focused on the removal of Cu(II), Pb(II), Cd(II), Ni(II), and Cr(III) ions from aqueous solutions and Nakuru industrial wastewater using sugarcane bagasse (NSCB) and valorised bagasse ash (VSCB), as alternative low-cost agricultural waste bio-sorbents. To achieve this goal, sugarcane bagasse was collected from Nzoia sugar industry in western Kenya, while the valorised bagasse

**Corresponding author: Email: eklangat2004@gmail.com;*

Cite as: *Lang'at, Ezekiel Kipkorir, Josiah Ouma Omolo, and Peter Olengo Ongoma. 2024. "Sugarcane Bagasse Based Adsorbents and Their Adsorption Efficacy on Removal of Heavy Metals from Nakuru Industrial Wastewater: Optimization, Kinetic and Thermodynamic Aspects". Asian Journal of Applied Chemistry Research 15 (4):276-93. https://doi.org/10.9734/ajacr/2024/v15i4311.*

was obtained by heating sugarcane bagasse sample in a muffle furnace at 300°C for three hours. Furthermore, batch adsorption studies were performed, and the effects of several factors, *i.e.* adsorbent particle size, pH, contact time, initial heavy metal ions concentration and temperature were investigated to optimise the removal efficiency of Pb, Cu, Cd, Ni, and Cr. The optimal adsorption conditions were pH of 5.0, adsorbent dosage of 0.1 g and ≤ 150µm particle size, equilibrium time of 60 minutes and at 25 degrees Celcius. The removal kinetics of the metal ions onto both adsorbents fitted well with the pseudo-second-order model. The removal kinetics of the metal ions onto both adsorbents fitted well with the pseudo-second-order model. The adsorption of Pb^{2+} and Ni^{2+} onto NSCB fitted better with the Freundlich isotherm model, while Cd^{2+}, Cu^{2+} and Cr^{3+} showed better fit for the Langmuir isotherm model. As for VSCB adsorbent, Cr^{3+} has a better fit with the Langmuir isotherm model whereas Pb^{2+}, Ni^{2+}, Cd^{2+}, and Cu^{2+} fitted well on the Freundlich isotherm model. Freundlich constant's (1/n) values and the separation factor (RL) from the Langmuir isotherm model indicate that the metal ions were favourably adsorbed onto the adsorbents. Langmuir isotherm model was used to estimate the maximum adsorption capacities (qmax) for Cu(II), Pb(II), Ni(II), Cd(II), and Cr(III). The negative free energy change (ΔG) values revealed that adsorption process of the metal ions onto NSCB and VSCB was spontaneous. Fourier Transform Infrared Spectroscopy (FTIR) was used for characterization studies. Interactions with metal ions caused the frequencies of the active functional groups, –OH, C=O and C=C, on the bio-sorbent surfaces to shift to higher values. Therefore, sugarcane bagasse and valorised bagasse have demonstrated higher potential to remove relatively all selected heavy metals in the industrial wastewater at controlled pH.

Keywords: Sugarcane bagasse; adsorption; heavy metals; wastewater.

1. INTRODUCTION

Water is a source of life [1]. However, the quality of the world's water is increasingly threatened due to freshwater resources becoming heavily polluted by heavy metals, pathogens, turbidity, oil, and its derivatives from industries and agricultural effluents [2,3]. Heavy metal contaminated water is a real threat for agriculture, fishing and human consumption [4,5]. Among the heavy metals, Cu^{2+}, Cr^{6+}, Mn^{2+}, Ni^{2+}, Fe^{3+}, Cd^{2+}, Pb^{2+}, and Zn^{2+} ions are of primary concern in aquatic and terrestrial environments because of their high toxicity, high mobility, and solubility [6]. These metals enter the human body either directly or through the food chain [7]. They tend to accumulate in the human body [8] when ingested and cause serious health disorders [9]. For example, Pb^{2+} poisoning can lead to low intelligence quotient, concentration issues in children, axon degeneration, edema, infertility, menstrual problems, and stillbirths in adults [10,11,12] while cadmium causes damage to the kidneys, lungs, and liver [13].

Currently, numerous conventional physicochemical methods such as electrochemical treatment, ion-exchange, precipitation, reverse osmosis, evaporation, and oxidation/reduction [14] have been used for the removal of heavy metal ions from wastewaters. However, these methods have had their limitations, the major ones being: initial high costs, not being eco-friendly as well as incomplete removal of large quantities of toxic sludge produced and a huge amount of energy needed [3]. Adsorption has been used for centuries by Egyptians for the removal of odours and purification of drinking water [15]. Adsorption is a viable alternative treatment method because it is cost-effective, simple to operate [16], requires low energy, offers good selectivity, allows for the recovery of heavy metals [17], and provides options for adsorbent regeneration [18,19]. Adsorption using activated carbon has been found to be an attractive process for the removal of heavy metals from industrial effluents and dyes from aqueous solutions [20]. However, the cost of activated carbon and the loss of adsorption efficiency after regeneration of the exhausted activated carbon have limited its use in effluent wastewater treatment.

Bio-adsorbents made from sugarcane bagasse are inexhaustible materials containing carbon-oxygen functional groups such as carboxyl, ketone, ester, aromatic rings, and hydroxyl groups [21]. These functional groups have capacity for adsorbing metal ions through mechanisms like chelation and electrostatic interactions [22], which offer greater selectivity for bio-sorption studies on heavy metal ions,